

The earliest Cambrian record of animals and ocean geochemical change

Adam C. Maloof^{1,†}, Susannah M. Porter², John L. Moore², Frank Ö. Dudás³, Samuel A. Bowring³, John A. Higgins¹, David A. Fike⁴, and Michael P. Eddy¹

¹Department of Geosciences, Princeton University, Guyot Hall, Washington Road, Princeton, New Jersey 08544, USA

²Department of Earth Science, University of California, Santa Barbara, California 93106, USA

³Department of Earth, Atmospheric and Planetary Sciences, Massachusetts Institute of Technology, Cambridge, Massachusetts 02139, USA

⁴Department of Earth and Planetary Sciences, Washington University, St. Louis, Missouri 63130, USA

ABSTRACT

The Cambrian diversification of animals was long thought to have begun with an explosive phase at the start of the Tommotian Age. Recent stratigraphic discoveries, however, suggest that many taxa appeared in the older Nemakit-Daldynian Age, and that the diversification was more gradual. We map lowest Cambrian (Nemakit-Daldynian through Tommotian) records of $\delta^{13}\text{C}_{\text{CaCO}_3}$ variability from Siberia, Mongolia, and China onto a Moroccan U/Pb– $\delta^{13}\text{C}_{\text{CaCO}_3}$ age model constrained by five U/Pb ages from interbedded volcanic ashes. The $\delta^{13}\text{C}_{\text{CaCO}_3}$ correlations ignore fossil tie points, so we assume synchronicity in $\delta^{13}\text{C}$ trends rather than synchronicity in first appearances of animal taxa. We present new $\delta^{13}\text{C}_{\text{org}}$, $^{87}\text{Sr}/^{86}\text{Sr}$, uranium, and vanadium data from the same carbonate samples that define the Moroccan $\delta^{13}\text{C}_{\text{CaCO}_3}$ curve. The result is a new absolute time line for first appearances of skeletal animals and for changes in the carbon, strontium, and redox chemistry of the ocean during the Nemakit-Daldynian and Tommotian ages at the beginning of the Cambrian. The time line suggests that the diversification of skeletal animals began early in the Nemakit-Daldynian, with much of the diversity appearing by the middle of the age. Fossil first appearances occurred in three pulses, with a small pulse in the earliest Nemakit-Daldynian (ca. 540–538 Ma), a larger pulse in the mid- to late Nemakit-Daldynian (ca. 534–530 Ma), and a moderate pulse in the Tommotian (ca. 524–522 Ma). These pulses

are associated with rapid reorganizations of the carbon cycle, and are superimposed on long-term increases in sea level and the hydrothermal flux of Sr.

INTRODUCTION

In his book *On the Origin of Species*, Charles Darwin suggested that one of the greatest challenges to his ideas was the “sudden appearance of groups of Allied Species in the lowest known fossiliferous strata” (Darwin, 1859, p. 306). He wrote (Darwin, 1859, p. 307):

“... if my theory be true, it is indisputable that before the lowest Silurian stratum was deposited, long periods elapsed, as long as, or probably far longer than, the whole interval from the Silurian age to the present day; and that during these vast, yet quite unknown, periods of time, the world swarmed with living creatures. ... To the question why we do not find records of these vast primordial periods, I can give no satisfactory answer.”

The dilemma Darwin faced was that if all life descended via gradual modification from a single common ancestor, then the complexity and diversity of fossils found in Cambrian strata (at that time referred to the lower part of the Silurian) demand a long interval of evolution prior to the beginning of the Cambrian. During Darwin’s time, there was no evidence of this life, and all that he could offer as explanation was the incompleteness of the geological record: The interval of time during which the ancestors to trilobites, brachiopods, molluscs, and other Lower Cambrian taxa evolved is not preserved in the rock record.

Beginning in the 1950s, discoveries of Precambrian microfossils in chert and shale and

of macroscopic Ediacara fossils (e.g., Tyler and Barghoorn, 1954; Barghoorn and Tyler, 1965; Ford, 1958; Glaessner and Wade, 1966; Schopf, 2000) helped solve this conundrum, but the sudden diversity of the Cambrian fossil record remained a puzzle (cf. Cloud, 1948, 1965). Despite abundant evidence for a variety of life extending back to at least 3.5 Ga, Precambrian fossils mostly record the evolution of bacteria and microbial eukaryotes. The earliest evidence for animals predates the Precambrian-Cambrian boundary by only ~100 m.y. (Xiao et al., 1998; Yin et al., 2007; Love et al., 2009; Maloof et al., 2010b), and the few unquestioned examples of Precambrian Bilateria are <15 m.y. older than the beginning of the Cambrian (Fedonkin and Waggoner, 1997; Martin et al., 2000; Jensen, 2003; Droser et al., 2005). Significant increases in trace fossil diversity and complexity across the boundary and the absence of soft-bodied animals in upper Precambrian Burgess Shale-type biotas (Xiao et al., 2002) suggest that the general absence of bilaterian animal fossils from upper Precambrian rocks is not a preservational artifact. Rather, it appears that animals originated and began to diversify relatively close to the base of the Cambrian. Although early studies using a “molecular clock” suggested that the divergences between major animal groups long predated the Cambrian (Wray et al., 1996; Bromham et al., 1998), some of the more recent work has produced dates that are closer to (if still older than) those supported by the fossil record (Aris-Brosou and Yang, 2003; Peterson et al., 2004, 2008). Furthermore, Konservat-Lagerstätten such as the Chengjiang biota and the Burgess Shale record a breathtaking array

[†]E-mail: maloof@princeton.edu

of soft-bodied animals by the late Early and Middle Cambrian (Briggs et al., 1994; Hou et al., 2004), respectively, and, together with more conventional skeletal assemblages, suggest a great radiation of animal life during the Early Cambrian.

These observations led scientists to focus in particular on two puzzling aspects of the Cambrian radiation, both encompassed by the term “Cambrian explosion” (cf. Marshall, 2006). The first is the dramatic increase in disparity (morphological distinctness) as represented by the supposed appearance of nearly all major animal body plans (equivalent to the animal phyla) within a geologically brief interval of time near the beginning of the Cambrian (e.g., Gould, 1989; Valentine, 1994, 2002, 2004). This problem was compounded by an apparent lack of evidence for “intermediate” taxa—taxa that lie close to the last common ancestor of different phyla in the metazoan tree (Marshall, 2006). The second difficulty is the high rate of diversification (increase in number of species) in the Early Cambrian, particularly the apparent spike in diversification during the Tommotian and Atdabanian ages (Fig. 1), spanning an interval that seemed short relative to subsequent radiations (e.g., Sepkoski, 1992; Zhuravlev, 2001; Marshall, 2006).

Evidence accumulated over the past 20 yr, however, suggests that both of these problems have been somewhat exaggerated. Although

Lower Cambrian fossils indicate that divergences among the major groups of animals must have occurred by that time, the assembly of the major animal body plans—the suites of characters that define the living phyla—in many cases took longer (Budd and Jensen, 2000). In other words, crown-group representatives of most phyla (i.e., those that possess all of the characters of the living groups) first appear later than the Early Cambrian, and in some cases much later. Most Early Cambrian animals are, in fact, the intermediate taxa or stem-groups that were thought to be missing from the early animal record (Budd and Jensen, 2000; Conway Morris and Peel, 1995; Shu et al., 2001; Budd, 2002; Caron et al., 2006; Skovsted et al., 2008).

Nonetheless, it is true that many Early Cambrian taxa are at least recognizably related to crown-group phyla, suggesting that many of the basic features that distinguish the major groups of animals had evolved by this time (Budd, 2008). In other words, the Early Cambrian diversification of animals is marked by high disparity. However, the observation that disparity reaches its peak early in a group’s history seems to reflect a general phenomenon, also observed in plants (Boyce, 2005), the Ediacara biota (Shen et al., 2008), Precambrian microfossils (Huntley et al., 2006), and within many individual animal clades, such as crinoids (Foote, 1997), gastropods (Wagner, 1995), and unguates (Jernvall

et al., 1996). Although of significant interest, this high disparity soon after a group’s appearance is not unique to the Cambrian.

The second puzzling aspect of the Cambrian explosion, the high rate of diversification, appears to be in part an artifact of a frequently incomplete Cambrian record with a dearth of reliable radiometric age constraints. Using radiometric dates of volcanic ash units interbedded in fossiliferous strata, workers discovered that the base of the Cambrian is ca. 542 Ma (Bowring et al., 1993; Grotzinger et al., 1995; Bowring et al., 2007), rather than 570 Ma (Harland et al., 1990) or ca. 600 Ma (Holmes, 1960; Harland et al., 1982). This newly compressed Cambrian Period led numerous authors to conclude that diversification rates had to be twice as fast as they already were thought to be. Despite these new geochronological constraints on the Ediacaran-Cambrian (E-C) boundary and the length of the Cambrian Period, the duration of individual Cambrian stages associated with specific animal radiations remained poorly constrained. Additional U/Pb dating of zircons in volcanic ash layers demonstrated that the Early Cambrian is in fact quite long, spanning 32 m.y. and nearly 60% of Cambrian time (Bowring et al., 1993; Grotzinger et al., 1995; Landing et al., 1998). Recent work suggests that the Nemakit-Daldynian Stage alone was 17 m.y. long (Landing et al., 1998; Maloof et al., 2005, 2010a). An equally important factor as the refined time scale is the recognition that the appearance of dozens of animal taxa at the base of the Tommotian Stage in the stratotype Nemakit-Daldynian–Tommotian (ND–T) boundary sections at Dvortsy and Ulakhan Sulugur (Siberia), which contributed to the classic view of an explosive early phase of diversification, actually reflects the presence of a significant unconformity just below that horizon (see following discussion). Other lowest Cambrian sections in northwestern Siberia and in Mongolia suggest instead that these “Tommotian” taxa appeared in a more gradual sequence in older rocks (Knoll et al., 1995b; Kaufman et al., 1996; Brasier et al., 1996). Thus, rather than being mostly devoid of fossils, the Nemakit-Daldynian Stage records the earliest diversification of Cambrian animals, spread out over 17 m.y.

Here, we examine in detail the Nemakit-Daldynian through Tommotian diversification of animals, and, in particular, the skeletal animals often referred to as “small shelly fossils.” We use carbon isotope chemostratigraphy of carbonates ($\delta^{13}\text{C}_{\text{CaCO}_3}$), derived from the same rocks that host the small shelly fossils, and calibrate the chemostratigraphy using U/Pb zircon geochronology of interbedded volcanic ashes. The result is a $\delta^{13}\text{C}_{\text{CaCO}_3}$ age model indepen-

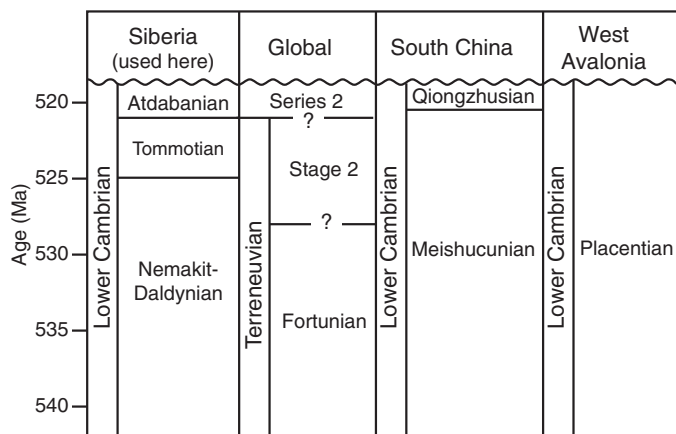


Figure 1. Lower Cambrian stratigraphic terminology from selected regions and the global standard. Global standard names are from the International Stratigraphic Chart (2009). Boundary ages for Siberia are from Maloof et al. (2005, 2010a). Correlations with South China and West Avalonia are from Steiner et al. (2007), although boundary ages are tentative. The lower boundary of the Lower Cambrian in each region is not necessarily synchronous. Because most of the sections discussed in this paper are from Siberia, and because the boundaries for global stages 2–4 have not yet been defined, we use the Siberian terminology.

dent of fossil first appearances. This method of correlation is preferred over biostratigraphy for two reasons: (1) the abundant evidence that Lower Cambrian fossil ranges are strongly facies-controlled (e.g., Brasier et al., 1994b; Lindsay et al., 1996a; Kouchinsky et al., 2007); and (2) the circularity associated with inferring paleobiological patterns from biostratigraphically correlated rock sequences. We find that there appear to be several pulses of fossil first appearances spanning the Nemakit-Daldynian–Tommotian interval: a small pulse (pulse_{ND}) occurring ca. 540–538 Ma and recorded only in Mongolia; a large pulse (pulse_{mND}) occurring between 534 and 530 Ma and observed in both China and Siberia; and a moderate pulse (pulse_r), occurring between 524 and 522 Ma during the Tommotian Stage.

Carbon isotopes in carbonates have long been recognized as a useful tool for stratigraphic correlation (e.g., Scholle and Arthur, 1980; Knoll et al., 1986; Magaritz et al., 1991; Kaufman et al., 1993; Narbonne et al., 1994; Brasier et al., 1994b; Knoll et al., 1995b; Jacobsen and Kaufman, 1999; Hayes et al., 1999; Veizer et al., 1999; Saltzman et al., 2000; Walter et al., 2000; Halverson et al., 2005; Maloof et al., 2005). However, carbon isotopes of both carbonate and organic matter also may preserve information about the global carbon cycle, and reorganization of the carbon cycle may be a cause or an effect (or both) of paleobiological change (e.g., Hayes and Waldbauer, 2006). We compare the paleontological patterns in the lowest Cambrian with the carbon isotope composition of carbonate ($\delta^{13}\text{C}_{\text{CaCO}_3}$) and organic matter ($\delta^{13}\text{C}_{\text{org}}$), and the strontium isotope ($^{87}\text{Sr}/^{86}\text{Sr}$) and trace element (Mn, Rb, Sr, V, Th, U) compositions of carbonate, and speculate about possible causal relationships between biological and environmental change during the earliest Cambrian. We show that the long-term Nemakit-Daldynian decline in $^{87}\text{Sr}/^{86}\text{Sr}$ is consistent with an increase in the hydrothermal alteration of oceanic crust and a rise in global sea level that spans the ND–T. Stratigraphic variability of uranium and vanadium indicates a nearly monotonic increase in the oxidation of the sediment-water interface on shallow-water carbonate platforms, consistent with the gradual increase in the depth of sediment bioturbation and in the diversity of animals. We find that pulse_{mND} coincides with a twofold increase in the amplitude of $\delta^{13}\text{C}_{\text{CaCO}_3}$ oscillations and a switch from a carbon cycle dominated by changes in the isotopic fractionation between inorganic and organic carbon (542–534 Ma and 525–517 Ma), to a carbon cycle dominated by changes in the relative rate of burial of carbonate and organic matter (534–525 Ma).

BACKGROUND

Paleontology of the Lowest Cambrian

Small Shelly Fossils

Among the most striking fossils of the lowest Cambrian are the so-called small shelly fossils (Matthews and Missarzhevsky, 1975). These consist of a variety of shells, sclerites, and other biomineralized structures produced by many independent metazoan lineages, and they are widespread in phosphatic limestones from this time. Although some of these skeletons were originally phosphatic, most were originally calcareous and later diagenetically phosphatized (Bengtson and Conway Morris, 1992; Porter, 2007, 2010), allowing for their easy study in samples prepared through acid maceration. Small shelly fossils are common from the lowest Cambrian through the Botomian in the upper Lower Cambrian, but they are only rarely found through the Middle Cambrian and above, reflecting in part the decline of their primary mode of preservation—secondary diagenetic phosphatization (Dzik, 1994; Porter, 2004a). Nemakit-Daldynian and Tommotian assemblages of small shelly fossils are particularly well described from the Siberian platform (reviewed in Sokolov and Zhuravleva, 1983; Missarzhevskiy, 1989; Rozanov and Zhuravlev, 1992), South China (reviewed in Qian, 1989, 1999; Qian and Bengtson, 1989), Mongolia (Voronin et al., 1982; Esakova and Zhegallo, 1996), and Avalonia (Brasier, 1984; Landing, 1988, 1991; Landing et al., 1989).

Small shelly fossils are significant because they record the beginnings of widespread biomineralization among animals. Probable biomineralized metazoans are known from the Ediacaran, but they are low in diversity: there are flanged, nested tubes (*Cloudina*; Grant, 1990; Hua et al., 2005), simple nested tubes (*Sinotubulites*; Chen et al., 2008), goblet-shaped fossils (*Namacalathus*; Grotzinger et al., 2000), and modular encrusting organisms (*Namapoikia*; Wood et al., 2002), all of which apparently disappear from the fossil record at the end of the Ediacaran (Amthor et al., 2003). Biomarkers recovered from sedimentary rocks suggest that demosponges were present by the latest Cryogenian (Love et al., 2009), and they may have produced spicules (Sperling et al., 2010), but there are very few specimens that have been identified as possible Cryogenian (Maloof et al., 2010b) or Ediacaran (Gehling and Rigby, 1996; Brasier et al., 1997; Reitner and Wörheide, 2002) sponge body fossils.

The anabaritids are among the earliest of the small shelly fossils to appear (Fig. 2A), and already may have been present in the terminal

Ediacaran (Knoll et al., 1995a; Brasier et al., 1996). Anabaritids are conical tubes, probably originally aragonitic, with prominent triradial symmetry; although their systematic position remains controversial, they have often been allied with cnidarians (see Kouchinsky et al., 2009). Later-appearing groups of tubular fossils include the phosphatic hyolithelminths (Fig. 2B) and aragonitic coleolids, the latter of which bear helically coiled ornamentation; their simple morphology hampers phylogenetic placement, although the former may be cnidarians (Vinn, 2006). The phosphatic carinacitiids and hexangulaconulariids may share affinities with the conulariids, probable scyphozoans (Conway Morris and Chen, 1992; Van Iten et al., 2010).

Another characteristic group of earliest Cambrian small shelly fossils are phosphatic spines termed protoconodonts (Fig. 2C), which are very similar in overall form, microstructure, and apparatus architecture to the grasping spines of modern chaetognaths (Szaniawski, 1982, 2002; Vannier et al., 2007). Protoconodonts would therefore demonstrate the emergence of macroscopic predation among animals.

Hyoliths are one of the most diverse and abundant groups of small shelly fossils. They are generally divided into two groups: the hyolithomorphs (Fig. 2D), which have a shell consisting of a conical conch, an operculum to cover the aperture of the conch, and two curving supports termed helens (Martí Mus and Bergström, 2005); and the orthothecimorphs (Fig. 2E), which lack helens and have less elaborate opercula and conchs than those of the hyolithomorphs (Malinky, 2009). Hyoliths have variously been considered to be a group of molluscs (Marek and Yochelson, 1976; Malinky and Yochelson, 2007) or a separate clade, possibly allied with the sipunculans (Runnegar et al., 1975; Kouchinsky, 2000). Although some orthothecimorphs are clearly related to hyolithomorphs, many Early Cambrian forms have such a simple morphology that they could well belong to separate groups (Malinky, 2009). There also are a variety of other conical fossils, such as *Cupitheca* (Fig. 2F), *Paragloborilus*, and *Neogloborilus*, that are not generally accepted as hyoliths and lack satisfactory placements elsewhere (Qian, 1989; Bengtson et al., 1990; Malinky and Skovsted, 2004; Li et al., 2007).

Many small shelly fossils do not represent the entire shell of an animal, but are instead isolated elements (sclerites) from a complex external skeleton (scleritome). Most of them remain problematic, since they are only known from disarticulated sclerites, but studies of their structure and microstructure have allowed several different groups of scleritome-bearing metazoans to be recognized. Prominent among these are the

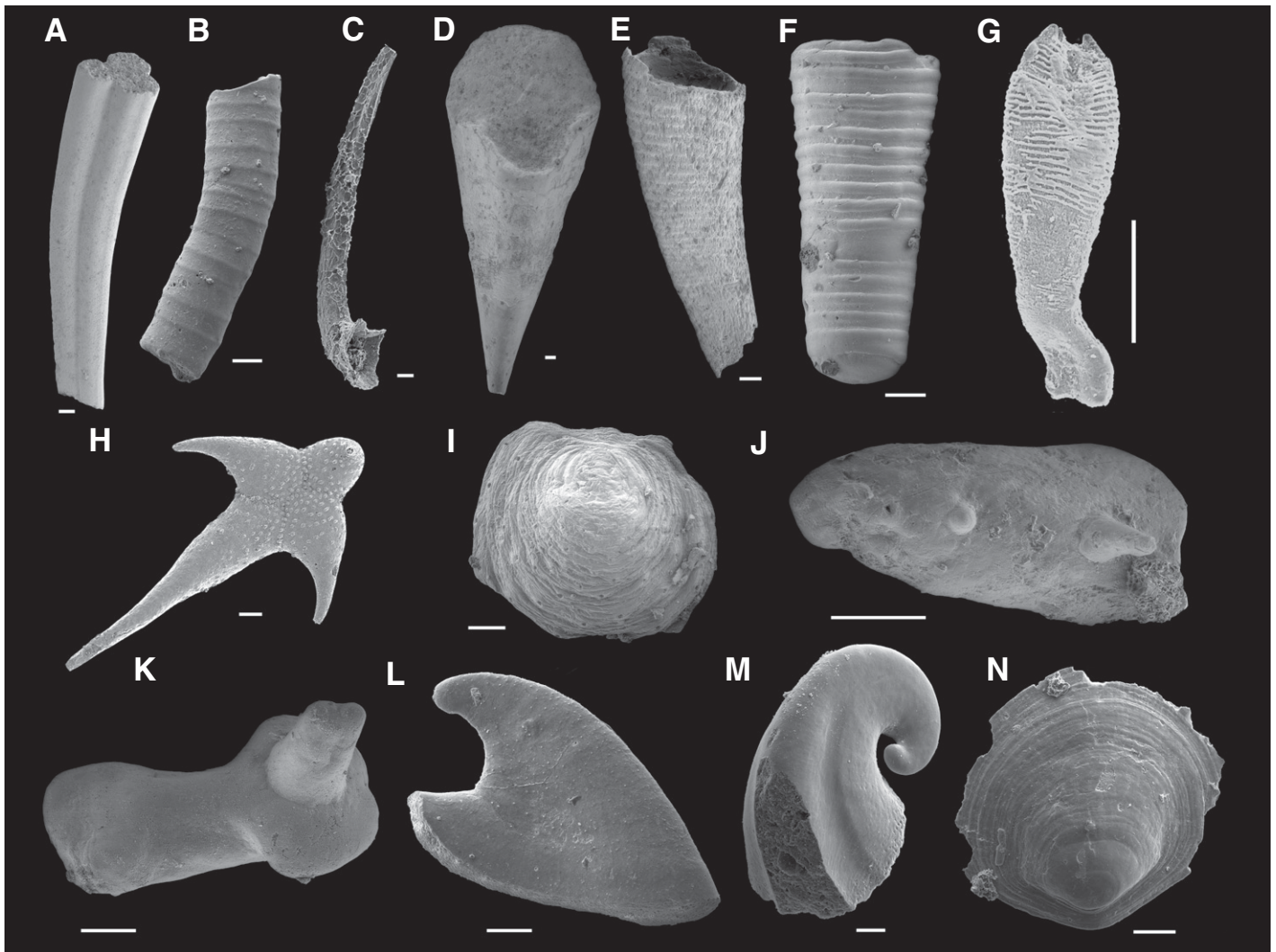


Figure 2. Cambrian small shelly fossils representing a variety of groups that first appear in the earliest Cambrian: (A) the anabaritid *Anabarites tripartitus*; (B) the hyolithelminth *Hyolithellus* sp.; (C) the protoconodont *Protohertzina unguiformis*; (D) a hyolithomorph hyolith; (E) the orthothecimorph hyolith *Conothecca brevica*; (F) the problematic tubular fossil *Cupitheca* sp.; (G) the coeloscleritophoran *Australohalkieria superstes*, a halkieriid; (H) the coeloscleritophoran *Archiasterella hirundo*, a chancelloriid; (I) the tommotiid *Micrina* sp.; (J) the paracarinachitid *Paracarinachites sinensis*; (K) the cambroclave *Cambroclavus fangxianensis*; (L) the mollusc *Anabarella simesi*; (M) the mollusc *Pelagiella deltoides*; (N) the cap-shaped fossil *Ocuranus finial*. All scale bars are 100 μm . (A) is from the Pestrotsvet Formation along the Dzhandara River, Siberia; (B) and (C) are from the Kuanchuanpu Formation at Shatan, Nanjiang, Sichuan, China; (D), (L), and (M) are from the Gowers Formation, Georgina Basin, Queensland, Australia; (E) and (K) are from the Xihaoping Member of the Dengying Formation at Xiaowan, Xixiang, Shaanxi, China; (F) is from the Parara Limestone, Horse Gully, South Australia; (G) is from the Monastery Creek Formation, Georgina Basin, Queensland, Australia; (H) and (I) are from the Parara Limestone, Currumulka Quarry, South Australia; (J) and (N) are from the Zhongyicun Member of the Zhujiqing Formation at Dailibaoqing, Xundian, Yunnan, China; (H) and (I) are from the Parara Limestone, Currumulka Quarry, South Australia. Image (A) is courtesy of Artem Kouchinsky and reprinted from Kouchinsky et al. (2009); (B) and (C) are courtesy of Michael Steiner and reprinted from Steiner et al. (2007) and Steiner et al. (2004a), respectively; (F) is courtesy of Chris Emerling; (G) is reprinted from Porter (2004b); (H) is reprinted from Porter (2008); (J) is courtesy of Marites Villarosa Garcia; (L), (M), and (N) are courtesy of Michael J. Vondrasco and are reprinted from Vondrasco et al. (2009, 2010).

coeloscleritophorans (Figs. 2G and 2H), which have hollow aragonitic sclerites (Bengtson and Missarzhevsky, 1981). Complete specimens representing different groups of coeloscleritophorans are known from Burgess Shale-type deposits, revealing that the chancelloriids were

sessile, radially symmetric, and superficially sponge-like (Bengtson and Hou, 2001; Janussen et al., 2002; Randell et al., 2005), while the halkieriids were bilaterally symmetric, slug-like animals (Conway Morris and Peel, 1995; Vinther and Nielsen, 2005). Their very different ap-

pearances have led many workers to conclude that the Coeloscleritophora is polyphyletic, but the similarity of their sclerites has led others to retain the group (Bengtson, 2005; Porter, 2008), as we do here. Less well understood coeloscleritophorans include the siphogonuchitids

(Qian and Bengtson, 1989; Conway Morris and Chapman, 1996) and sachtids (Bengtson et al., 1990).

Another major group of scleritome-bearing metazoans is the phosphatic tomotiids (Fig. 2I). Recent discoveries have allowed the partial reconstruction of several different tomotiids, showing that they range from forms with a bivalved shell to others with a tube covered with numerous irregular sclerites; their microstructure closely resembles that of linguliform brachiopods, and the tomotiids are probably stem-group brachiopods (Skovsted et al., 2008, 2009a, 2009b; Holmer et al., 2008; Balhasar et al., 2009; Kouchinsky et al., 2010).

A wide variety of other earliest Cambrian sclerites remain more enigmatic; these include the nail- or tack-shaped cambroclaves (Fig. 2K; Bengtson et al., 1990; Conway Morris and Chen, 1991; Conway Morris et al., 1997), rows of spine-bearing plates called paracarinachitids (Fig. 2J; Qian and Bengtson, 1989; Conway Morris and Chen, 1991), the phosphatic plates of *Tumuliduria* (Bengtson et al., 1987), and a variety of spine- or tooth-shaped fossils such as *Cyrtochites*, *Fomitchella*, *Kaiyangites*, *Rhombocorniculum*, and *Yunnanodus* (Bengtson, 1983; Qian and Bengtson, 1989; G. Li et al., 2003; Qian et al., 2004; Yao et al., 2005). Mobergellans are round phosphatic plates generally interpreted as opercula from a tube-like form of uncertain identity, although they have also been argued to be isolated sclerites or univalved limpet-like shells (Bengtson, 1968; Conway Morris and Chapman, 1997; Skovsted, 2003).

The most diverse group of small shelly fossils with clear affinities to an extant taxon is the molluscs (Figs. 2L and 2M). Most molluscs from the earliest Cambrian have been classified as helcionelloids, a group that ranges to the Ordovician and is characterized by univalved shells that range in shape from limpet-like caps to high cones to helically coiled forms; they probably include both epifaunal and shallow infaunal species (Gubanov and Peel, 2000). Long considered to be monoplacophorans, the systematic position of helcionelloids is unclear, and they may not be monophyletic; they have variously been considered as a paraphyletic stem group from which all other conchiferan molluscs are derived (Runnegar and Pojeta, 1974), as ancestral only to the cephalopods and rostroconchs (Peel, 1991), as early gastropods (Parkhaev, 2001, 2008), or as an entirely extinct group of early molluscs (Yochelson, 1978; Geyer, 1994). Asymmetrically coiled forms such as *Aldanella* and *Pelagiella* are superficially reminiscent of gastropods and have long been interpreted as such (Runnegar, 1981), but they also may be helcionelloids that have exaggerated the

asymmetry commonly seen in the more nearly planispirally coiled forms (Gubanov and Peel, 2000); they have also been interpreted as coiled “worm” tubes unrelated to molluscs (Bockelie and Yochelson, 1979).

A wide variety of low, cap-shaped shells that superficially resemble limpet-like molluscs are also present (referred to herein as “cap-shaped fossils”; Qian and Bengtson, 1989; Peel and Skovsted, 2005). Some of these may indeed represent univalved molluscs (Ponder et al., 2007), but others have been interpreted as isolated valves from the scleritome of a halkieriid or other coeloscleritophoran (Bengtson, 1992b; Conway Morris and Peel, 1995), isolated valves from a superficially brachiopod-like animal (Bengtson et al., 1990; Parkhaev, 1998), and isolated plates from a polyplacophoran (Fig. 2N; Vendrasco et al., 2009). Another problematic group that may be allied with molluscs is the stenotheccoids, which had a bivalved shell with bilaterally symmetric valves similar to those of brachiopods (Yochelson, 1969; Kouchinsky, 2001).

Sponge spicules have occasionally been reported from pre-trilobitic assemblages (Zhuravleva in Sokolov and Zhuravleva, 1983; Pel'man et al., 1990), as have rare fragments that have been interpreted as the remains of bivalved arthropods (Skovsted et al., 2006). Occasional phosphatized soft-bodied remains, most notably eggs and embryos, are also associated with the biomineralized small shelly fossils. A variety of spectacularly preserved embryos have been reported from the lowest Cambrian, including the probable cnidarian *Olivoides* (Yue and Bengtson, 1999), the ecdysozoan worm *Markuelia* (Donoghue et al., 2006a), and several unnamed forms, some of which may be from a segmented animal (Steiner et al., 2004b; Donoghue et al., 2006b).

Other Metazoan Body Fossils

Body fossils of animals larger than those that produced the small shelly fossils do not become widespread until the appearance of archaeocyaths in the Tommotian. Archaeocyaths were long considered problematic, but are now generally regarded as being sponge-grade metazoans (Rowland, 2001); they made calcitic cup-like structures and were probably filter feeders. Along with calcified microbes, archaeocyaths were important framework-builders of bioherms in the Tommotian of Siberia (Riding and Zhuravlev, 1995; Kruse et al., 1995). Archaeocyaths were restricted to the Siberian platform in the Tommotian, and did not spread elsewhere until the Atdabanian (Zhuravlev, 1986a). Other large, sessile, calcareous organisms appear in the Tommotian, often in association with archaeocyaths, includ-

ing radiocyaths (Zhuravlev, 1986b), which have variously been interpreted as sponges or calcareous algae, and the corallomorph *Cysticyathus*, interpreted as a cnidarian (Debrenne et al., 1990; Kruse et al., 1995).

Some of the animals recorded by small shelly fossils are also known from larger specimens. For example, there are several known occurrences of centimeter-scale helcionelloid molluscs (Dzik, 1991; Martí Mus et al., 2008), hyoliths (Orłowski and Waksmundzki, 1986), and larger calcareous tubular problematica and coleolids, some of which formed small biostromes (Landing, 1993). Other larger shelly fossils include brachiopods. Early brachiopods include *Khasagtina* from the Nemakit-Daldynian of Mongolia, interpreted as a kutorginid (Ushatinskaya, 1987), and the Tommotian paterinids *Aldanotreta* and *Cryptotreta* from Siberia (Laurie, 2000); the supposed Tommotian obolellid *Nochoroiella* (Grigor'eva et al., 1983) may not be a brachiopod (Popov and Holmer, 2000).

Soft-bodied animals have a poor fossil record during the earliest Cambrian. Most Ediacara-type fossils disappear by the end of the Ediacaran, but a few are now known to have survived into the basal Cambrian (e.g., Jensen et al., 1998). Burgess Shale-type deposits do not become important until the Atdabanian, with the Sirius Passet (northern Greenland) and Chengjiang (South China) biotas. The oldest known Burgess Shale-type deposits are from South China, in the Hetang Formation of Anhui Province (Xiao et al., 2005) and the lowermost Niutitang Formation of Guizhou and Hunan Provinces (Steiner et al., 1993, 2001; Mehl and Erdtmann, 1994; Zhao et al., 1999), all of uncertain Tommotian or Atdabanian age. These faunas are dominated by sponges, including hexactinellids and demosponges; those of the Niutitang Formation also include bivalved arthropods similar to *Perspicaris*. Finally, small organic-walled tubes called sabelliditids are common in lowermost Cambrian rocks (Urbanek and Mierzejewska, 1977; Ivantsov, 1990), and likely appear first during the Ediacaran Period; they have often been compared with tubes constructed by modern pogonophoran worms, but this assignment is unlikely.

Trace Fossils

Lowest Cambrian trace fossils offer a record of the evolution of macroscopic, primarily soft-bodied, animals. They are also among the few fossils to be found in siliciclastic rocks from this time, and consequently have been the focus of study in the hope that they could offer a means of biostratigraphic correlation (e.g., Crimes, 1987). Although a variety of metazoan traces

are known from the Ediacaran, they mostly represent very simple, typically unbranched horizontal traces formed at or very near the sediment surface (Jensen et al., 2006). Deeper burrowing does not become widespread until the appearance of treptichnids, which are now known from the uppermost Ediacaran (Jensen et al., 2000; Gehling et al., 2001). The first appearance of *Treptichnus pedum* (previously known as *Phycodes pedum* and sometimes called *Trichophycus pedum*) in the Chapel Island Formation at Fortune Head, Newfoundland, defines the global stratotype for the Ediacaran-Cambrian boundary (Brasier et al., 1994a; Landing, 1994) and broadly corresponds in age to the last appearance of the soft-bodied Ediacara biota (Seilacher, 1984; Brasier, 1996). Treptichnids consist of a series of short segments alternating in a zigzag-like pattern, probably representing a series of feeding and dwelling traces of a worm-like animal feeding on detritus on the sediment surface (Jensen, 1997; Dzik, 2005). These and other early deep burrows were not common enough to thoroughly mix the upper sediment layers. Unlike those of the rest of the Phanerozoic, earliest Cambrian silts at the sediment surface remained relatively firm, and there was a sharp sediment-water interface (Droser et al., 2002). Widespread microbial mats similar to those characteristic of Ediacaran and older seafloors persisted, and some trace fossils record animals grazing on these microbial mats (Dornbos et al., 2004; Weber et al., 2007). Bioturbation became much more intense in the Atdabanian (Droser and Bottjer, 1988); eventually this increase in bioturbation would result in the destruction of microbial mats and the production of a much soupy, water-rich layer at the sediment surface, in what has been termed the Cambrian substrate revolution (Bottjer et al., 2000). While the makers of most trace fossils from the earliest Cambrian remain unclear (although some workers have interpreted treptichnids and other traces such as *Didymaulichnus* as the products of priapulids or similar worms; Dzik, 2005; Vannier et al., 2010), a variety of arthropod scratch marks and resting traces are known from strata preceding the first trilobites in the upper part of the Lower Cambrian (Crimes, 1987; Weber and Zhu, 2003).

Nonmetazoan Fossils

A variety of nonmetazoan fossils also are known from the lowest Cambrian. Among protists, these include siliceous radiolarian-like fossils (Braun et al., 2007) and agglutinated tubes (*Platysolenites* and *Spirosolenites*) regarded as foraminiferans (McIlroy et al., 2001). Acritarch diversity is low at the beginning of the Cambrian, following the disappearance of the

Doushantuo-Pertatataka acritarchs during the Ediacaran. Acritarchs increase in both diversity (Knoll, 1994; Vidal and Moczyłowska-Vidal, 1997) and disparity (Huntley et al., 2006) through the Early Cambrian. It has been suggested that this diversification is a result of the appearance of metazoans capable of consuming plankton (Butterfield, 1997), reflecting the ecological principle that the introduction of predators can drive diversification of their prey (Stanley, 1973).

Calcified cyanobacteria (such as *Renalcis*, *Epiphyton*, and *Obruchuvella*) diversify through the earliest Cambrian (Riding, 2001), form bioherms in the Nemakit-Daldynian of Siberia (Luchinina, 1999) and Mongolia (Kruse et al., 1996) and thrombolites in the Tommotian of Morocco (Latham and Riding, 1990), and continue to be important framework builders in Tommotian archaeocyathan reefs (Riding and Zhuravlev, 1995; Kruse et al., 1995). Helically coiled probable cyanobacterial filaments are known from some small shelly fossil assemblages (Peel, 1988; Qian and Bengtson, 1989). Coccoidal and filamentous microfossils sometimes are preserved in chert together with acritarchs; some resemble cyanobacteria, but some tubular forms likely are not cyanobacterial (Yao et al., 2005; Dong et al., 2009).

A few compressions of possible macroscopic algae have been described from the Nemakit-Daldynian Yanjiahe Formation of the Yangtze Gorges area, Hubei Province, South China (Guo et al., 2008); they are accompanied by problematic conical and tubular fossils that may be metazoans. Vendotaenids are problematic fossils of possible algal or bacterial origin (Cohen et al., 2009), and are represented in the Nemakit-Daldynian by *Tyrasotaenia* (Gnilovskaya, 1985).

Chemostratigraphic Correlation

Carbon isotopes have proven useful for identifying the E-C boundary where sedimentary environments or lithologies are not conducive to the preservation of *Treptichnus pedum*. In numerous mixed carbonate-siliciclastic systems such as the Mackenzie Mountains, Canada (Narbonne et al., 1994); Death Valley, California (Corsetti and Hagadorn, 2000); the Olenek Uplift, northeastern Siberia (Fedonkin, 1985; Knoll et al., 1995a); the Dzabkhan basin, southwestern Mongolia (Brasier et al., 1996; but see Ragozina et al., 2008); and South China (Zhu et al., 2001b; Weber et al., 2007), the first appearance of *Treptichnus pedum* occurs just above a deep negative $\delta^{13}\text{C}_{\text{CaCO}_3}$ excursion (from 0‰ to 2‰ down to -4‰ to -7‰ and back again). In carbonate-dominated successions

that do not preserve *Treptichnus pedum*, such as Oman (Amthor et al., 2003; Bowring et al., 2007) and Morocco (Maloof et al., 2005), the E-C boundary has been identified using this marker carbon-isotope excursion (Amthor et al., 2003; Maloof et al., 2005). In Oman, weighted mean $^{206}\text{Pb}/^{238}\text{U}$ dates of 542.3 ± 0.2 Ma and 541.0 ± 0.2 Ma, below and during the $\delta^{13}\text{C}_{\text{CaCO}_3}$ excursion, respectively, constrain the age of the carbon isotope excursion (Bowring et al., 2007). These ages are broadly consistent with a recalculated weighted mean $^{206}\text{Pb}/^{238}\text{U}$ date of 540.61 ± 0.88 (see Appendix section A5) on a tuff unconformably below sediments containing the first *Treptichnus pedum* in the Nama basin of southern Namibia (Grotzinger et al., 1995). The negative $\delta^{13}\text{C}_{\text{CaCO}_3}$ anomaly occurs just after the last appearance of the calcified metazoan *Namacalathus* and *Cloudina* (Grotzinger et al., 2000; Amthor et al., 2003).

The $\delta^{13}\text{C}_{\text{CaCO}_3}$ records also help calibrate Nemakit-Daldynian time and locate the Nemakit-Daldynian-Tommotian boundary in sections that lack appropriate small shelly fossils or early archaeocyaths (Maloof et al., 2010a). Although isotope records may be truncated by stratigraphic hiatuses, the morphology of $\delta^{13}\text{C}_{\text{CaCO}_3}$ curves between hiatuses remains intact and may be compared from section to section. Furthermore, we document a monotonic decline in $^{87}\text{Sr}/^{86}\text{Sr}$ through the Nemakit-Daldynian and Tommotian that provides a unique test of the $\delta^{13}\text{C}_{\text{CaCO}_3}$ correlations. In the following section, we describe the geological setting of the key lowest Cambrian sites, and discuss the construction of an age model for the Nemakit-Daldynian through Atdabanian. The result is a U/Pb-calibrated age model that is based on $\delta^{13}\text{C}_{\text{CaCO}_3}$ and $^{87}\text{Sr}/^{86}\text{Sr}$ correlations, that is independent of fossil first appearances, and that we use to elucidate the evolution of small shelly fossils and the geochemistry of Early Cambrian oceans.

Geological Setting and Correlations of Key Lowest Cambrian Sites

Siberia, southwest Mongolia, and South China are the only locations with more or less continuous Nemakit-Daldynian to Atdabanian records of small shelly fossils and $\delta^{13}\text{C}_{\text{CaCO}_3}$. Morocco is the only location with an expanded Nemakit-Daldynian to Atdabanian record of U/Pb-calibrated $\delta^{13}\text{C}_{\text{CaCO}_3}$ and $^{87}\text{Sr}/^{86}\text{Sr}$. Stratigraphic section locations are depicted in approximate Early Cambrian (Fig. 3) and modern (Fig. 4) geographic coordinates. However, the plate reconstruction in Figure 3 should be considered tentative and almost certainly incorrect in detail (uncertainties and assumptions are described in Appendix section A8). In the following

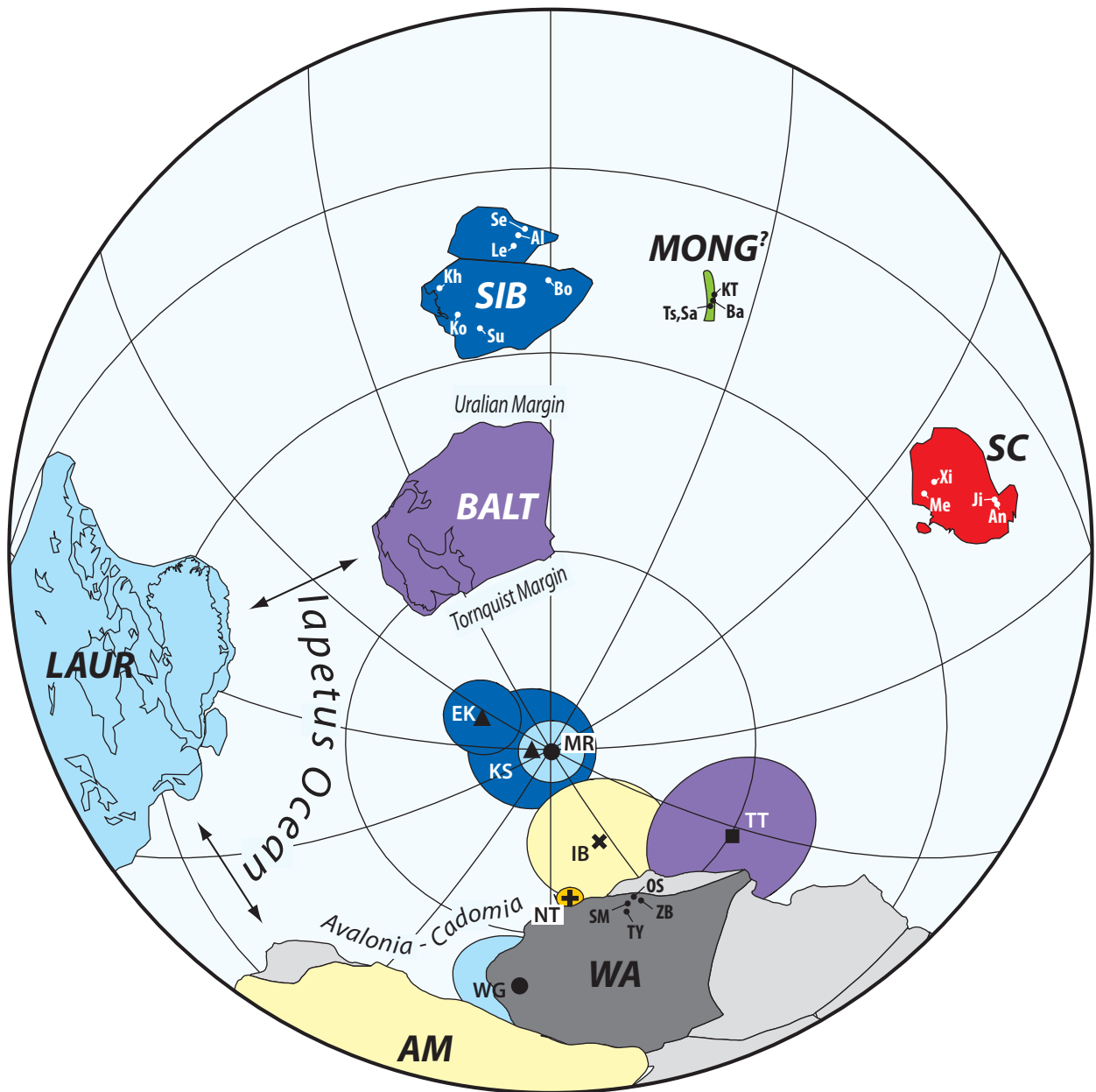


Figure 3. Tentative paleogeographic reconstruction for ca. 525 Ma (following Hoffman, 1991; Cawood and Pisarevsky, 2006; McCausland et al., 2007). Cratons are labeled: LAUR—Laurentia, AM—Amazonia, WA—West Africa, BALT—Baltica, SIB—Siberia, MONG—Mongolia, and SC—South China. West Gondwana is positioned such that the paleomagnetic pole from the 525 ± 5 Ma Itabaiana dikes (IB) of Amazonia (Trindade et al., 2006) is near the South Pole. Laurentia is positioned so that the paleomagnetic pole from the Mont Rigaud and Chatham-Grenville (MR) syenitic intrusions (McCausland et al., 2007) is near the South Pole. Siberia is located so that the 533–523 Ma paleomagnetic poles from the Kessyusa sandstone (KS) and Erkeket limestone (EK) from the Khorbusuonka section (Ko; Fig. 4B) are near the South Pole. Baltica is positioned so that the paleomagnetic pole from the 540–520 Ma Torneträsk Formation siltstone is near the South Pole. Mongolia and South China have no Lower Cambrian paleomagnetic constraints. Paleomagnetic poles (Table A1) and rotations (Table A2) can be found in Appendix section A8. Lower Cambrian stratigraphic sections are labeled: Morocco: ZB—Zawyat n’ Bougzoul, OS—Oued Sdas, TY—Talat n’ Yissi, SM—Sidi M’Sal; Siberia: Se—Selinde, Al—Aldan (Dvortsy and Ulakhan Sulugur), Le—Lena (Isit’ and Zhurinsky Mys), Kh—Khorbusuonka, Bo—Bol’shaya Kuonamka, Ko—Kotuikan, Su—Sukharikha; Mongolia: Ts,Sa—Tsagaan Gol and Salaany Gol, Ba—Bayan Gol, KT—Kvete-Tsakhir-Nuruu; and South China: Me—Meishucun, Xi—Xiaotan, An—Anjiahe, Ji—Jijiapo. This plate reconstruction is fraught with uncertainties and assumptions and only should be considered as a very general guide to the relative location of continents during the Early Cambrian (see Appendix section A8 for details).

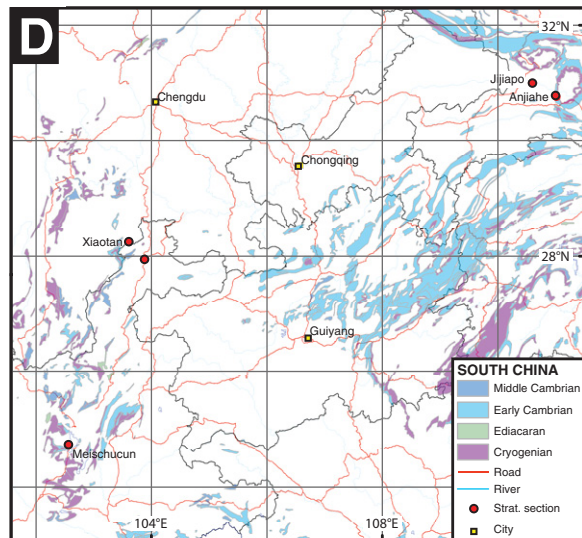
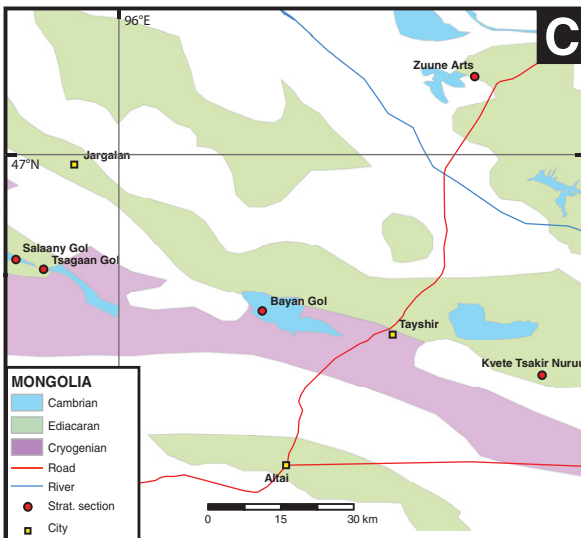
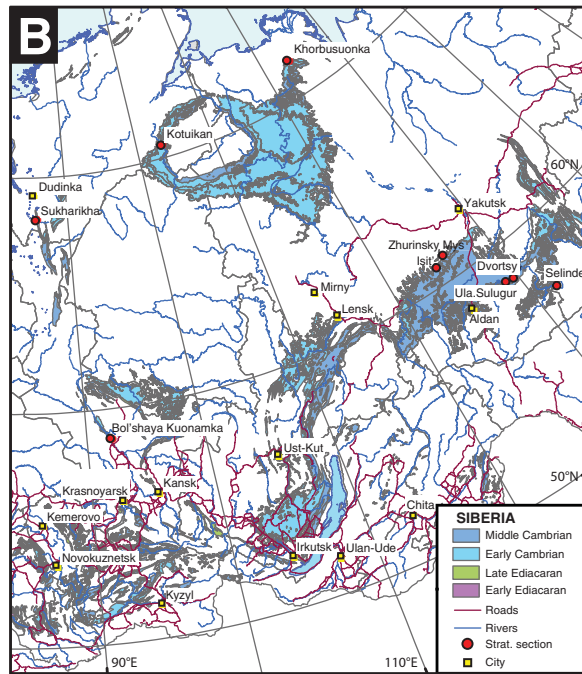
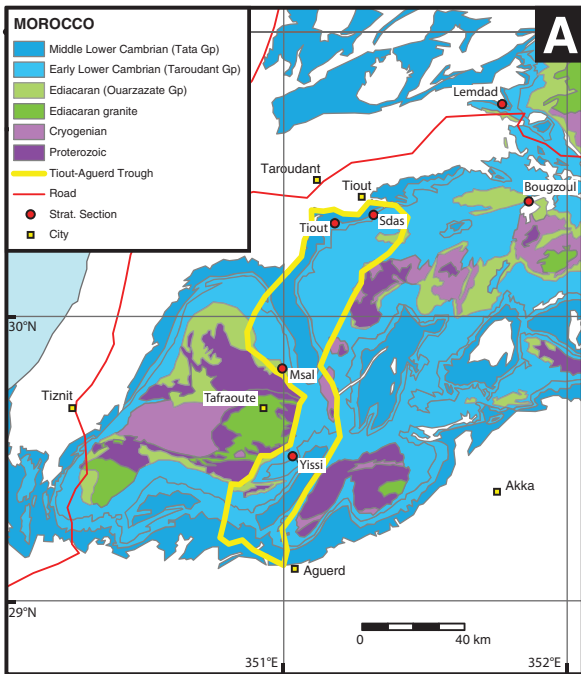
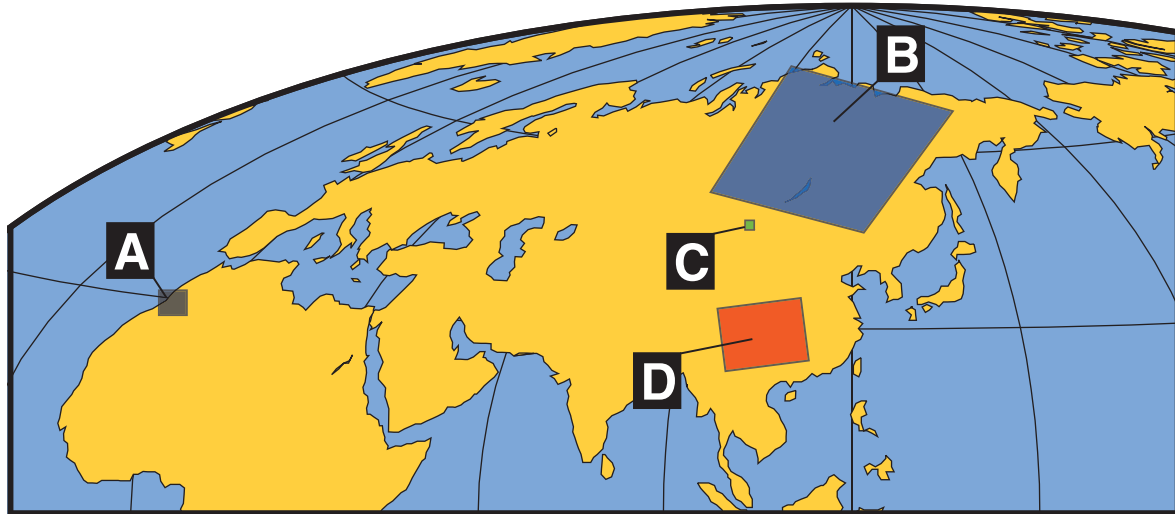


Figure 4. Geological maps for (A) Morocco (modified from Saadi et al., 1985); (B) Siberia (modified from Nalivkin, 1965); (C) Mongolia (modified from Terman, 1973), and (D) China (modified from Ma, 2004). Paleogeographic locations for these maps are depicted in Early Cambrian coordinates in Figure 3.

sections, we summarize the geological setting and basic correlation of each of the key lowest Cambrian sites that we use to construct the global age model.

Morocco

The western Anti-Atlas margin of Morocco (Fig. 4A) preserves the most expanded Lower Cambrian record of carbonates in the world. Following rift volcanism (577–560 Ma) and succeeding deposition of mixed carbonates and siliciclastics in isolated grabens, as much as 2.5 km of dominantly carbonate sediment accumulated on the thermally subsiding continental shelf (Malooof et al., 2005). Volcanic ash beds punctuate this stratigraphy, and four of these tuffs have yielded weighted mean $^{206}\text{Pb}/^{238}\text{U}$ isotope dilution–thermal ionization mass spectrometry (ID-TIMS) ages with ± 150 k.y. precision or better (e.g., Malooof et al., 2005, 2010a). With these four ashes (and a weighted mean $^{206}\text{Pb}/^{238}\text{U}$ age of 515.56 ± 1.16 Ma, recalculated [see Appendix section A5] from the published $^{207}\text{Pb}/^{206}\text{Pb}$ age of 517.0 ± 1.5 Ma [Landing et al., 1998] from an upper Tata Group ash in the Lemdad syncline; Fig. 4A) and $\delta^{13}\text{C}_{\text{CaCO}_3}$, $^{87}\text{Sr}/^{86}\text{Sr}$, and physical stratigraphy from the four most complete sections in the western Anti-Atlas (Fig. 4A), we built the age model depicted in Figure 5. The most uncertain calibration point is the E-C boundary itself, which, in the absence of *Treptichnus pedum*, is identified based on the morphology of the $\delta^{13}\text{C}_{\text{CaCO}_3}$ curve alone. The labeled $\delta^{13}\text{C}_{\text{CaCO}_3}$ peaks (1p–7p and II–IV) were named in Siberia (e.g., Kouchinsky et al., 2007). We interpret the lack of sequence boundaries and smooth $\delta^{13}\text{C}_{\text{CaCO}_3}$ record in Morocco to indicate that there are no significant intervals of missing time in the stratigraphic succession.

Unfortunately, the Nemakit-Daldynian and Tommotian Stages in Morocco, recorded in the Taroudant Group, are difficult to distinguish biostratigraphically. No small shelly fossils have been reported from the dolomitic Adoudonian Formation (Fig. 4A; 540–524 Ma in Fig. 5). Thrombolites in the upper half of the predominantly limestone Lie de Vin Formation (ca. 521 Ma in Fig. 5) contain calcified remains of cyanobacteria such as *Renalcis* (Latham and Riding, 1990), but no small shelly fossils or archaeocyaths have been found. The overlying limestone-dominated Tata Group (520–516 Ma) records a transition to more energetic marine

conditions than those found in the Taroudant Group (Geyer, 1989). The upper Igoudine Formation (ca. 519 Ma in Fig. 5) contains the oldest known skeletal fossils from Morocco and includes trilobites, archaeocyaths, brachiopods, and cancelloririids of Atdabanian age (Geyer and Landing, 1995).

Siberia

Across the Siberian Platform (Fig. 4B), upper Ediacaran and Cambrian sediments unconformably overlie a wide range of rocks of Proterozoic age. The location of the E-C boundary was interpreted to be constrained by a weighted mean $^{207}\text{Pb}/^{206}\text{Pb}$ ID-TIMS zircon date of 543.9 ± 0.24 Ma for a reworked volcanoclastic breccia near the base of the Nemakit-Daldynian at Khorbusuonka (Bowring et al., 1993). The zircons in this breccia have lost Pb, but for the most concordant grains, the $^{206}\text{Pb}/^{238}\text{U}$ dates are 542.8 ± 1.3 Ma, herein interpreted as the maximum age for the rock. This 542.8 ± 1.3 Ma date should be used when comparing this result to other $^{206}\text{Pb}/^{238}\text{U}$ dates in this paper. Excellent preservation of small shelly fossils in lowest Cambrian strata allows for a direct link between biostratigraphy and chemostratigraphy. As a result, the stage system for the Lower Cambrian on the Siberian Platform, where it is divided into the Nemakit-Daldynian, Tommotian, Atdabanian, Botomian, and Toyonian (Repina and Rozanov, 1992; Rozanov et al., 2008), has become widely used worldwide (Fig. 1).

The Tommotian was originally defined as encompassing all of the subtrilobitic Lower Cambrian (Rozanov and Missarzhevsky, 1966; Rozanov et al., 1969); the stratotype is on the Aldan River in the southeastern Siberian Platform, where its lower boundary is defined near the top of the Yudoma Formation at the level where archaeocyaths first appear together with a great diversity of small shelly fossils (Rozanov, 1984; Repina and Rozanov, 1992). The discovery that small shelly fossils appear more gradually in sections elsewhere in Siberia led to proposals for a pre-Tommotian stage, with broadly correlative strata being referred to as the Nemakit-Daldynian (see Khomentovskiy and Karlova, 1992) or Manykayan (Missarzhevsky, 1982, 1983) stages, based on type sections in the Anabar Uplift. Following designation of the global stratotype for the base of the Cambrian at Fortune Head in Newfound-

land (Brasier et al., 1994a; Landing, 1994), it generally has been accepted that the Nemakit-Daldynian is earliest Cambrian in age, although some workers would prefer to continue regarding the base of the Tommotian as the base of the Cambrian (most recently, Rozanov et al., 2008; Khomentovskiy, 2008).

Correlation of lowest Cambrian strata across the Siberian Platform has been hampered by lateral facies variations and unconformities of uncertain duration. Although a great deal of biostratigraphic work has been done on the lowest Cambrian of Siberia, the precise correlations of sections in different areas remain contentious (compare, for example, Val'kov, 1987; Missarzhevsky, 1989; Repina and Rozanov, 1992; Khomentovskiy and Karlova, 1992, 1993, 2002, 2005; Vasil'eva, 1998). Most authors do at least recognize a lower Nemakit-Daldynian interval characterized by anabaritids, protoconodonts, and coeloscleritophorans, followed by an upper Nemakit-Daldynian interval with a wider range of small shelly fossils, and then the Tommotian with a great variety of small shelly fossils accompanying the first appearance of archaeocyaths.

The base of the Tommotian is defined by an unconformity at the type sections at Dvortsy and Ulakhan Sulugur: the upper part of the Yudoma Formation is karsted, and the Tommotian fossils reported from these layers are in cavity fill deposited with the overlying Pestrotsvet Formation (see Khomentovskiy and Karlova, 1993, 2002). The duration of the hiatus below the Pestrotsvet Formation has been controversial; the sudden appearance of many taxa that appear more gradually in other sections suggests that it was relatively long (e.g., Knoll et al., 1995b; Kaufman et al., 1996). According to an alternative view, this hiatus was relatively short and the sudden appearance of many taxa reflects their migration from other parts of Siberia (Khomentovskiy and Karlova, 2002, 2005). Carbon isotope chemostratigraphy supports the presence of a long unconformity beneath the stratotype of the Tommotian, recorded elsewhere by strata in the northwestern Siberian Platform (Kouchinsky et al., 2007), the western and eastern Anabar Uplift (Knoll et al., 1995b; Kaufman et al., 1996; Kouchinsky et al., 2001), and the southeastern Siberian Platform (Kouchinsky et al., 2005).

Malooof et al. (2005) mapped the carbon isotope records from Ulakhan Sulugur (Brasier et al., 1993) and Dvortsy (Magaritz et al., 1991) onto the $\delta^{13}\text{C}_{\text{CaCO}_3}$ curve from Morocco and located the Nemakit-Daldynian–Tommotian boundary at the zero crossing in the record of declining $\delta^{13}\text{C}_{\text{CaCO}_3}$ after the last positive anomaly (6p; Fig. 5), where Malooof et al. (2010a)

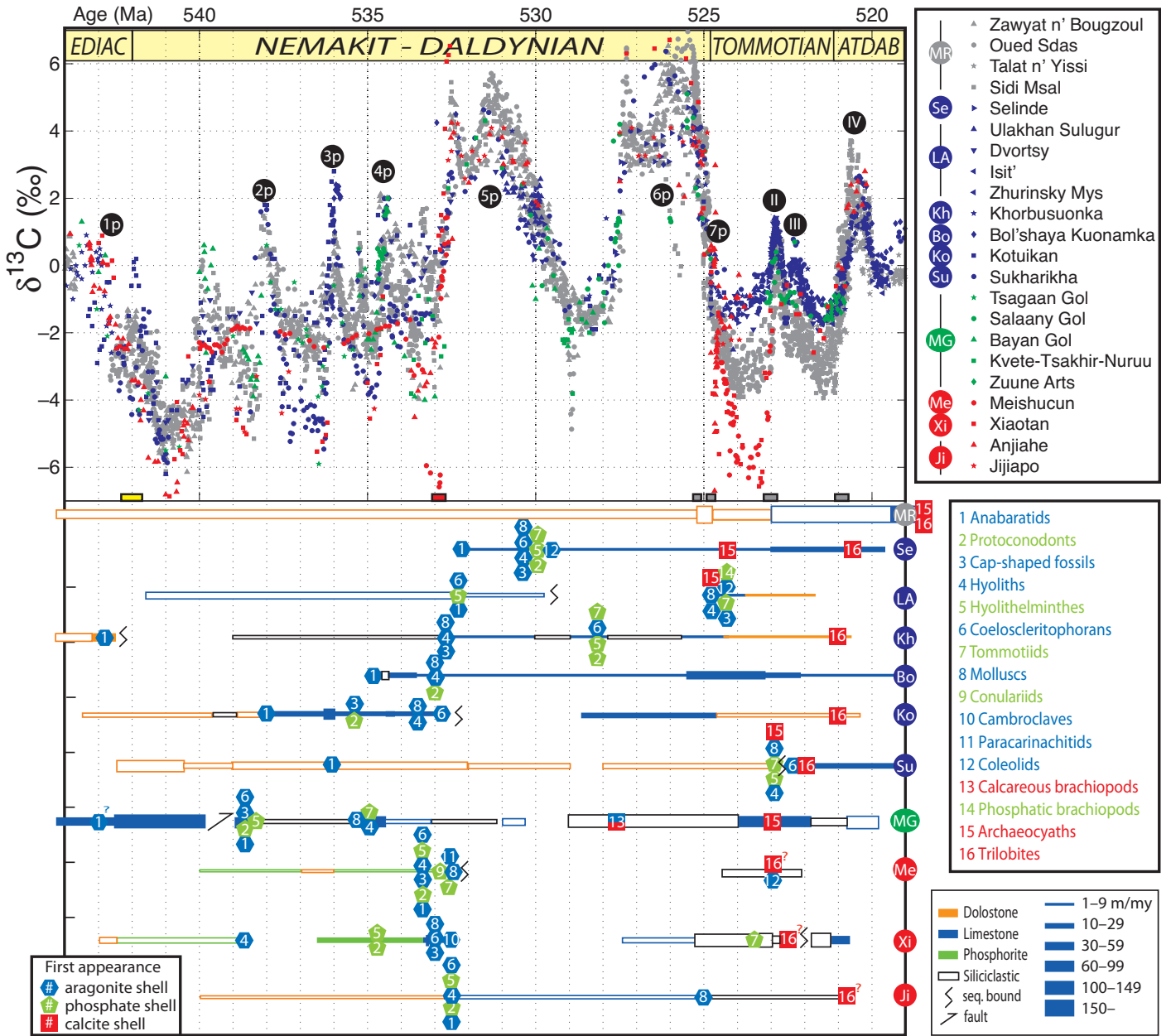


Figure 5. Carbon isotopes and fossil ranges plotted against age. The age model for the Moroccan data (gray shapes: Zawyat n' Bougzoul, Oued Sdas, and Talat n' Yissi [Maloof et al., 2005], and Sidi M'sal [Maloof et al., 2010a]) assumes constant sediment accumulation rates between U/Pb zircon tie points. U/Pb tie points are illustrated as gray (Morocco: Maloof et al., 2005, 2010a), red (China: Brooks et al., 2006), and yellow (Oman: Bowring et al., 2007) rectangles, the centers and widths of which represent the ages and 2σ error bars, respectively, of each analysis. Each group of colored shapes represents $\delta^{13}\text{C}_{\text{CaCO}_3}$ data from a different stratigraphic section. Siberia (blue)—Selinde River (Kouchinsky et al., 2005), Ulakhan Sulugur (Aldan River; Brasier et al., 1993), Dvortsy (Aldan River; Magaritz et al., 1986; Brasier et al., 1993), Isit' and Zhurinsky Mys (Lena River; Magaritz et al., 1991; Kirschvink et al., 1991), Khorbusuonka River (Olenek Uplift; Knoll et al., 1995a), Bol'shaya Kuonamka (Anabar Uplift; Kouchinsky et al., 2001), Kotuikan River (Anabar Uplift; Knoll et al., 1995b; Kaufman et al., 1996), Sukharikha River (Kouchinsky et al., 2007). Mongolia (green)—Tsagaan Gol, Salaany Gol, Bayan Gol, Kvete-Tsakhir-Nuruu, and Zuune Arts (Brasier et al., 1996). China (red)—Meishucun (Brasier et al., 1990), Xiaotan (Zhou et al., 1997), Anjiahe (Ishikawa et al., 2008), and Jijiapo (M. Zhu, 2010, personal commun.). The labeled $\delta^{13}\text{C}_{\text{CaCO}_3}$ peaks (1p–7p and II–IV) were named in Siberia (e.g., Kouchinsky et al., 2007). Sections for which both $\delta^{13}\text{C}_{\text{CaCO}_3}$ and biostratigraphy are available are plotted below, with line-width representing sedimentation rates inferred from the age model in meters per million years (m/m.y.), and line color representing dominant lithology (dolostone, limestone, phosphorite, or mixed siliciclastics). The lines are filled if they represent a fossiliferous interval, and they are hollow if they are unfossiliferous. Blue hexagons, green pentagons, and red squares depict the first appearance of organisms producing aragonite, apatite, and calcite skeletons, respectively.

reported an ash with a weighted mean $^{206}\text{Pb}/^{238}\text{U}$ date of 524.837 ± 0.092 Ma. This placement is consistent with combined biostratigraphic and $\delta^{13}\text{C}_{\text{CaCO}_3}$ data from the rest of Siberia (Brasier et al., 1993; Khomentovsky and Karlova, 1993; Knoll et al., 1995a, 1995b; Rowland et al., 1998; Kouchinsky et al., 2001, 2007), where the first appearance of archaeocyaths occurs stratigraphically above the last large positive $\delta^{13}\text{C}_{\text{CaCO}_3}$ anomaly (6p; Fig. 5). (Selinde may be an exception to this pattern, where archaeocyath debris appears to occur stratigraphically below the last large positive $\delta^{13}\text{C}_{\text{CaCO}_3}$ anomaly; Kouchinsky et al., 2005.) In particular, the most complete Siberian record, from the Sukharikha River (Fig. 4B), matches the Nemakit-Daldynian to Atdabanian $\delta^{13}\text{C}_{\text{CaCO}_3}$ curve of Morocco peak-for-peak (Malooof et al., 2005; Kouchinsky et al., 2007; Fig. 5). This calibration places the ND-T boundary at a recognizable and radiometrically dated $\delta^{13}\text{C}_{\text{CaCO}_3}$ shift and constrains the duration of the Nemakit-Daldynian Stage to 17 m.y.

Mongolia

The Dzabkhan basin of southwestern Mongolia (Fig. 4C) was formed on the margins of a ribbon continent that experienced andesitic volcanism at ca. 800 Ma (Badarch et al., 2002), prior to rifting from southern Siberia in the earliest Cryogenian (Kuzmichev et al., 2001). Platformal carbonates and siliciclastics of the Tsagaan Oloom Formation (1500 m thick) accumulated during Cryogenian and Ediacaran rifting and subsequent thermal subsidence (Macdonald et al., 2009). Diamictites in the succession have been interpreted as glacial in origin (Lindsay et al., 1996b), and recent mapping and $\delta^{13}\text{C}_{\text{CaCO}_3}$ chemostratigraphy correlated the younger of two glacial deposits to the Marinoan ice age (Macdonald et al., 2009), which ended ca. 635 Ma (Hoffmann et al., 2004; Condon et al., 2005). A significant Ediacaran hiatus preceded obduction of ca. 570 Ma ophiolites to the south of the Dzabkhan basin (Khain et al., 2003), which suggests there was south-dipping subduction (in present-day coordinates) that led to rapid accumulation of the upper Tsagaan Oloom Formation (Zuune Arts Member) in a flexural basin (Macdonald et al., 2009). The Ediacaran-Cambrian boundary has been placed in the uppermost Tsagaan Oloom Formation where $\delta^{13}\text{C}_{\text{CaCO}_3}$ descends from 1‰ (1p; Fig. 5) to a nadir of -6‰ (W; Brasier et al., 1996), and anabaritids and small burrows first appear (Khomentovsky and Gibsher, 1996) (Fig. 5).

The overlying Bayan Gol and Salaany Gol Formations (1000–1500 m thick) contain a diversity of Lower Cambrian small shelly fossils (Voronin et al., 1982; Esakova and Zhegallo, 1996) and consist of stacked sequences

of fine siliciclastics and laminated limestones shoaling upward into platformal carbonates (Lindsay et al., 1996a). We correlate the E (Salaany Gol, Section 2, Unit 7; Bayan Gol, Section 3B, Unit 21; and Kvote-Tsakhir-Nuruu, Section 4, Unit 7) and F (Salaany Gol, Section 2, Unit 11/12) 4‰–5‰ $\delta^{13}\text{C}_{\text{CaCO}_3}$ peaks of Brasier et al. (1996) in the upper Bayan Gol Formation with the pair of terminal Nemakit-Daldynian positive $\delta^{13}\text{C}_{\text{CaCO}_3}$ excursions, 5p and 6p, respectively (Fig. 5).

China

The Yangtze Platform of South China (Fig. 4D) began as a rifted margin during the breakup of Rodinia, with ca. 820 to ca. 780 Ma bimodal volcanic rocks flooring the basin (Li, 1998; Z. Li et al., 2003). The overlying Cryogenian succession includes two glacial deposits and is capped by the Doushantuo Formation, the base of which has a weighted mean $^{206}\text{Pb}/^{238}\text{U}$ ID-TIMS zircon age of 635.2 ± 0.6 Ma (Condon et al., 2005). The upper Doushantuo Formation has a weighted mean $^{206}\text{Pb}/^{238}\text{U}$ ID-TIMS zircon age of 551.1 ± 0.7 Ma (Condon et al., 2005), and is overlain by uppermost Ediacaran recrystallized dolostones of the Dengying Formation. The cause of slow but long-lived subsidence during Ediacaran–Cambrian time on the Yangtze Platform is poorly understood—the entire Lower Cambrian succession is usually contained within 120 m of condensed, phosphatic dolomites and argillites.

In South China, the lowest Cambrian is referred to as the Meishucunian Stage (Qian, 1977), with trilobites first appearing in the overlying Qiongzhusian Stage. The biostratigraphy of the Meishucunian recently has been revised (Qian et al., 2001; Steiner et al., 2007). The lowermost part of the Meishucunian is dominated by anabaritids and protoconodonts, and a correlation with the lower Nemakit-Daldynian has generally been accepted; higher zones in the Meishucunian have been more difficult to correlate (Qian and Bengtson, 1989). Recent work has favored the view that the Meishucunian includes equivalents to both the Nemakit-Daldynian and Tommotian (Steiner et al., 2007). As trilobites first appear at the base of the Atdabanian in Siberia and the base of the Qiongzhusian in South China, these levels often have been regarded as correlative, although the correctness of this interpretation remains undemonstrated; different correlations suggest that the base of the Qiongzhusian is above (Steiner et al., 2007) or below (Qian et al., 2001) the base of the Atdabanian.

Some workers have attempted to define the E-C boundary in South China by the stratigraphically highest negative $\delta^{13}\text{C}_{\text{CaCO}_3}$ excursion below the first appearance of *Treptichnus pedum*

and small shelly fossils, but even this placement has been controversial (Luo et al., 1991; Brasier et al., 1990; Zhang et al., 1997; Shen and Schidlowski, 2000; Zhu et al., 2001a). Further complicating basinwide and global correlations, the lower Nemakit-Daldynian (542–533 Ma) of South China is not dominated by the 1‰–3‰ positive $\delta^{13}\text{C}_{\text{CaCO}_3}$ excursions with frequencies of 0.5–1 m.y. that are so characteristic of Morocco, Siberia, and Mongolia (Fig. 5). The most distinctive Nemakit-Daldynian $\delta^{13}\text{C}_{\text{CaCO}_3}$ tie point in China is the first shift toward $\geq +4\%$ values (peak 5p; Fig. 5). This shift is well developed at Xiaotan (Zhou et al., 1997), Anjiahe (Ishikawa et al., 2008), and Jijiapo (M. Zhu, 2010, personal commun.), and the beginning of the shift is pinned at Meishucun (Brasier et al., 1990) by a tuff from Bed 5 that has a weighted mean $^{206}\text{Pb}/^{238}\text{U}$ ID-TIMS zircon age of ca. 533 Ma (Brooks et al., 2006; see also Compston et al., 2008; Jenkins et al., 2002) (Fig. 5). This Bed 5 tuff provides the best estimate for the durations of the pair of upper Nemakit-Daldynian positive $\delta^{13}\text{C}_{\text{CaCO}_3}$ excursions.

RESULTS

Small Shelly Fossils

One surprising result from Figure 5 (also see Fig. 6) is evidence for early appearances of calcareous brachiopods, archaeocyaths, and trilobites. Calcareous brachiopods are thought to have appeared in the mid-Tommotian, after the appearance of phosphatic brachiopods (Ushatinskaya, 2001, 2008), but our age model suggests that *Khasagtina*, accepted as an early calcareous brachiopod of possible kutorginid affinity (Ushatinskaya, 1987; Bengtson, 1992a; Popov and Williams, 2000), comes from rocks that are late Nemakit-Daldynian in age, ca. 528 Ma (Ushatinskaya, 1987). (Note that there is conflicting evidence regarding kutorginid brachiopod mineralogy; some may have had a partially aragonitic shell [James and Klappa, 1983]. The mineralogy of *Khasagtina* is not known.) Evidence for Nemakit-Daldynian archaeocyaths is more questionable, and is based on fragments of archaeocyaths reported from Selinde in rocks inferred by our age model to be ca. 530 Ma (2.7 m and 5 m above the base of the Pestrotsvet Formation; Korshunov et al., 1969; Khomentovsky and Karlova, 2002). However, specimens are not illustrated in those reports, making evaluation difficult, and other detailed stratigraphic studies place the first appearance of archaeocyaths in much higher rocks (21 m above the base of the Pestrotsvet Formation, inferred by our age model to be ca. 525 Ma), suggesting the earlier reports may have been in error (Voronova et al., 1983; Repina et al., 1988; Kouchinsky

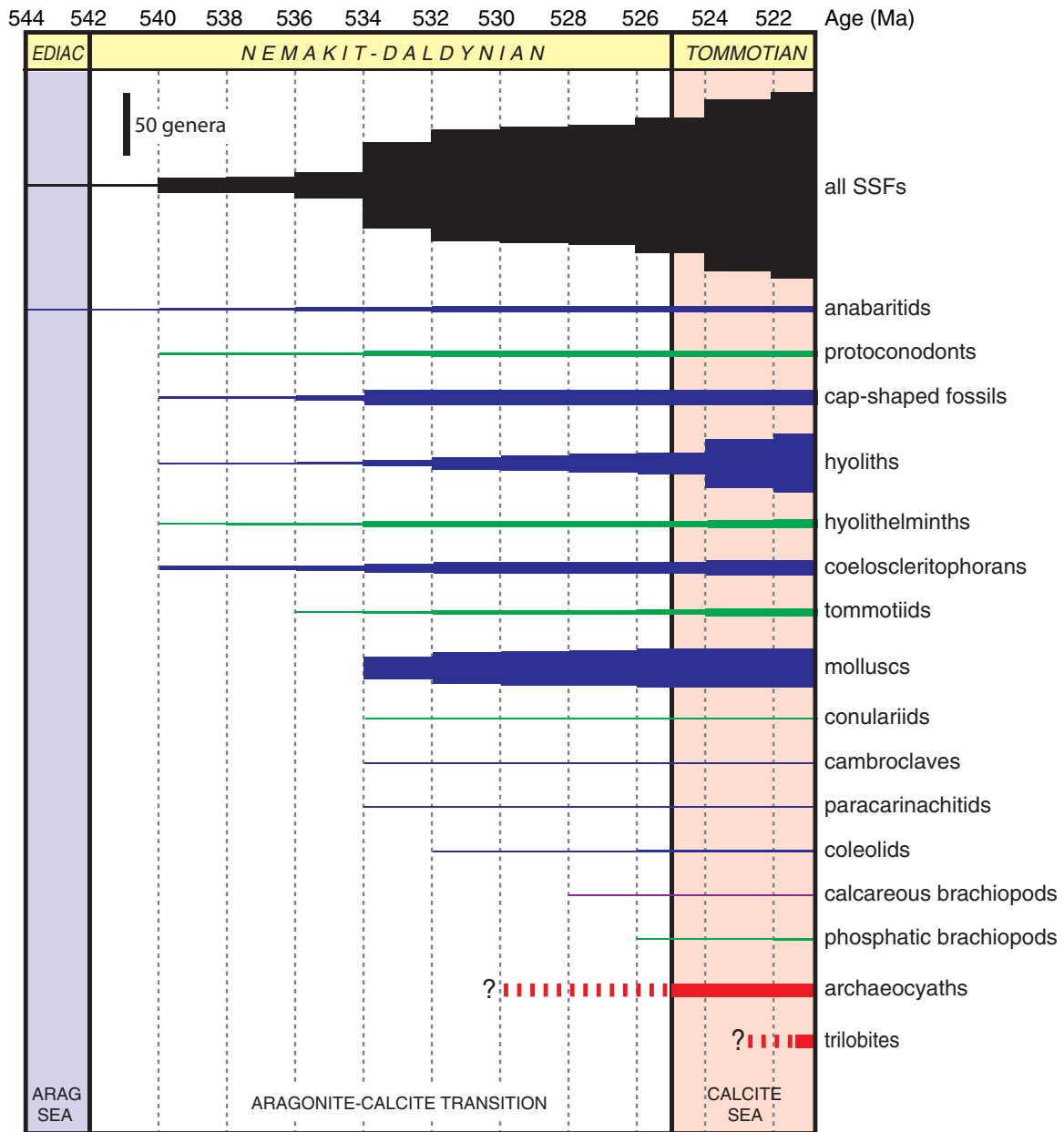


Figure 6. The timing of animal appearances in the earliest Cambrian and temporal constraints on aragonite and calcite seas. Spindles show the total number of small shelly fossil (SSF) genera that have appeared by a particular time (i.e., the number of genera that appear in older time bins plus the number of new genera); they do not indicate standing diversity. Archaeocyaths and trilobites are not represented by spindle diagrams; only their presence or absence is shown. Colors indicate mineralogy of skeletons: blue—aragonitic; green—phosphatic; red—calcitic; purple (calcareous brachiopods)—either calcitic or aragonitic. (Note that although we depict them here as distinct, recent evidence suggests that the shells of calcareous and phosphatic brachiopods are homologous with those of tommotiids [Skovsted et al., 2008; Balthasar et al., 2009].) See Figures A2–A4 for more details of genus occurrence data. Constraints on aragonite and calcite seas are from Mg/Ca in fluid inclusions (see Porter, 2007, 2010, and references cited therein) and are consistent with the $^{87}\text{Sr}/^{86}\text{Sr}$ record (Fig. 9). The timing of the aragonite-calcite transition in the Nemakit-Daldynian is not well constrained and could have occurred at any time between 542 Ma and 525 Ma.

et al., 2005). Although the mid-Tommotian age for trilobites from the Meishucun and Xiaotan sections reflects the best fit between the Chinese and Moroccan $\delta^{13}\text{C}_{\text{CaCO}_3}$ curves, this fit is poorly constrained, and the first appearance of trilobites in China could be much younger. However, the age constraints on trilobites from Sukharikha are much better; the fit between $\delta^{13}\text{C}$ curves from Sukharikha and Morocco has almost no mismatch (Fig. 5), and the rocks in which the trilobites occur correlate with strata from Morocco that are radiometrically constrained to be older than 520.93 ± 0.14 Ma and younger than 522.85 ± 0.22 Ma (Maloof et al., 2010a). Interestingly, archaeocyaths typical of Atdabanian strata elsewhere also appear at this horizon, suggesting a mismatch between biostratigraphic and chemostratigraphic boundaries (Kouchinsky et al., 2007).

Figure 6 summarizes the first appearance data of the groups highlighted in Figure 5, color-coded according to skeletal mineralogy. A factor of particular note is the sequence of mineral acquisition. The first taxa to appear are either aragonitic or phosphatic; the first calcitic taxa do not appear until either the late Nemakit-Daldynian or the beginning of the Tommotian (depending on the original mineralogy of the calcareous brachiopod *Khasagtina* and the first appearance of archaeocyaths at Selinde). No new acquisitions of aragonitic skeletons occur after the Nemakit-Daldynian until the appearance of the kilbuchophyllid corals in the Ordovician and scleractinian corals in the Triassic (Porter, 2010). The sequence of first appearances of aragonitic and calcitic taxa shown in Figure 6 also is observed within each section, suggesting that it is a relatively robust pattern. As shown in Figure 5, all aragonitic taxa appear either before or at the same time as calcitic taxa. In combination with evidence that seawater chemistry favored aragonite precipitation during the late Precambrian and favored calcite precipitation during the Tommotian (Porter, 2007; see section “Strontium”; Fig. 6), the pattern shown in Figures 5 and 6 supports the hypothesis that carbonate skeletal mineralogy is determined by the chemistry of seawater at the time carbonate skeletons first evolve in a clade (Porter, 2007, 2010; Zhuravlev and Wood, 2008). Although several phosphatic groups are known to appear later in the Early Cambrian (e.g., the problematic *Mobergella*, *Tumulduria*, and *Rhombocorniculum* in the Tommotian and bradoriids and *Microdictyon* in the Atdabanian), the clustered appearance of important Early Cambrian phosphatic biomineralizers may be meaningful, perhaps reflecting seawater chemistry responsible for widespread phosphogenesis at this time (e.g., Cook and Shergold, 1984).

Another factor of note in Figure 6 is the pattern of first appearances of small shelly fossil taxa. It is important to emphasize that the thickness of each segment in the spindles shown in Figure 6 does not indicate standing diversity; rather, it records the total number of genera that had appeared by the indicated time bin, calculated as the number of genera that appeared in earlier time bins plus the number of new genera that appear at that time. Thus, the spindles represent cumulative first appearances; they do not take into account extinctions, which are difficult to infer from our database. Because a taxon's time of origin always predates its appearance in the fossil record, the cumulative number of first appearances shown in Figure 6 should be understood as a minimum estimate: we can state how many small shelly fossil genera must have evolved by a certain time, but the real number may be much higher. A number of notable patterns emerge from these data. First, the major groups of small shelly fossils (anabaritids, protoconodonts, etc.) appear early: five are present by 540 Ma, and all except the coleolids appear by 532 Ma. This proliferation of higher taxa seems to outpace proliferation of genera within each taxon, consistent with the observation (see section “Introduction”) that disparity reaches its peak early in a group's history (although small shelly fossils are a polyphyletic assemblage). Second, although outpaced by the proliferation of higher taxa, small shelly fossil genera do appear quite early as well, with 46% of the small shelly fossil taxa known from Nemakit-Daldynian and Tommotian sections studied here appearing by 534–532 Ma, and 72% appearing by 526–524 Ma. This result suggests a gradual unfolding of diversity through the Nemakit-Daldynian (Brasier et al., 1996; Knoll et al., 1995a), rather than a burst at or just before the Tommotian boundary. Finally, Figure 6 indicates that the dominant contributors to small shelly fossil diversity are molluscs and hyoliths, with more minor contributions from cap-shaped fossils and coelocleritophorans. If these four groups are closely related (Marek and Yochelson, 1976; Bengtson, 1992b; Vinther and Nielsen, 2005), then the Nemakit-Daldynian and Tommotian diversification of small shelly fossils predominantly reflects the radiation of a single clade.

Figure 7 shows the number of small shelly fossil genera that first appear in each time bin, for all sections combined (global data) and for different subsets of sections (each region by itself or all sections but one). The global data suggest several pulses of fossil first appearances: a pulse (pulse_{eND}) between 540 and 538 Ma, a pulse (pulse_{mND}) between 534 and 530 Ma, and a pulse (pulse_r) between 524 and 522 Ma. Pulse_{eND} appears to be recorded

primarily in Mongolia and could reflect local preservational conditions within the Bayan Gol section. In contrast, pulse_{mND} and pulse_r appear to be insensitive to the removal of any particular section and are recorded in both China and Siberia (although pulse_{mND} is shifted later in Siberia). These pulses may reflect a global preservational bias (e.g., the effects of eustasy or ocean geochemistry), real pulses in diversification, or perhaps both (cf. Peters, 2005).

Isotopes and Trace Elements

So far, we only have considered $\delta^{13}\text{C}_{\text{CaCO}_3}$ as a tool to generate a fossil-independent age model within which the paleontological data from Siberia, Mongolia, and China can be interpreted (Fig. 5). This analysis contains the implicit assumption that $\delta^{13}\text{C}_{\text{CaCO}_3}$ in platform carbonates records a global signal. Workers frequently call upon the observation that $\delta^{13}\text{C}_{\text{CaCO}_3}$ time series may be matched peak-for-peak between separate continents as the strongest evidence for a global signal (e.g., Halverson et al., 2005; Maloof et al., 2005; Macdonald et al., 2009). However, synchronous $\delta^{13}\text{C}_{\text{CaCO}_3}$ signals in globally distributed platform carbonates may not necessarily reflect a change in global ocean dissolved inorganic carbon (DIC). For example, global processes such as climate and sea-level change may affect the distribution of mineralogies and the depositional and diagenetic environments that control $\delta^{13}\text{C}_{\text{CaCO}_3}$ on shallow-water carbonate platforms, so that some changes in platform $\delta^{13}\text{C}_{\text{CaCO}_3}$ do not mimic changes in the $\delta^{13}\text{C}$ of open-ocean DIC (Swart, 2008). Along similar lines, Hayes and Waldbauer (2006) proposed that temporal changes in the global importance of diagenetic reactions (e.g., methanogenesis) in sediments could produce globally similar patterns of local alteration. We consider this assumption extensively in Appendix section A9, and conclude that the dominant $\delta^{13}\text{C}_{\text{CaCO}_3}$ signal recorded in Lower Cambrian carbonate platform sediments primarily reflects changes in the isotopic composition of global DIC.

Carbonate Carbon

The $\delta^{13}\text{C}_{\text{CaCO}_3}$ chemostratigraphies of Morocco, Siberia, Mongolia, and China depict a superposition of $\delta^{13}\text{C}_{\text{CaCO}_3}$ oscillations with different characteristic periods and amplitudes. High-frequency signals with periods $\leq 10^5$ yr and amplitudes of 1‰–3‰ are present as regionally and often globally reproducible signals between 542 and 533 Ma, and as globally well-defined excursions at other times, such as the negative spike at 529 Ma (Fig. 5). Even higher-order variability of <1‰ amplitude may be present, but the sampling density is too coarse to

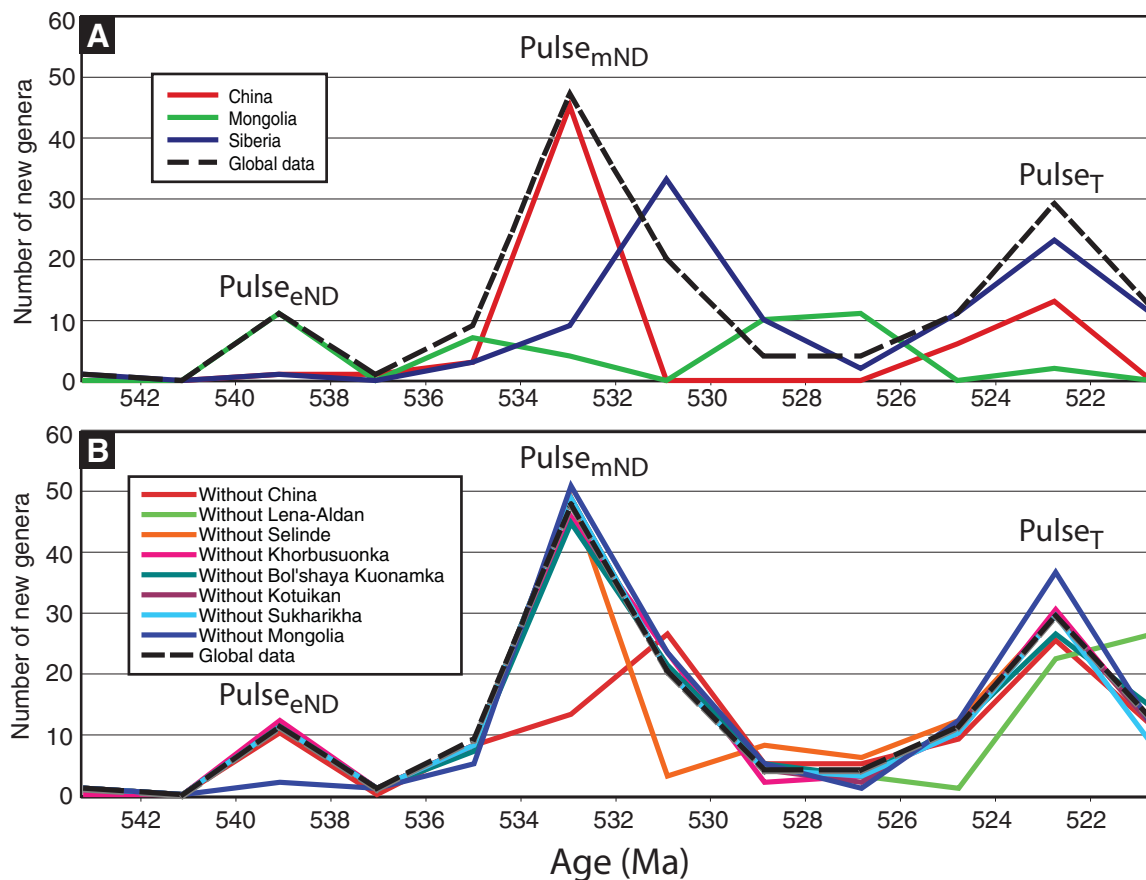


Figure 7. Number of new genera appearing in each 2 m.y. time bin calculated for (A) all sections (global data) and for each region, and (B) all sections except one (as indicated).

determine whether or not this variability reflects temporally coherent oscillations. The $\delta^{13}\text{C}_{\text{CaCO}_3}$ variations of substantially longer period (4–7 m.y.) and larger amplitude (8‰–11‰) dominate the middle to upper Nemakit-Daldynian, while moderate-frequency oscillations with periods of $\sim 10^6$ yr and amplitudes of 2‰–4‰ characterize the Tommotian–Atdabanian.

From a subset of the same carbonate samples that we used to generate the $\delta^{13}\text{C}_{\text{CaCO}_3}$ chemostratigraphy, we develop $\delta^{13}\text{C}_{\text{org}}$, $^{87}\text{Sr}/^{86}\text{Sr}$, uranium, and vanadium time series. In the following paragraphs, we document these additional time series and interpret them in the context of the $\delta^{13}\text{C}_{\text{CaCO}_3}$ and paleobiological records.

Organic Carbon

Throughout most of the Phanerozoic Eon, paired records of carbonate carbon ($\delta^{13}\text{C}_{\text{CaCO}_3}$) and coeval bulk organic carbon ($\delta^{13}\text{C}_{\text{org}}$) suggest a model in which the organic carbon in marine sediments is derived and isotopically fractionated from contemporaneous DIC. In contrast, $\delta^{13}\text{C}_{\text{CaCO}_3}$ and $\delta^{13}\text{C}_{\text{org}}$ records from Cryogenian

(ca. 720–635 Ma; Swanson-Hysell et al., 2010) and Ediacaran (635–542 Ma; Calver, 2000; Fike et al., 2006; McFadden et al., 2008) carbonate successions display relatively invariant $\delta^{13}\text{C}_{\text{org}}$, despite large changes to $\delta^{13}\text{C}_{\text{CaCO}_3}$. Rothman et al. (2003) originally observed this behavior in the Hayes et al. (1999) compilation of globally averaged $\delta^{13}\text{C}_{\text{CaCO}_3}$ and $\delta^{13}\text{C}_{\text{org}}$ data and proposed a controversial model for the late Neoproterozoic carbon cycle in which a very large, semi-refractory, ^{13}C -depleted dissolved or particulate organic carbon (DOC or POC) reservoir maintained nearly constant carbon isotope composition and, through incorporation into sediments, overwhelmed the isotopic signal from contemporaneous primary-biomass-fractionating DIC. In contrast, the carbon isotope composition of the relatively small DIC pool would be susceptible to large negative swings associated with DOC/POC remineralization.

Past reconstructions of the global organic carbon cycle using $\delta^{13}\text{C}$ of bulk organic carbon (e.g., Rothman et al., 2003) rely on the assumption that the $\delta^{13}\text{C}$ of the measured organic carbon ($\delta^{13}\text{C}_{\text{org}}$) is relatively unaltered by dia-

genesis and reflects young organic carbon incorporated into the sediment at the time of deposition. Possible sources of uncertainty include the effect of thermal maturation and oxidation on bulk total organic carbon (TOC) $\delta^{13}\text{C}_{\text{org}}$ values (Des Marais et al., 1992), contamination by migrating hydrocarbons, and contamination by weathered detrital organic carbon. Although quantifying the effects of contamination and diagenetic alteration on bulk TOC $\delta^{13}\text{C}_{\text{org}}$ values is beyond the scope of this study, there are several qualitative points that may be important. First, a basinwide decrease in TOC due to thermal maturation or oxidation will tend to shift TOC toward more enriched $\delta^{13}\text{C}_{\text{org}}$ values, changing the absolute value of the difference (ϵ) between $\delta^{13}\text{C}_{\text{CaCO}_3}$ and $\delta^{13}\text{C}_{\text{org}}$ but not $\delta^{13}\text{C}_{\text{org}}$ trends (Des Marais et al., 1992). Second, contamination by migrating hydrocarbons should be porosity and permeability dependent. As a result, the effects of contamination on the $\delta^{13}\text{C}_{\text{org}}$ value of bulk TOC are expected to depend on lithofacies and the degree of early diagenetic cementation (see Fig. A1 in Appendix). Finally, contamination by detrital C_{org} may be a

significantly underappreciated source of TOC in Precambrian shallow-marine sediments. Recent work on the recycling of ancient TOC in modern tectonically active continental margins indicates that at sites with high sedimentation rates, up to 30% of the TOC in marine sediments is detrital (Aller et al., 1996; Blair et al., 2003; Drenzek et al., 2009). Also, it is important to note that the organic carbon contents of these sediments are not trivial (0.1–1 wt% TOC; Blair et al., 2003), suggesting that wt% TOC may not be a sufficient predictor of detrital contamination. Efficient reburial of TOC in these environments is thought to be due to the short time that the fossil organic carbon is exposed to oxidizing conditions (Blair et al., 2003). Lower concentrations of the major oxidants in seawater (O_2 , SO_4^{2-}) in the late Precambrian and early Phanerozoic should be associated with less oxidative exposure and more efficient reburial of fossil organic carbon globally (i.e., not just in active margin sediments). A large contribution of fossil organic carbon should be associated with damped (or invariant) bulk TOC $\delta^{13}C_{org}$ values.

Despite the potential complications associated with interpreting bulk TOC $\delta^{13}C_{org}$ values in ancient rocks, the Rothman et al. (2003) hypothesis of a large and dynamic DOC pool is an intriguing one in light of the large variability in the isotopic composition of carbonate carbon ($\delta^{13}C_{CaCO_3}$). The form and size of the required organic carbon pool depends crucially on the time scale of the observed $\delta^{13}C_{CaCO_3}$ excursions (Higgins and Schrag, 2006) and the oxidant budget of the ocean (Bristow and Kennedy, 2008). Rothman et al. (2003) proposed DOC pools 100–1000 times larger than those of today (DOC is $\sim 45 \mu M$ in the deep ocean today; Hansell and Carlson, 2001) in order to get the observed decoupling of $\delta^{13}C_{CaCO_3}$ and $\delta^{13}C_{org}$, but these values assume roughly modern concentrations of DIC in the ancient ocean: the carbon cycle dynamics depend critically on the relative sizes of DOC and DIC, not the absolute size of DOC. Today, millimolar-level concentrations of DOC are common in lake environments (O’Loughlin and Chin, 2004; Smith et al., 1993; Takacs et al., 2001; Giri et al., 2004), in marine pore waters (Lahajnar et al., 2005), and in the euxinic waters of the Black Sea (Agatova et al., 1989, 2001; Torgunova, 1994), where even the oxic upper waters have DOC elevated up to 5 \times that of normal seawater (Cauwet et al., 2002).

The apparent end of $\delta^{13}C_{org}$ invariance in the latter stages of the Shuram-Wonoka isotope anomaly ca. 551 Ma (Condon et al., 2005) has been interpreted as the demise of the large DOC source (Fike et al., 2006), perhaps associated with the radiation of benthic microsuspension feeders such as sponges and some of the

Ediacara fauna (Sperling et al., 2007). In Oman, the Ediacaran–Cambrian boundary $\delta^{13}C$ excursion appears to display excellent covariance in $\delta^{13}C_{CaCO_3}$ and $\delta^{13}C_{org}$ (Fike, 2007), but, to our knowledge, no detailed paired $\delta^{13}C_{CaCO_3}$ and $\delta^{13}C_{org}$ record has previously been generated from Lower Cambrian carbonates. We describe $\delta^{13}C_{org}$ methods in Appendix section A2 and display new data from Morocco in Figures 8 and A1 (see Appendix).

Figure 8 depicts no Neoproterozoic-like invariance in $\delta^{13}C_{org}$, but instead shows that $\delta^{13}C_{CaCO_3}$ and $\delta^{13}C_{org}$ are uncorrelated from 542 to 532.5 Ma and 524.85 to 520.5 Ma, and are correlated from 532.5 to 524.85 Ma. The $\delta^{13}C_{org}$ curve is reproduced from two stratigraphic sections that are separated by over 100 km and contain significantly different facies associations representing outer-shelf (Oued Sdas, MS-7) and inner-shelf (Sidi M’Sal, MS-16) environments (Maloof et al., 2010a). Some workers have expressed concern that carbonates with low total organic carbon may be prone to contamination by external sources of organic carbon. The Moroccan samples have TOC ~ 0.05 wt%, typical of many Neoproterozoic and Phanerozoic carbonates, and we observe no correlation between $\delta^{13}C_{org}$ and TOC (Fig. A1B [see Appendix]) or lithofacies (Fig. A1 [see Appendix]), suggesting that porosity- and permeability-dependent contamination associated with migrating hydrocarbons was not important. Furthermore, the lack of correlation among $\delta^{13}C_{org}$, TOC, and lithofacies suggests that size and density sorting during sediment transport of fossil carbon particles did not preferentially concentrate fossil carbon into specific lithologies (and thus fossil carbon may not impact $\delta^{13}C_{org}$).

Paired Carbonate and Organic Carbon

Coherent excursions in the $\delta^{13}C$ record of the global DIC reservoir of the magnitude and duration observed in the Cambrian are difficult to reconcile with our current understanding of the budgets and dynamics of the global carbon cycle on geologic time scales. Carbon isotope excursions of 5‰–10‰ over 0.1–2.0 m.y. require both extreme changes in the ratio of organic carbon to total carbon outputs ($f_{org} = C_{org}/C_{total}$) and extreme absolute rates of carbon throughput. Maloof et al. (2010a) calculated response times to a step change in f_{org} from 0.4 to 0.14 (these f_{org} values were calculated from $\delta^{13}C_{CaCO_3}$ and $\delta^{13}C_{org}$ values assuming steady-state carbon cycling [Kump and Arthur, 1999] for various [DIC] and carbon burial (F_{burial}) and input fluxes ($F_{input} = F_{burial}$ in steady state). For F_{burial} and [DIC] similar to those of modern oceans, this change in f_{org} would require 3.5 m.y. to generate a $\delta^{13}C_{CaCO_3}$ excursion similar in magnitude to that seen at

the ND-T boundary (post-6p negative excursion; Fig. 5; Maloof et al., 2010a). Larger [DIC] or smaller F_{burial} lead to more sluggish response times (Bartley and Kah, 2004). For example, a steady-state model of the ND-T boundary negative $\delta^{13}C_{CaCO_3}$ shift (post-6p; Fig. 5) constrained to last 330–686 k.y. will only work for modern values of [DIC] if F_{burial} is four times larger than today, or if the change in f_{org} was much more extreme than the beginning and ending values for $\delta^{13}C_{CaCO_3}$ suggest. Furthermore, most authors believe that the Cambrian Period had elevated [DIC], up to 9 mM (Bernier et al., 1983), due to the higher pCO_2 required to compensate for a 5% weaker Sun (Bahcall et al., 2001) and to explain the lack of glaciation (Hambrey and Harland, 1981). High atmospheric pCO_2 could have been maintained with lower [DIC] if ocean pH was very low and calcium concentrations were high enough to maintain $CaCO_3$ saturation (Higgins et al., 2009), although we have no evidence for such a low-pH ocean. For [DIC] ~ 9 mM, an F_{burial} 16 times larger than modern carbon burial flux is required to generate the observed $\delta^{13}C_{CaCO_3}$ shift in ca. 500 k.y.

On time scales >100 k.y., $F_{input} = F_{burial}$ should reflect volcanic (e.g., Bernier et al., 1983) and metamorphic (e.g., Evans et al., 2008) outgassing rates of CO_2 . To explain the lowest Cambrian $\delta^{13}C_{CaCO_3}$ shifts, Cambrian volcanoes or orogenies (e.g., Squire et al., 2006) must have been 4–16 times more potent CO_2 producers than those of today (see section “Strontium”). It is important to note that on geologic time scales, the high rates of volcanic/metamorphic outgassing required by our data must be balanced by carbon sinks ($CaCO_3$, C_{org} , or both). Although absolute rates of carbonate burial are difficult to extract from the geologic record, the observation that large carbonate depositional systems on shallow continental shelves may have extended poleward of the Antarctic Circle (Appendix section A8; Fig. 3) is consistent with higher overall rates of carbonate burial during this time.

If we consider the Phanerozoic system where organic carbon is derived from contemporaneous DIC, the long-term steady-state (i.e., greater than the relaxation time of the ocean-atmosphere carbon cycle, which presently is a few hundred thousand years; Holser et al., 1988) carbon-isotopic mass balance for the ocean can be written:

$$\delta^{13}C_{in} = (1 - f_{org})\delta^{13}C_{CaCO_3} + (f_{org})(\delta^{13}C_{CaCO_3} - \epsilon), \quad (1)$$

where $\delta^{13}C_{in}$ is the isotopic composition of DIC entering the ocean (approximately mantle composition), $\delta^{13}C_{CaCO_3}$ is the isotopic composition of the oceanic DIC pool derived from chemical weathering, ϵ is the difference between DIC

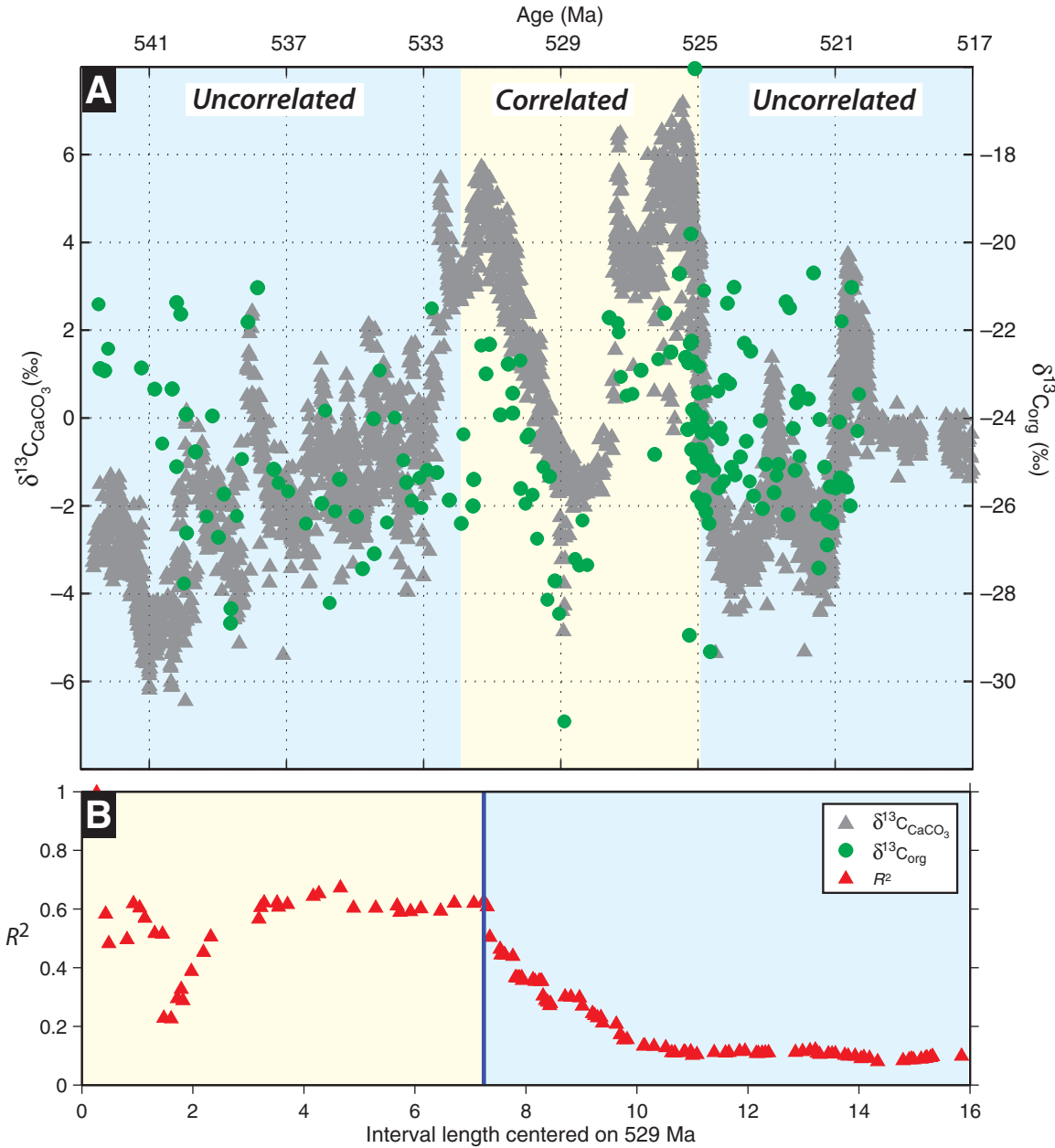


Figure 8. (A) Paired carbonate (gray) and organic carbon (green) $\delta^{13}\text{C}$ data from Morocco with intervals of correlation and lack of correlation highlighted in yellow and blue, respectively. (B) The evolution of R^2 (calculated from the correlation between $\delta^{13}\text{C}_{\text{CaCO}_3}$ and $\delta^{13}\text{C}_{\text{org}}$) as a function of the size of a symmetric analysis window centered at ca. 529 Ma. At a distance of ± 3.5 m.y. from 529 Ma (i.e., within the yellow window), R^2 remains greater than 0.6, while analysis windows expanding beyond this region show declining R^2 .

and organic carbon (often dominated by the kinetic isotope fractionation associated with the uptake of carbon by photoautotrophs), and $f_{\text{org}} = C_{\text{org}}/C_{\text{total}}$ is the fraction of carbon buried that is organic (Kump, 1991). Changes in f_{org} correspond to changes in the burial fluxes of oxidized and reduced carbon species. Changes in ϵ correspond to changes in the difference between the isotopic compositions of those carbon

end members. Assuming that the global carbon cycle in the Cambrian can be approximated by the steady state described in Equation 1, we suggest that the lower Nemakit-Daldynian and Tommotian intervals of uncorrelated $\delta^{13}\text{C}_{\text{CaCO}_3}$ and $\delta^{13}\text{C}_{\text{org}}$ and relatively low $\delta^{13}\text{C}_{\text{CaCO}_3}$ volatility (Fig. 8) were dominated by local variability in the carbon isotopic composition of organic matter associated with variability in biological

fractionation, organic matter preservation, or contamination by ancient organic carbon weathered from the continents. Unlike DIC, which is generally thought to be globally homogeneous on time scales longer than the 10^3 yr mixing time of the ocean, C_{org} can be dominated by local influences (associated with carbon fixation mechanisms and rates, degree of remineralization, and trophic structure). These factors can

lead to local changes in $\delta^{13}\text{C}_{\text{org}}$, separate from and superimposed on any changes in $\delta^{13}\text{C}_{\text{org}}$ inherited from changing the isotopic composition of DIC, which is the source for the carbon. In contrast, we interpret the upper Nemakit-Daldynian interval of correlated $\delta^{13}\text{C}_{\text{CaCO}_3}$ and $\delta^{13}\text{C}_{\text{org}}$, high $\delta^{13}\text{C}_{\text{CaCO}_3}$ volatility, and virtually no small shelly fossil first appearances (Fig. 5) as dominated by changes in f_{org} , perhaps associated with changes in oceanic redox conditions, carbon to phosphorus ratios of buried organic matter, or phosphate versus nitrate limitation (Saltzman, 2005; Maloof et al., 2005).

Over the ≥ 100 k.y. time scale required to achieve carbon-isotopic steady state, phosphate (PO_4^{3-}) is likely to be the limiting nutrient for primary productivity (Broecker and Peng, 1982; Smith, 1984; Lenton and Watson, 2000; Tyrrell, 1999; Schrag et al., 2002). It follows that the burial of organic carbon is controlled by the riverine flux of PO_4^{3-} to the ocean and its removal in sediments and hydrothermal systems (Kump, 1988; Schrag et al., 2002). As pointed out by Schrag et al. (2002) and Junge et al. (1975), an increase in silicate weathering would lead to an increase in the flux of both riverine PO_4^{3-} and alkalinity to the oceans, enhancing the burial of organic and carbonate carbon in approximately equal proportions and keeping f_{org} (and thus $\delta^{13}\text{C}_{\text{CaCO}_3}$) about the same. This argument suggests that positive $\delta^{13}\text{C}_{\text{CaCO}_3}$ and $\delta^{13}\text{C}_{\text{org}}$ swings in the Early Cambrian ocean must have been driven by increasing burial of C_{org} relative to PO_4^{3-} . Unfortunately, the processes that control the relative rates of C_{org} and P burial are not well understood. Because the vast majority of P delivered to sediments is associated with C_{org} , and most C_{org} that is delivered to sediments is respired, it is the processes that influence the leak of P back to the ocean that will ultimately control the rate of P burial relative to C_{org} . There is some evidence from organic compounds that local anoxia enhances the leak of PO_4^{3-} back to seawater, allowing for higher rates of C_{org} burial relative to PO_4^{3-} . On short time scales, this feedback has been argued to amplify anoxia, although on million-year time scales, enhanced burial of C_{org} will lead to the accumulation of atmospheric O_2 and a return to more oxic conditions (Ingall and Van Cappellen, 1990; Ingall et al., 1993; Van Cappellen and Ingall, 1996; Ingall and Jahnke, 1997). Exactly how this mechanism could produce the oscillations in $\delta^{13}\text{C}_{\text{CaCO}_3}$ observed in the Cambrian is not clear. In addition, recent studies found the unexpected result that apatite precipitation and sequestration of PO_4^{3-} are favored in anoxic conditions (Goldhammer et al., 2010).

The large carbon isotope excursions that characterize the Cambrian are remarkable for

both their magnitude and the short duration over which they occur. The covariance between $\delta^{13}\text{C}_{\text{CaCO}_3}$ and $\delta^{13}\text{C}_{\text{org}}$ during most of the large-amplitude changes suggests that the carbon isotope excursions are related to changes in the $\delta^{13}\text{C}$ of contemporaneous DIC and not to diagenesis (e.g., Derry, 2010) or the dynamics of a large, homogeneous DOC pool (e.g., Rothman et al., 2003). Given the caveats involved in interpretation of bulk TOC $\delta^{13}\text{C}_{\text{org}}$ data, the lack of correlation during periods of high-frequency, low-amplitude $\delta^{13}\text{C}_{\text{CaCO}_3}$ excursions is likely due to local variability in $\delta^{13}\text{C}_{\text{org}}$, unrelated to the $\delta^{13}\text{C}$ of DIC or buffering by detrital C_{org} . However, in the context of our current understanding of the global carbon cycle on geologic time scales, the magnitude and rapidity of the carbon isotope excursions require extreme changes in the relative rates of C_{org} and CaCO_3 burial and rates of volcanic outgassing that are up to an order of magnitude larger than modern fluxes. Decarbonation of carbonaceous sediments (CaCO_3 and C_{org}), either in subduction zones or in metamorphic terranes, a likely source of some of the additional carbon. Although it is uncertain to what extent higher rates of continental metamorphism are expected during periods of supercontinent assembly, the earliest Cambrian is associated with the latter stages of the breakup of southern Rodinia and the assembly of Gondwana (Figs. 3 and 10). Though it is tempting to regard the volatility in f_{org} and high rates of carbon throughput as having a common cause, exactly how tectonic processes influence organic carbon burial and atmospheric O_2 remains a mystery (but see Campbell and Squire [2010] for one hypothesis).

Strontium

During the earliest Cambrian, seawater $^{87}\text{Sr}/^{86}\text{Sr}$, as recorded in carbonate rocks from Morocco, Siberia, Mongolia, and China, declined monotonically by ~ 0.0006 (Fig. 9A). Seawater chemistry is thought to have alternated throughout Earth history between states that favor aragonite production (during intervals referred to as aragonite seas) and those that favor calcite production (during calcite seas). The major control on mineralogy is thought to be the Mg/Ca ratio of seawater, with ratios above ~ 2.0 favoring aragonite, and lower ratios favoring calcite (Stanley and Hardie, 1998; Lowenstein et al., 2001). We explore the implications of the observed shift from aragonite to calcite seas during the Early Cambrian (Fig. 5; Porter, 2007) and the associated decline in the $^{87}\text{Sr}/^{86}\text{Sr}$ of seawater (Figs. 9A and A9 [see Appendix]) for changes in the chemistry of seawater through the Cambrian using a numerical model of the global magnesium, calcium, and strontium cycles.

Modeled processes include carbonate and silicate weathering, high-temperature hydrothermal alteration of oceanic crust, burial of carbonate minerals, and dolomitization (see Appendix section A11). Mechanisms for a decline in the Mg/Ca ratio of seawater on time scales of tens of millions of years include an increase in the rate of high-temperature hydrothermal alteration of the oceanic crust or an increase in the rate of dolomite formation (Holland and Zimmermann, 2000; Hardie, 1996).

Rising global sea level in the Early Cambrian (e.g., Miller et al., 2005; Haq and Schutter, 2008) is consistent with increased submergence of shallow-water carbonate platforms, higher rates of dolomitization, and a consequent decline in the Mg/Ca ratio of seawater. The effect of an increase in dolomitization on the Sr isotopic composition of seawater is difficult to constrain, although it is likely to be small. Thus, an increase in dolomitization through the Cambrian may help to explain the observed decrease in the Mg/Ca ratio of seawater and shift from aragonite to calcite seas, but it does not help to explain the decline in $^{87}\text{Sr}/^{86}\text{Sr}$ or the rise in sea level.

An increase in the rate of hydrothermal alteration of oceanic crust is consistent with the observed decrease in the $^{87}\text{Sr}/^{86}\text{Sr}$ of seawater between 543 and 521 Ma (e.g., Edmond, 1992; Richter et al., 1992). If caused only by changes in the rate of hydrothermal alteration of oceanic crust, a 0.0006 decline in the $^{87}\text{Sr}/^{86}\text{Sr}$ of seawater would require a $2.25\times$ increase in the flux of seawater through high-temperature hydrothermal systems at mid-ocean-ridge crests, from 3.75×10^{13} kg seawater per year to 8.4×10^{13} kg seawater per year (Fig. 9; Table 1). A smaller increase in the hydrothermal flux of seawater would be required if the $^{87}\text{Sr}/^{86}\text{Sr}$ of the weathering flux declined appreciably during this interval. For example, model calculations indicate that no change in hydrothermal flux of seawater would be required if the $^{87}\text{Sr}/^{86}\text{Sr}$ of the weathering flux declined from 0.7105 to 0.7096 from 543 to 521 Ma (Table 1). Such a decline in the $^{87}\text{Sr}/^{86}\text{Sr}$ of the weathering flux could be accommodated by any combination of a reduction in the rate of silicate weathering, an increase in the rate of carbonate weathering or recrystallization, or a reduction in the average $^{87}\text{Sr}/^{86}\text{Sr}$ of weathered carbonate and silicate rocks (Edmond, 1992). Observations of rising eustatic sea level through this interval (Miller et al., 2005; Haq and Schutter, 2008) do not favor increased rates of carbonate weathering.

The recrystallization of metastable carbonates, specifically the conversion of aragonite to low-Mg calcite, can have a significant effect on the Sr concentration and isotope budget of

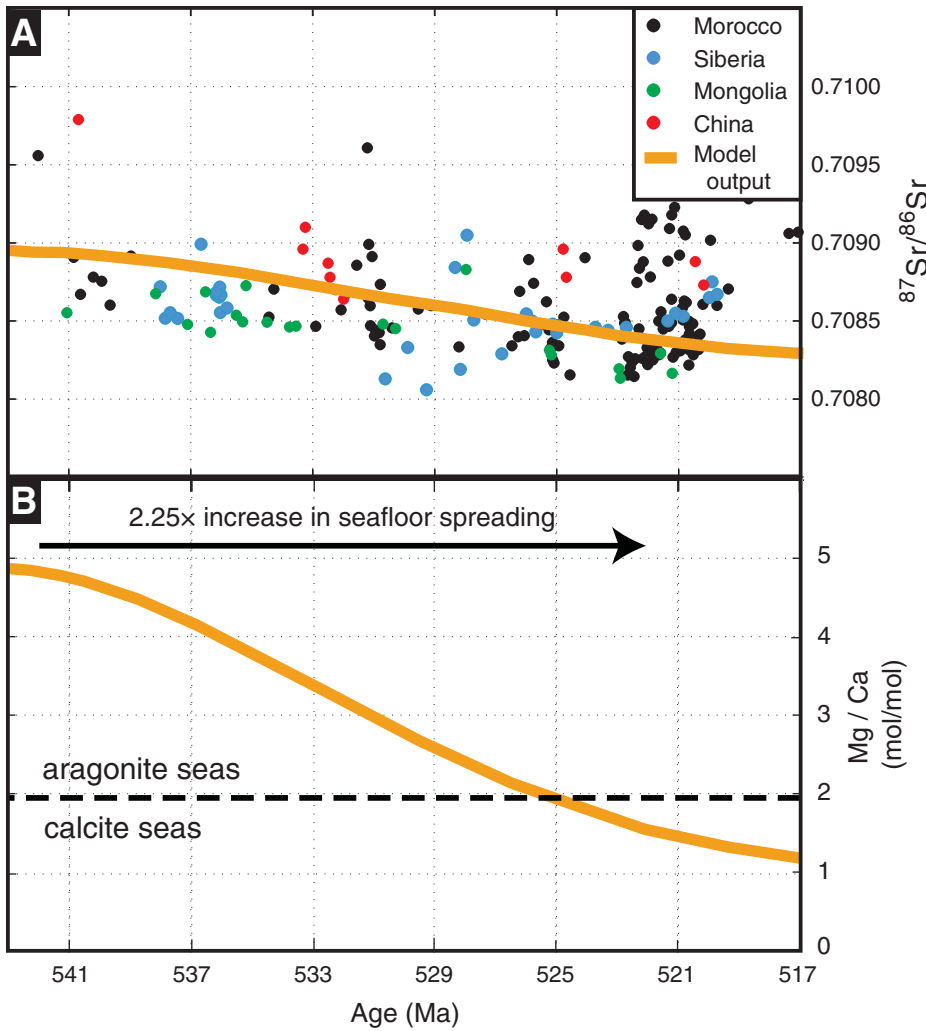


Figure 9. (A) Time evolution of $^{87}\text{Sr}/^{86}\text{Sr}$ from Morocco (this paper), Siberia (Derry et al., 1994; Knoll et al., 1995a; Nicholas, 1996; Kaufman et al., 1996), Mongolia (Brasier et al., 1996), and China (Ishikawa et al., 2008; Sawaki et al., 2008). The unfiltered $^{87}\text{Sr}/^{86}\text{Sr}$ record and a description of filter design are reported in Appendix section A10. (B) Modeled impact on Mg/Ca for a 2.25x increase in the hydrothermal flux of $^{87}\text{Sr}/^{86}\text{Sr}$ over 20 m.y.

seawater (Stoll and Schrag, 1998). Aragonite contains roughly 5–9 times more Sr than does low-Mg calcite precipitated from seawater. Because aragonite is metastable at Earth’s surface conditions, it tends to recrystallize to low-Mg calcite on a range of time scales (Swart et al., 2001; James et al., 2005). In the process, 80%–90% of the Sr contained in the primary aragonite is released back to seawater. Thus, the volume

of aragonite buried in sediments represents a potential source of relatively unradiogenic Sr that will be mobilized if rates of aragonite burial or recrystallization change. It is difficult to say how rates of recrystallization might be affected by rising sea level, but the reduction in aragonite burial associated with the shift from aragonite to calcite seas at ca. 525 Ma is expected to have diminished the flux of Sr associated with recrystallization

as the volume of sedimentary aragonite was progressively depleted. Although not modeled here, the loss of this additional source of carbonate Sr may help to explain the apparent inflection in the $^{87}\text{Sr}/^{86}\text{Sr}$ of seawater toward higher values after 525 Ma.

Model calculations indicate that a 55% decline in the rate of silicate weathering would be required to explain the observed decline in the $^{87}\text{Sr}/^{86}\text{Sr}$ of seawater (Table 1). However, there is no independent evidence for a cooling that could cause a change of this magnitude, and Early Cambrian plate reconstructions suggest that the climate may have warmed during this interval to allow for development of high-latitude shallow-water carbonate microbialites (see Appendix section A8; Fig. 3). It is well known that changes in the weathering of rocks containing highly radiogenic Sr can have a large effect on the $^{87}\text{Sr}/^{86}\text{Sr}$ value of the weathering flux (e.g., Edmond, 1992; Richter et al., 1992; Derry and France-Lanord, 1996; Galy et al., 1999). Thus, for instance, chemical weathering of exhumed lower-crustal granulites in Pan-African orogens (Squire et al., 2006; Campbell and Squire, 2010) may have supplied unradiogenic material to rivers and lowered the $^{87}\text{Sr}/^{86}\text{Sr}$ of seawater. While a change in the $^{87}\text{Sr}/^{86}\text{Sr}$ of the weathering flux may be significant, we believe that an increase in the rate of hydrothermal alteration of oceanic crust is likely the most important contributor to the observed decline in $^{87}\text{Sr}/^{86}\text{Sr}$, because a hydrothermal explanation is consistent with independent observations of a decrease in the Mg/Ca ratio of seawater and the switch from aragonite to calcite seas across the ND-T boundary (Fig. 5; Porter, 2007).

The simplest way to increase the rate of hydrothermal alteration of oceanic crust is to increase the total length of mid-ocean ridges around the world. If total hydrothermal alteration scales linearly with ridge length, then an approximate doubling of ridge length over 20 m.y. would be required. The late Neoproterozoic to Early Cambrian is a time of continent dispersal during the breakup of Rodinia. Centered around Laurentia (North America) (Hoffman, 1991), the breakup of northern Rodinia spalled future east Gondwanan continents (e.g., Australia, Antarctica, India, South China) across the incipient Panthalassa Ocean starting as early as

TABLE 1. PARAMETERS USED IN MODELING THE Sr CYCLE

Model run	$^{87}\text{Sr}/^{86}\text{Sr}_{\text{sil}}$ weathering (1)	$^{87}\text{Sr}/^{86}\text{Sr}_{\text{CaCO}_3}$ weathering (1)	Silicate/carbonate weathering (1) $\times 10^{10}$ mol/yr (% carbonate/% silicate)	High-T hydrothermal (2) ($\times 10^{13}$ kg H ₂ O/yr)	$^{87}\text{Sr}/^{86}\text{Sr}$ hydrothermal (1)
Initialization	0.7150	0.7070	1.89, (43/57)	3.75	0.7030
(+) high-T hydrothermal	0.7150	0.7070	1.89, (43/57)	3.75 to 8.4	0.7030
(-) $^{87}\text{Sr}/^{86}\text{Sr}$ of weathering	0.7150 to 0.7141	0.7070 to 0.7061	1.89, (43/57)	3.75	0.7030
(-) silicate weathering	0.7150	0.7070	1.89, (43/57) to 1.48, (32/68)	3.75	0.7030

Note: (1) Allègre et al. (2010); (2) Elderfield and Schultz (1996).

ca. 800 Ma (Wingate et al., 1998; Z. Li et al., 2003; Pisarevsky et al., 2003) and perhaps culminating with the final rift-to-drift transition from the modern western margin of North America in the Early Cambrian (Bond and Kominz, 1984; Bond et al., 1988). In contrast, southern Rodinia (or Pannotia) did not break apart into Laurentia, Baltica (northern Europe), Siberia, and west Gondwana (now Africa and South America) until latest Ediacaran (Fig. 3), with a well developed rift-to-drift transition and opening of the Iapetus Ocean in the Early Cambrian (Bond et al., 1984, 1988). The opening of Iapetus alone could have doubled mid-ocean-ridge lengths.

Parsons (1982) and Rowley (2002) used the area/age versus age distribution of modern oceanic lithosphere to suggest that there have been no significant changes in global seafloor production rates over the past 180 m.y. Seafloor production is a function of both ridge length and seafloor spreading rates. The primary source of error in such ridge-production estimates is the inherent uncertainty in reconstructing the now-subducted ridges in the Pacific and Tethyan Ocean basins. In those studies that contradict Parsons (1982) and Rowley (2002) and suggest a 5%–20% mid-Cenozoic (Conrad and Lithgow-Bertelloni, 2007) and 50%–100% long-term Cretaceous–Tertiary (Kominz, 1984; Engebretson et al., 1992) decrease in crust production, it is the seafloor production along these subducted ridges that is responsible for the discrepancy. Unfortunately, none of these studies has enough seafloor area to work with to determine how ridge length and production changed during the early stages of the breakup of Pangea (200–170 Ma), a time when plate reconfiguration and continent dispersal were most analogous to the Early Cambrian. Therefore, we consider it possible that ridge length and ridge production could both increase during the breakup of a supercontinent.

A doubling of ridge length would lead to an increase in ridge volume of $\sim 5 \times 10^6$ – 25×10^6 km³ for average half-spreading rates of 1–5 cm yr⁻¹. Assuming transgressing shorelines on a planet with a similar distribution of continental elevations as today, this change in the mid-ocean-ridge system would cause a 10–70 m sea-level rise (e.g., Pitman, 1978). However, Gurnis (1990) suggested that increased ridge production would be offset by faster subduction and lead to an increase in the negative dynamic topography near convergent margins, thus diminishing the sea-level rise associated with the ridge volume change. Husson and Conrad (2006) disputed the idea that ridge-displaced water could be stored in trenches by showing that, if plate acceleration is enabled by a change

in mantle viscosity, the effect of dynamic topography on basin volume, and thus sea level, is nearly removed. In summary, changes in ridge production (and thus plate velocities) likely will lead to a net increase in eustatic sea level, but the amplitude, and even the sign, of the associated dynamic topographic influence on eustasy is difficult to determine (Conrad and Husson, 2009). No glacial sediments of definitive Early Cambrian age have been found (Hambrey and Harland, 1981), so glacioeustasy is not a viable alternative for sea-level change (but see Norin, 1937; Runkel et al., 2010; Landing and MacGabhann, 2010).

A sea-level rise of 10–70 m is consistent with the general observation that virtually every continent underwent progressive flooding starting sometime in the Early Cambrian (e.g., the “Cambrian transgression” of Matthews and Cowie, 1979; McKie, 1993) and culminating in the Middle–Late Ordovician “Sauk” highstand (e.g., Sloss, 1963; Haq and Schutter, 2008). However, the relative position of shorelines is not a direct measure of eustasy, because changes in subsidence and sediment supply also influence shoreline location. Numerous workers have attempted to use sequence stratigraphic boundaries such as flooding surfaces and erosional unconformities preserved in the sedimentary records of cratonic basins as more accurate indicators of relative sea-level change (Vail et al., 1977; Haq et al., 1987; Miller et al., 2005; Haq and Schutter, 2008). The sub-Tommotian unconformity and subsequent northwest-to-southeast transgression of the Siberian platform (see section “Siberia”) is an example of a Lower Cambrian flooding event. Correlations of sequence boundaries of similar ages from different continents are what have led to interpretations of global eustatic change, although such correlations are challenging because interpolation between Lower Cambrian sections without radiometrically dated ash beds or sufficient bio- and chemostratigraphy can lead to age uncertainties as large as 10 m.y. Furthermore, even sequence stratigraphic observations are notoriously poor indicators of eustasy, as coastlines around the world are in constant motion relative to sea level due to the dynamics of mantle convection (e.g., Moucha et al., 2008).

Despite all of these caveats, we propose that the Lower Cambrian ⁸⁷Sr/⁸⁶Sr record presented here is consistent with an increase in the rate of hydrothermal alteration of seafloor basalt and the consequent transition from an aragonite to a calcite sea (Fig. 9). A feature associated with the increase in mid-ocean-ridge production is a global sea-level rise that flooded parts of all the continents (e.g., Worsley et al., 1984). Rela-

tive sea-level rise was diachronous, depending on the initial elevation of the continent and dynamic topography. The increase in mid-ocean-ridge production also should have led to an increase in the rate of volcanic outgassing and climate warming, which may help to explain the existence of the Moroccan carbonate belt at remarkably high latitude (e.g., McCausland et al., 2007; Fig. 3).

The new Lower Cambrian ⁸⁷Sr/⁸⁶Sr record nicely connects the composite Neoproterozoic and Phanerozoic ⁸⁷Sr/⁸⁶Sr curves compiled by Halverson et al. (2007, 2010) and Veizer et al. (1999), respectively (Fig. 10). Halverson et al. (2007) used this compilation to challenge the idea that orogenesis leads to a rise in marine ⁸⁷Sr/⁸⁶Sr (Raymo et al., 1988; Asmerom et al., 1991; Edmond, 1992; Kaufman et al., 1993) by pointing out that the culminations in both Rodinia and Pangea assembly correspond to nadirs in the ⁸⁷Sr/⁸⁶Sr curve. The isolation of supercontinent interiors from moisture sources probably plays the crucial role in reducing the continental weathering flux of Sr to the oceans (Donnadieu et al., 2004; Halverson et al., 2007). The rifting of northern Rodinia brought moisture to previously dry cratons, increasing the weathering flux of ⁸⁷Sr/⁸⁶Sr and swamping any increase in the hydrothermal flux due to the generation of new mid-ocean ridges. The acceleration in the rate of ⁸⁷Sr/⁸⁶Sr increase at the base of the Cryogenian may have been caused by the glacial removal of a long-lived continental regolith that accumulated during the 1.5 b.y. gap between Proterozoic ice ages (Swanson-Hysell et al., 2010).

The rifting of southern Rodinia and the opening of the Iapetus Ocean may have caused the Lower Cambrian dip in ⁸⁷Sr/⁸⁶Sr because, by then, continents were sufficiently dispersed to receive consistent moisture and maintain chemical weathering of their interiors, while the increase in Iapetus mid-ocean-ridge length contributed a new hydrothermal ⁸⁷Sr/⁸⁶Sr source to the ocean. No single process can elegantly explain the time-evolution of marine ⁸⁷Sr/⁸⁶Sr over the past 1000 m.y.; however, the monotonic ND-T decline in ⁸⁷Sr/⁸⁶Sr provides a useful companion to $\delta^{13}\text{C}_{\text{CaCO}_3}$ for interbasinal correlation, and may signal a change in hydrothermal flux and Mg/Ca in the ocean that had an important impact on the skeletal mineralogy of animals that evolved during the Early Cambrian.

Uranium and Vanadium

The concentration of redox-sensitive trace elements in seawater, and their incorporation into marine carbonates, depends critically on the oxidation state of the ambient water column (e.g., Schröder and Grotzinger, 2007). In particular, both V and U become enriched in

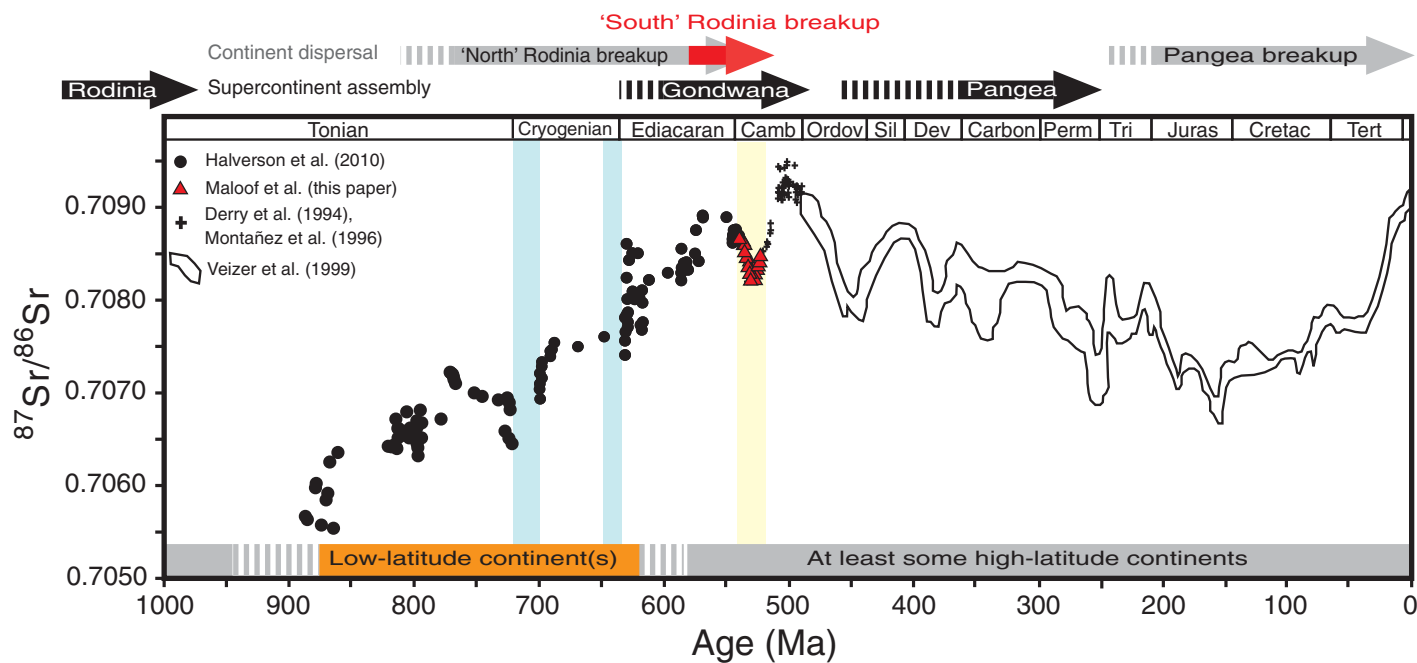


Figure 10. Time evolution of $^{87}\text{Sr}/^{86}\text{Sr}$ during the Neoproterozoic and Phanerozoic, modified after Halverson et al. (2007). Snowball Earth intervals are highlighted in light blue (Hoffman et al., 1998), intervals dominated by low-latitude continents are highlighted in orange, and periods of supercontinent assembly (black) and dispersal (gray and red) are marked. The new Lower Cambrian data from Morocco nicely connect previously published Neoproterozoic (Halverson et al., 2007, 2010) and stratigraphically higher Cambrian (Derry et al., 1994; Montañez et al., 1996) $^{87}\text{Sr}/^{86}\text{Sr}$ curves. The Lower Cambrian decline in $^{87}\text{Sr}/^{86}\text{Sr}$ occurs during the final rifting of “south” Rodinia and the opening of the Iapetus Ocean.

sediments deposited under anoxic conditions (Jones and Manning, 1994; Piper, 1994; Piper and Isaacs, 1995). V enrichment usually occurs at redox conditions typical of nitrate reduction, while U enrichment generally corresponds to redox conditions typical of sulfate reduction in the marine environment (Jones and Manning, 1994; Piper and Isaacs, 1995). Although the trace-element proxy for seawater redox conditions originally was developed for the study of siliciclastic sediments, the method recently has been applied to carbonate strata (e.g., Schröder and Grotzinger, 2007; Amthor et al., 2003).

After applying a filter designed to exclude diagenetically altered samples from the $^{87}\text{Sr}/^{86}\text{Sr}$ analysis and correcting for contamination by terrestrial clays using Th content (see Appendix section A10), we overlay normalized U and V records from Morocco on the $\delta^{13}\text{C}_{\text{CaCO}_3}$ curve (Fig. 11). The salient long-term trend is a monotonic decline in the concentrations of both elements over the duration of the Nemakit-Daldynian, Tommotian, and Atdabanian Stages. This long-term decline is particularly impressive because, if the rate of hydrothermal alteration of oceanic crust increased over the same interval, as postulated in section “Strontium,” then the hydrothermal input of U and V to the ocean also should have increased, leading to

larger oceanic reservoirs and generally more U and V in sediments.

Decreasing U and V suggest progressive oxidation of the sediment-water interface, consistent with the observation that both bioturbation (e.g., Crimes, 1987) and benthic biodiversity (see section “Small Shelly Fossils”) increase through the same interval (in Morocco and globally). Furthermore, the U and V signals are consistent in four stratigraphic sections (Fig. A9, see Appendix), indicating that the oxygenation of shelfal waters occurred simultaneously across more than 300 km² of the Anti-Atlas margin.

The only significant short-term perturbations to this trend are positive U and V anomalies during the negative $\delta^{13}\text{C}_{\text{CaCO}_3}$ excursions between 5p–6p, 6p–7p, and III–IV. These positive U and V anomalies are similar to those found in carbonates and shales associated with the E-C boundary negative $\delta^{13}\text{C}_{\text{CaCO}_3}$ excursion in Iran, Oman, and China (Kimura and Watanabe, 2001; Amthor et al., 2003; Schröder and Grotzinger, 2007; Wille et al., 2008). This association suggests that these negative $\delta^{13}\text{C}_{\text{CaCO}_3}$ anomalies may not be entirely controlled by global reductions in f_{org} or ϵ , but may have been driven partly by isotopic gradients caused by local upwelling of basinal waters that provided isotopically light carbon and enough reducing power to drive

increases in U and V. This hypothesis must be tested with trace-element time series that span the Lower Cambrian from other continents.

DISCUSSION

In this paper, we map lowest Cambrian records of $\delta^{13}\text{C}_{\text{CaCO}_3}$ variability from Siberia, Mongolia, and China onto the Moroccan U/Pb– $\delta^{13}\text{C}_{\text{CaCO}_3}$ age model constrained by five single-zircon U/Pb ages from interbedded volcanic ashes (Fig. 5). We also present new $\delta^{13}\text{C}_{\text{org}}$, $^{87}\text{Sr}/^{86}\text{Sr}$, uranium, and vanadium data from the same carbonate samples that define the Moroccan U/Pb– $\delta^{13}\text{C}_{\text{CaCO}_3}$ age model. The result is a new absolute time line of first appearances of skeletal animals (Figs. A2–A4 [see Appendix]) that avoids the circularity associated with using biostratigraphic correlations and that is presented in the context of coincident changes in the cycling of carbon and trace elements in the ocean. Better than ever before, we are now capable of determining the absolute timing of biological and environmental change in the earliest Cambrian.

The time line of small shelly fossil first appearances indicates the following (Figs. 6 and 7).

(1) All aragonitic taxa appeared in the Nemakit-Daldynian, before the first appearances

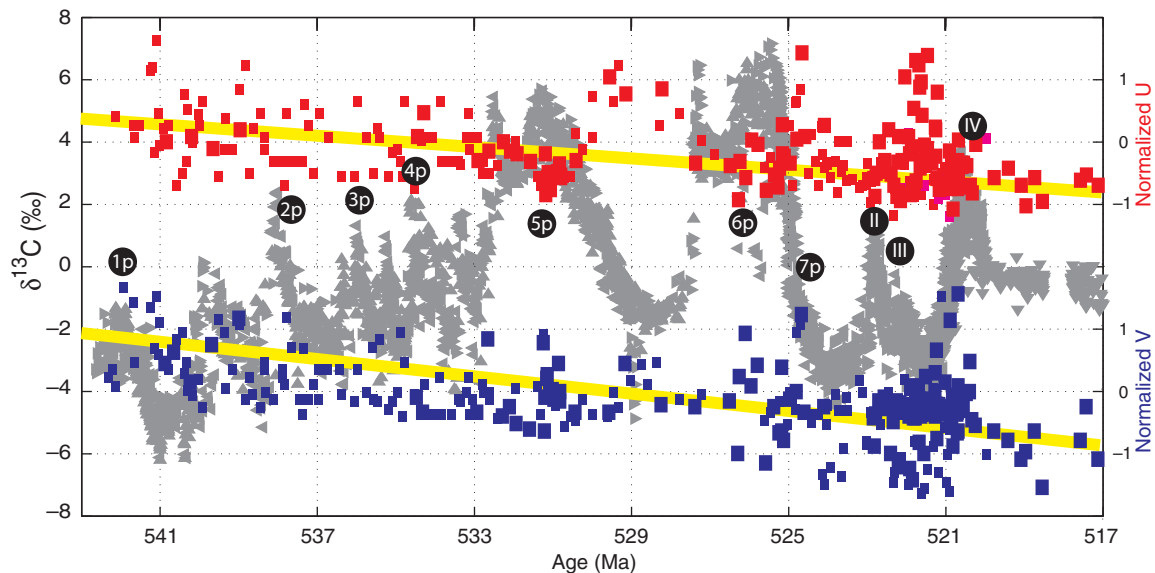


Figure 11. Time evolution of uranium (red) and vanadium (blue) against $\delta^{13}\text{C}_{\text{CaCO}_3}$ (gray) in Moroccan carbonates. Large and small squares depict samples that pass and fail, respectively, the combined [Sr] and Mn/Sr test for diagenetic alteration (see Appendix section A10). Regardless of whether we include all data or only the filtered data, linear regressions (yellow lines) depict a statistically significant decline in U and V with time: all U data $R^2 = 0.25$, $p = 1.11 \times 10^{-12}$; filtered U data $R^2 = 0.19$, $p = 2.71 \times 10^{-7}$; all V data $R^2 = 0.30$, $p = 6.54 \times 10^{-15}$; filtered V data $R^2 = 0.25$, $p = 9.22 \times 10^{-10}$.

of calcitic taxa, confirming earlier studies (Porter, 2007; Zhuravlev and Wood, 2008), and suggesting that the Mg/Ca ratio of seawater determines skeletal mineralogy at the time that carbonate skeletons first evolve in a clade. Phosphatic taxa appear through the Nemakit-Daldynian as well, although their first appearances are not restricted to this time interval (unlike those of aragonitic taxa).

(2) The major groups of small shelly fossils appear early; five appear by 540–538 Ma, and all but one appear by 534–532 Ma.

(3) By the middle of the Nemakit-Daldynian (534–532 Ma), nearly half of the total number of small shelly fossil genera recorded in our data set had appeared, and by the end of the Nemakit-Daldynian, nearly three-quarters had appeared, suggesting that diversification of these animals occurred throughout the Nemakit-Daldynian, rather than being concentrated at the end of that time. The dominant contributors to the pattern of first appearances are the molluscs and hyoliths, and to a lesser extent cap-shaped fossils and coeloscleritophorans, all of which may be closely related.

(4) Three pulses in fossil first appearances, the smallest in the early Nemakit-Daldynian, ca. 540–538 Ma ($\text{pulse}_{\text{eND}}$), the largest in the middle Nemakit-Daldynian, ca. 534–530 Ma ($\text{pulse}_{\text{mND}}$), and the third in the Tommotian, ca. 524–522 Ma (pulse_{T}), may reflect peaks in

small shelly fossil diversification, but could also reflect the influence of local ($\text{pulse}_{\text{eND}}$) or global ($\text{pulse}_{\text{mND}}$, pulse_{T}) preservational biases.

Although we do not understand the causes of these pulses or of the large-scale changes in the Early Cambrian carbon cycle, it may be significant that just subsequent to the largest pulse ($\text{pulse}_{\text{mND}}$), the first of the two large reorganizations of the carbon cycle during the Early Cambrian occurred. At ca. 533 Ma, $\delta^{13}\text{C}_{\text{CaCO}_3}$ begins to rise and eventually reaches $\geq +4\text{‰}$ for the first time. From 533 to 525 Ma, the $\delta^{13}\text{C}_{\text{CaCO}_3}$ oscillations are twice as large and ~ 4 times less frequent than in the previous 9 m.y. Furthermore, by 532 Ma, $\delta^{13}\text{C}_{\text{org}}$ behavior has changed from being uncorrelated with $\delta^{13}\text{C}_{\text{CaCO}_3}$ (variability in the carbon isotopic composition of organic matter associated with differences in biology, preservation, or contamination by ancient organic carbon weathered from the continents) to being correlated with $\delta^{13}\text{C}_{\text{CaCO}_3}$ ($\delta^{13}\text{C}$ changes dominated by changes in global f_{org}). Similarly, the third pulse (pulse_{T}) occurs after the 8‰ negative $\delta^{13}\text{C}_{\text{CaCO}_3}$ shift that accompanies the Nemakit-Daldynian–Tommotian boundary. This negative $\delta^{13}\text{C}_{\text{CaCO}_3}$ shift lasted just 506 ± 126 k.y. (Maloof et al., 2010a) and corresponds to the switch from f_{org} -dominated carbon cycle volatility back to much smaller-amplitude $\delta^{13}\text{C}_{\text{CaCO}_3}$ oscillations and $\delta^{13}\text{C}_{\text{org}}$ variability affected

by local changes in biology, preservation, or contamination.

Superimposed on this 1–10 m.y. time scale variability in skeletal animal first appearances and the carbon cycle, there is a 20 m.y. monotonic decline in uranium, vanadium, and $^{87}\text{Sr}/^{86}\text{Sr}$. The uranium and vanadium records suggest long-term oxidation of the sediment-water interface in shallow continental shelf environments, and are consistent with the Lower Cambrian record of increasing depth and thoroughness of bioturbation. The $^{87}\text{Sr}/^{86}\text{Sr}$ record is consistent with a relative increase in the hydrothermal flux of Sr to the ocean that would have led to a gradual decrease in the Mg/Ca ratio of seawater (Fig. 9). This change in Mg/Ca ratio predicts a switch from aragonite to calcite seas at ca. 525 Ma, which is reflected in a change from aragonite to calcite in the mineralogies of animals that evolve carbonate biomineralization associated with the youngest pulse of first appearances near the Nemakit-Daldynian–Tommotian boundary (Porter, 2007).

The increase in the rate of hydrothermal alteration of basalt also is consistent with an increase in mid-ocean-ridge length associated with the initial opening of the Iapetus Ocean (Fig. 3) and a rise in global sea level. The diachronous flooding of at least part of all the continents during the Early Cambrian could be associated with this predicted rise in global sea level, although

dynamic topography associated with mantle convection must have had an equally large impact on the regional sea level observed in the stratigraphy of continental margins. Regardless of the origin of the observed flooding of continental margins (Matthews and Cowie, 1979; McKie, 1993; Haq and Schutter, 2008), recent work by Peters (2005) supports the long-standing hypothesis (Newell, 1952, 1962; Valentine and Moores, 1970; Schopf, 1974; Simberloff, 1974; Hallam and Wignall, 1999) that the total global area of flooded continental shelves, and thus the total area of shallow marine habitat, controls the rate of taxonomic origination and extinction.

A wide variety of different causes for the Cambrian “explosion” have been presented over the years (reviewed by Marshall, 2006), including environmental triggers, increased genetic complexity, and feedbacks relating to increasing ecological complexity. The environmental parameter most commonly invoked as a trigger for animal radiation is atmospheric pO_2 , which could have reached a threshold level in the earliest Cambrian that allowed for larger organisms with complex physiologies and abilities to create collagen-containing tissues (Towe, 1970). There is no independent evidence for a rise in atmospheric oxygen at the Ediacaran-Cambrian boundary, however. An explanation for the processes responsible for the radiation of animals, and of whether the radiation was a consequence or a cause of associated geochemical changes, requires a thorough understanding of the pattern of that radiation, to which this paper contributes.

CONCLUSIONS

In his chapter on the imperfection of the geological record, Darwin alludes in passing to a different explanation for the supposed sudden appearance of animals in the lowest fossiliferous strata. He writes “[w]e should not forget that only a small portion of the world is known with accuracy” (Darwin, 1859, p. 307). It is this explanation—the incompleteness of our knowledge—that has turned out to be closer to the truth. The problem of missing fossil ancestors was solved by the discovery of the Precambrian fossil record, the problem that nearly all the animal phyla appear in the Lower Cambrian with no evidence of intermediate taxa was solved by the recognition that most Lower Cambrian fossils represent stem-groups of living phyla, and the problem of the explosive diversification of animals at the start of the Tommotian was solved by improved correlation and radiometric dating of Lower Cambrian sequences—to which we contribute here—showing that this diversification was drawn out over more than 20 m.y.

APPENDIX

A1. $\delta^{13}C_{CaCO_3}$ Methods

No previously unpublished $\delta^{13}C_{CaCO_3}$ data are reported in this paper. For Morocco (Maloof et al., 2005, 2010a), clean dolostones and limestones with minimal siliclastic components and secondary veining or cleavage were targeted. Samples were slabbed and polished perpendicular to bedding and ~5 mg of powder were microdrilled from individual laminations for isotopic analysis. Aliquots of approximately 1 mg of powder were heated to 200°C to remove volatile contaminants and water. Samples were then placed in individual borosilicate reaction vessels and reacted at 76°C with three drops of H_3PO_4 in a Finnigan MAT Kiel I preparation device coupled directly to the inlet of a Finnigan MAT 251 triple collector–isotope ratio–mass spectrometer, and $\delta^{13}C$ and $\delta^{18}O$ data were acquired simultaneously. $\delta^{13}C$ and $\delta^{18}O$ are reported in the standard delta notation as the ‰ difference from the Vienna Peedee belemnite (VPDB) standard. Precision and accuracy of data were monitored through daily analysis of at least six standards, which were run to ratchet sample suites at the beginning, middle, and end of the day’s runs. Measured precision was maintained at better than 0.1‰ (1 σ) for both $\delta^{13}C$ and $\delta^{18}O$.

A2.1. $\delta^{13}C_{org}$ Methods

Organic carbon isotopic values for Morocco were obtained from the total organic carbon (TOC) of insoluble residues. After removing the outside layer of surface oxidation and large veins, whole-rock samples were crushed into powder. Insoluble residues for organic carbon isotope analysis were obtained by acidifying these whole-rock powders in 6 N HCl for 24 h to dissolve all carbonate minerals. Care was taken to ensure that acid was added and acidification continued until there was absolutely no visible carbonate dissolution, so that the analyses would not be affected by contamination from residual inorganic carbon. The insoluble residues were then rinsed with deionized (DI) water, dried, and loaded into tin capsules for isotopic analysis. At the Massachusetts Institute of Technology (MIT) and Washington University, samples were flash combusted at 1030°C in a Costech ECS 4010 Elemental Analyzer. The resulting CO_2 gas was analyzed by continuous flow on a Delta V Plus continuous flow–isotope ratio–mass spectrometer. The $\delta^{13}C_{org}$ values were calibrated against the NBS 22 standard using the accepted value of $\delta^{13}C_{org} = -30.03‰$. Reproducibility (typically better than 0.5‰) was verified by duplicate sample analyses and regularly interspersed international standards (IAEA-CH-6, $-10.45‰$). The $\delta^{13}C_{org}$ values are reported in standard delta notation relative to VPDB. Organic C concentrations were measured using standards with known carbon concentration and the intensity of mass 44. TOC values for the bulk samples were calculated by combining the carbon concentration data with measurements of the ratio of insoluble residue to original pre-decarbonated powder. The values of $\delta^{13}C_{CaCO_3}$, $\delta^{13}C_{org}$, ϵ , and TOC are plotted together in Figure A1.

A2.2. Carbon Cycle Systematics

If f_{org} ($f_{org} = C_{org}/C_{total}$ is the fraction of carbon buried that is organic) is constant, the $\delta^{13}C_{CaCO_3}$ versus ϵ (ϵ is the difference between DIC and organic carbon, often dominated by the kinetic isotope effect associated with the uptake of carbon by photoautotrophs) plot (Fig. A1C) should have a slope equal to f_{org} and

a y-intercept equal to $\delta^{13}C_{in}$: 0.2–0.3 and $-6‰$, respectively, for the Cenozoic (Rothman et al., 2003). However, Figure A1C has a slope of unity and an intercept of $-22.6‰$, typical of Cryogenian and Ediacaran carbonates, where $\delta^{13}C_{CaCO_3}$ varies but $\delta^{13}C_{org}$ does not (Rothman et al., 2003). Because the $\delta^{13}C_{org}$ signal is damped by a factor of 1.5–2 with respect to $\delta^{13}C_{CaCO_3}$, and because data in the cross plot span a variety of events and >20 m.y., the $\delta^{13}C_{CaCO_3}$ - ϵ cross plot is misleading and demonstrates that blind use of cross plots without stratigraphic context and event-by-event analysis can be dangerous. The damping of the $\delta^{13}C_{org}$ signal may reflect the possibility that some part of the $\delta^{13}C_{CaCO_3}$ signal recorded in restricted platform carbonates does not represent open-ocean DIC (Appendix section A9), or that some part of the $\delta^{13}C_{org}$ signal reflects ancient organic matter (be it DOC or recycled sedimentary carbon).

A3. $^{87}Sr/^{86}Sr$ Methods

Available $^{87}Sr/^{86}Sr$ data for Siberia, Mongolia, and China were gleaned from the literature with little possibility for quality control. All $^{87}Sr/^{86}Sr$ data from Morocco were acquired at the MIT Radiogenic Isotope Laboratory. The 5–10 mg aliquots of carbonate from the same powders prepared for $\delta^{13}C_{org}$ were first reacted sequentially in an ultrasonic bath 3–5 times for 15–45 min in 1.0 mL of 0.2 M ammonium acetate to exchange loosely bound Sr cations, which included radiogenic ^{87}Sr derived from ^{87}Rb decay (Gao et al., 1996; Montañez et al., 1996; Bailey et al., 2000). Three 15–30 min sequential ultrasonic washes in water removed residual ammonium and some of the suspended clay fraction. The remaining carbonate was reacted for 5 min with 1.0 mL 1.4 M acetic acid, and insoluble residue was removed by centrifugation. Sr was isolated via standard chromatographic techniques using EICHRoM SR-spec resin and eluted with ultrapure H_2O . Samples were analyzed by thermal ionization mass spectrometry (TIMS) on a Micromass IsoProbe T in dynamic mode. All data were corrected for internal mass bias using $^{86}Sr/^{88}Sr = 0.1194$. Analyses were referenced against NBS SRM 987 (0.710250), with a long-term average of 0.710240 and 2 σ external precision of 0.000014 ($N > 100$).

A4. Elemental Concentration Methods

Elemental concentrations (e.g., Ca, Mg, Fe, Mn, Rb, Sr, Th, U, V) for Morocco samples were determined by inductively coupled plasma–mass spectrometry (ICP-MS). All samples were prepared by digesting a 0.5 g aliquot from the same carbonate powder used for $\delta^{13}C_{org}$ and $^{87}Sr/^{86}Sr$ in aqua regia at 90°C in a microprocessor-controlled digestion block for 2 h. This digestion was not total and would not dissolve silicates or oxides. The solution was diluted and analyzed by ICP-MS using a Perkin Elmer SCIEX ELAN 6100 at ActLabs. One blank was run for every 68 samples, along with digested certified reference materials USGS GXR-1, GXR-2, GXR-4, and GXR-6. An in-house control was run every 33 samples. Internal control standards and a duplicate were analyzed after every 10 samples. External error (1 σ), determined by repeat analyses, was 7% for all elements, with the best precision achieved for Ca, Mg, and Sr.

A5. U/Pb Geochronology Methods

No new geochronological data are reported in this paper. However, all of the ages from Morocco, Siberia, China, and Oman used to construct our age

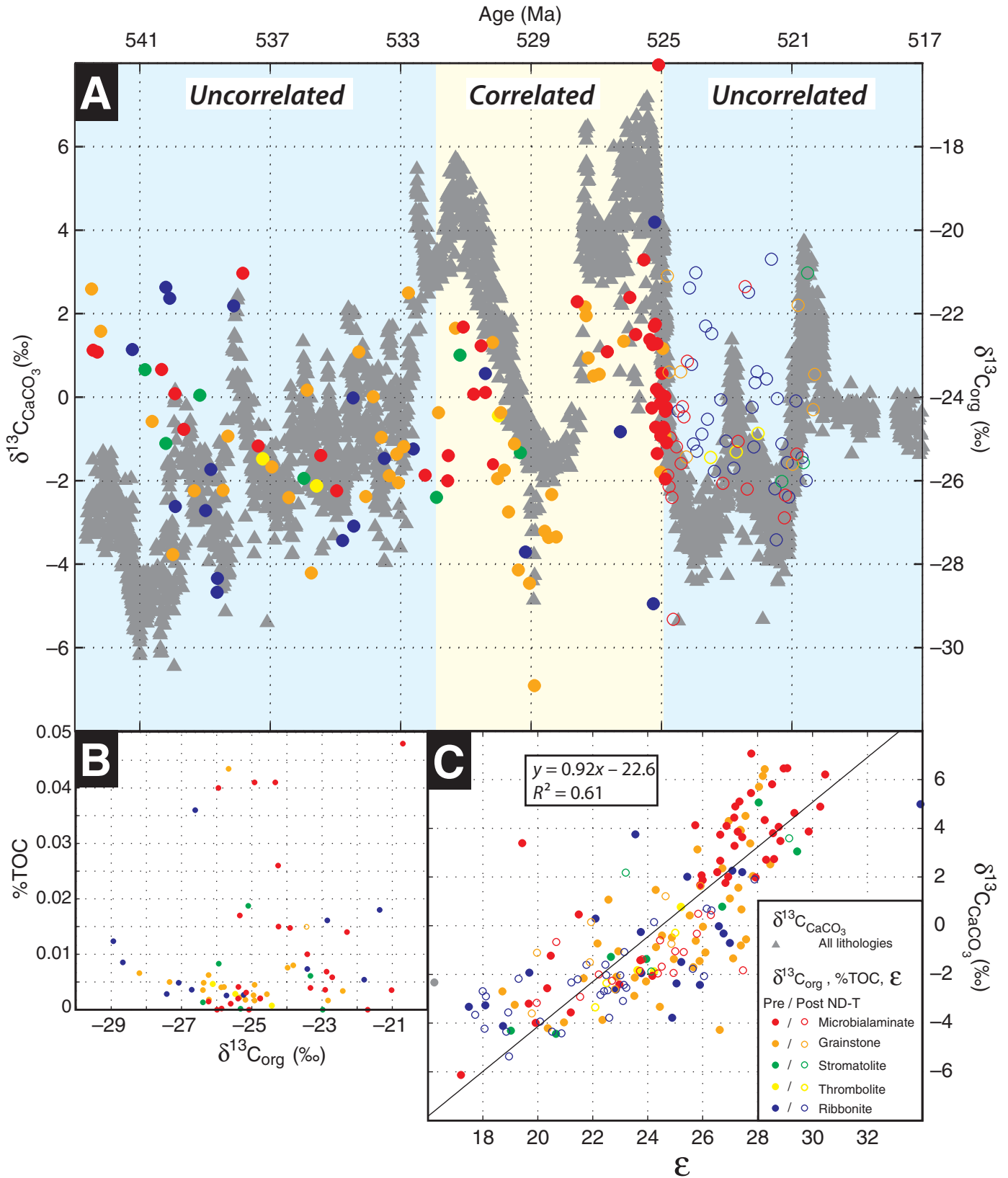


Figure A1. Paired carbonate and organic carbon $\delta^{13}\text{C}$ from the same carbonate samples from Oued Sdas and Sidi M'Sal. Data are color coded for lithology. (A) $\delta^{13}\text{C}_{\text{CaCO}_3}$ - $\delta^{13}\text{C}_{\text{org}}$ variation through time, with intervals of correlated and uncorrelated behavior highlighted in yellow and blue, respectively. (B) Total organic carbon (TOC) versus $\delta^{13}\text{C}_{\text{org}}$. (C) $\delta^{13}\text{C}_{\text{CaCO}_3}$ versus ϵ , with a linear fit computed using the reduced major axis method.

model were obtained at the MIT geochronology laboratory over the past two decades. During that time, techniques have evolved. Perhaps the most important change in technique is the routine application of Mattinson's (2005) chemical abrasion technique. In the chemical abrasion method, high-temperature annealing repairs radiation damage in zircon and prevents preferential leaching of Pb relative to U during multistep digestions. Annealed zircons were dissolved in two steps with the initial HF digestion step preferentially dissolving the most damaged zircon, which is most likely to be affected by postcrystallization Pb loss, isolating the highest quality low-U zircon for final analysis.

Prior to routine use of chemical abrasion, many analyses were affected by Pb loss, despite mechanical abrasion. In these situations, the $^{207}\text{Pb}/^{206}\text{Pb}$ date is older than the $^{207}\text{Pb}/^{235}\text{U}$ date, which is in turn older than the $^{206}\text{Pb}/^{238}\text{U}$ date. In many of these cases, the most precise estimate for the age of an ash bed was derived by taking the weighted mean $^{207}\text{Pb}/^{206}\text{Pb}$ date of the most concordant analyses, with the $^{206}\text{Pb}/^{238}\text{U}$ date often being much younger. In samples treated by chemical abrasion, it is common to calculate weighted mean $^{206}\text{Pb}/^{238}\text{U}$, $^{207}\text{Pb}/^{235}\text{U}$, and $^{207}\text{Pb}/^{206}\text{Pb}$ dates for each sample based on coherent clusters of data for which all scatter can be explained by analytical uncertainty alone. Most high-precision zircon data exhibit a slight but systematic discordance (with $^{206}\text{Pb}/^{238}\text{U} < ^{207}\text{Pb}/^{235}\text{U} < ^{207}\text{Pb}/^{206}\text{Pb}$ dates) likely related to inaccuracy in one or both of the U decay constants (Mattinson, 2000, 2010; Schoene et al., 2006). Thus, it has become accepted to use the weighted mean $^{206}\text{Pb}/^{238}\text{U}$ date as the most precise and accurate representation of the eruption/depositional age, and we follow this practice here. Mattinson (2010) also proposed that a new decay constant should be calculated for ^{235}U , assuming that the decay constant for ^{238}U is accurate, such that the two U-Pb dates will be concordant. In the soon-to-be-published version of the geological time scale (GTS2010), an attempt has been made to propagate decay constant uncertainties and to correct the ^{235}U decay constant for legacy data (M. Schmitz, 2010, oral communication). In general, the net effects are to decrease the published $^{207}\text{Pb}/^{206}\text{Pb}$ dates and to significantly increase the age uncertainties. However, if the analyses are rendered concordant after the correction, one can use the higher-precision weighted mean $^{206}\text{Pb}/^{238}\text{U}$ date. Thus, for legacy data, Pb-Pb and U-Pb dates should not be used interchangeably when calculating durations or rates. A good example is sample 94-N-11 (Grotzinger et al., 1995), for which ten multigrain fractions resulted in a $^{207}\text{Pb}/^{206}\text{Pb}$ date of 543.3 ± 1.0 Ma, and a weighted mean $^{206}\text{Pb}/^{238}\text{U}$ date of 540.61 ± 0.88 Ma. Recalculating the data with a new decay constant yielded a weighted mean. The preferred weighted mean $^{206}\text{Pb}/^{238}\text{U}$ age is much closer to the estimate for the E-C boundary in Oman (Bowring et al., 2007) based in CATIMS $^{206}\text{Pb}/^{238}\text{U}$ data. Where relevant, we report both the originally published and recalculated ages.

A6. U/Pb- $\delta^{13}\text{C}_{\text{CaCO}_3}$ Age Model

The $\delta^{13}\text{C}_{\text{CaCO}_3}$ record from Morocco is directly constrained by four weighted mean $^{206}\text{Pb}/^{238}\text{U}$ zircon dates from ash beds within the carbonate stratigraphy: 525.343 ± 0.088 Ma (Malooof et al., 2005, 2010a), 524.837 ± 0.092 Ma (Malooof et al., 2010a), 523.17 ± 0.16 Ma (Malooof et al., 2010a), 520.93 ± 0.14 Ma (Landing et al., 1998; Compston et al., 1992; Malooof et al., 2010a), and one weighted mean $^{207}\text{Pb}/^{206}\text{Pb}$ zircon date of 517 ± 1.5 Ma (Landing et al., 1998). When

the ca. 517 Ma $^{207}\text{Pb}/^{206}\text{Pb}$ age is recalculated using new decay constants (see Appendix section A5), five single grains have a weighted mean $^{206}\text{Pb}/^{238}\text{U}$ date of 515.56 ± 1.03 Ma. The oldest four of these dates are labeled with gray bars along the bottom of Figure 5. Two other indirect radiometric ages are used as tie points for the Morocco $\delta^{13}\text{C}_{\text{CaCO}_3}$ record. The onset (1p; Fig. 5) of the Ediacaran-Cambrian boundary negative $\delta^{13}\text{C}_{\text{CaCO}_3}$ excursion is pinned to a weighted mean $^{206}\text{Pb}/^{238}\text{U}$ zircon date of 542.3 ± 0.2 Ma from Oman (yellow bar in Fig. 5; Bowring et al., 2007). The beginning of the first $\geq +4\text{‰}$ positive $\delta^{13}\text{C}_{\text{CaCO}_3}$ excursion (5p; Fig. 5) is pinned to a weighted mean $^{206}\text{Pb}/^{238}\text{U}$ zircon date from Bed 5 Meishucun of ca. 533 Ma (Brooks et al., 2006; Jenkins et al., 2002; red bar in Fig. 5). Between each of these radiometric tie points, sediment accumulation rates are assumed to be constant. We pay particular attention to each predicted change in sediment accumulation rate to determine whether these changes are consistent with visible sedimentary or stratigraphic evidence. For example, in Morocco, the transition between the Adoudounian and Lie de Vin Formations heralds an increase in siliciclastic input to the basin, and a simultaneous increase in relative sea level and sedimentation rate within the Tiout-Aguerd Trough (Malooof et al., 2005, 2010a).

Next, individual $\delta^{13}\text{C}_{\text{CaCO}_3}$ records from Siberia, Mongolia, and China are stretched to best fit the Moroccan U/Pb- $\delta^{13}\text{C}_{\text{CaCO}_3}$ age model. The least ambiguous correlation is for Sukharikha (Kouchinsky et al., 2007), where the $\delta^{13}\text{C}_{\text{CaCO}_3}$ curve matches Morocco peak for peak in remarkable detail (Fig. 5). Several workers have already generated a suite of consistent correlations between $\delta^{13}\text{C}_{\text{CaCO}_3}$ stratigraphies within Siberia (Magaritz et al., 1986, 1991; Kirschvink et al., 1991; Brasier et al., 1993, 1994; Knoll et al., 1995b; Kaufman et al., 1996; Brasier and Sukhov, 1998; Kouchinsky et al., 2001, 2005, 2007). We tune all of these individual records to Morocco, taking note of each change in sedimentation rate required to fit the age model. For example, the base of the Tommotian Stage is defined by an unconformity at the type sections at Dvortsy and Ulakhan Sulugur, leading to a controversy over the duration of this sedimentary hiatus (e.g., Knoll et al., 1995b; Kaufman et al., 1996; Khomentovsky and Karlova, 2002, 2005). The U/Pb- $\delta^{13}\text{C}_{\text{CaCO}_3}$ age model supports the hypothesis that a substantial unconformity breaks the stratotype section of the Tommotian, while a well-structured $\delta^{13}\text{C}_{\text{CaCO}_3}$ curve exists elsewhere in Siberia during this time interval.

The Mongolian carbonates are mixed with siliciclastics for which there are no $\delta^{13}\text{C}_{\text{CaCO}_3}$ records. However, despite these gaps, a strong correlation can be made to virtually every positive $\delta^{13}\text{C}_{\text{CaCO}_3}$ excursion observed in Morocco and Siberia (except perhaps 3p; Fig. 5). In particular, the $+4\text{‰}$ to $+5\text{‰}$ $\delta^{13}\text{C}_{\text{CaCO}_3}$ peaks E (Salaany Gol, Section 2, Unit 7; Bayan Gol, Section 3B, Unit 21; and Kvetse-Tsakhir-Nuruu, Section 4, Unit 7) and F (Salaany Gol, Section 2, Unit 11/12) of Brasier et al. (1996) in the upper Bayan Gol Formation match well with the upper Nemakit-Daldynian (533–525 Ma) positive $\delta^{13}\text{C}_{\text{CaCO}_3}$ excursions 5p and 6p, respectively (Fig. 5). The favored age model also is consistent with the $^{87}\text{Sr}/^{86}\text{Sr}$ records from Morocco, Siberia, and Mongolia (Fig. 9).

China is pinned to the Moroccan U/Pb- $\delta^{13}\text{C}_{\text{CaCO}_3}$ age model by the first appearance of *Treptichnus pedum* and the $\delta^{13}\text{C}_{\text{CaCO}_3}$ -defined Ediacaran-Cambrian boundary, as well as the ca. 533 Ma date from Bed 5 at Meishucun (Brooks et al., 2006; Jenkins et al., 2002). However, several aspects of the Chinese $\delta^{13}\text{C}_{\text{CaCO}_3}$ record do not match Morocco, Siberia, and Mongolia.

For example, although the lower Nemakit-Daldynian (542–534 Ma) contains the right number of negative $\delta^{13}\text{C}_{\text{CaCO}_3}$ excursions, $\delta^{13}\text{C}_{\text{CaCO}_3}$ never reaches the $+1\text{‰}$ to $+2\text{‰}$ peaks characteristic of Morocco, Siberia, and Mongolia. Also, although there is no better place in the Lower Cambrian to place it, the nadir between 7p and II is deeper in China than in Morocco, Siberia, or Mongolia (Fig. 5). The Shiyantou and Yu'anhan formations that contain this nadir are dominated by silt and sand, and perhaps the $\delta^{13}\text{C}_{\text{CaCO}_3}$ from these units is not reliable. Nevertheless, at the ± 1 m.y. level, the proposed age model for China is the best fit to the $\delta^{13}\text{C}_{\text{CaCO}_3}$ and $^{87}\text{Sr}/^{86}\text{Sr}$ records from Morocco, Siberia, and Mongolia.

All of the stretches applied to generate the age model are collected in the GSA Data Repository.¹ With the best-fit U/Pb- $\delta^{13}\text{C}_{\text{CaCO}_3}$ age model constructed independent of the fossil record, small shelly fossil first appearances from different continents may be studied in the context of relative and absolute time (Fig. 5; see next section).

A7. Small Shelly Fossil Methods

Occurrence data for small shelly fossils were obtained from the literature for sections from which carbon isotopic data are available, using the following sources: Sukharikha—Voronova and Rozanov in Rozanov et al. (1969), Meshkova (1974), Luchina et al. (1997), and Kouchinsky et al. (2010); Kotuikan—Missarzhevsky in Rozanov et al. (1969), Val'kov (1975), and Savitsky et al. (1980); Bol'shaya Kuonamka—Val'kov (1975); Khorbusuonka—Karlova and Vodanyuk (1985) and Karlova (1987); Zhurinsky Mys—Sysoev (1972) and Grigor'eva and Varlamov in Rozanov and Sokolov (1984); Isit'—Missarzhevsky and Rozanov in Rozanov et al. (1969), Sysoev (1972), Meshkova (1974), and Grigor'eva and Repina in Rozanov and Sokolov (1984); Dvortsy—Krylov et al. in Rozanov et al. (1969), Sysoev (1972), Val'kov (1983), Grigor'eva in Rozanov and Sokolov (1984), and Fedorov et al. in Repina and Rozanov (1992); Ulakhan Sulugur—Krylov et al. in Rozanov et al. (1969), Grigor'eva in Rozanov and Sokolov (1984), and Fedorov et al. in Repina and Rozanov (1992); Selinde—Korshunov et al. (1969), Val'kov (1982), Voronova et al. (1983), Khomentovsky and Karlova (1986), and Repina et al. (1988); Salaany Gol—Korobov and Missarzhevsky (1977), Voronin et al. (1982), Endonzhamts and Lkhasuren (1988), and Esakova and Zhegallo (1996); Bayan Gol—Khomentovsky and Gibsher (1996) and Esakova and Zhegallo (1996); Kvetse-Tsakhir-Nuruu—Esakova and Zhegallo (1996); Meishucun—Qian (1989) and Qian and Bengtson (1989); Jijiapo—Chen (1984); and Xiaotan—Li et al. (2001). The stratigraphic data in these publications were compared with those associated with the isotopic data to assign fossil occurrences with the closest available isotopic sample (see GSA Data Repository [see footnote 1]). Where fossils were stated to be present from an unspecified level within a unit from which several isotopic measurements are available (e.g., Bed 3 in the Meishucun section, for which there are three samples with isotopic measurements), the fossil occurrences were assigned to the stratigraphically highest sample. If no isotopic measurements

¹GSA Data Repository item 2010293, Microsoft Excel Workbook containing stratigraphic, geochemical and biostratigraphic data presented in this paper, is available at <http://www.geosociety.org/pubs/ft2010.htm> or by request to editing@geosociety.org.

were available from the bed in which fossils occurred, the fossil occurrences were associated with the closest overlying isotopic measurement. These procedures are conservative in that first appearances are placed as late as possible. In any case, the age of most such units falls within a single time bin, and thus the choice of the sample to which to assign fossil occurrences does not influence the overall patterns presented here (e.g., all of Bed 3 in the Meishucun section is assigned an age of 534–533 Ma). In the sections at Dvortsy and Ulakhan Sulugur, the upper layers of the Yudoma Formation are karsted, and the fossils in these layers may be younger material in cavern fill (e.g., Khomentovsky and Karlova, 1993; but see Khomentovsky, 1997); as a result, all material in the upper Yudoma Formation at these localities was associated with the stratigraphically lowest isotopic measurement from the overlying Pestrosvet Formation.

In many cases, the taxonomy of the fossils has been revised since the publication of the references listed here. Consequently, the lists of species from the various sections were compared with the most recent and authoritative systematic literature in order to place them in the most appropriate genera and higher groups (see Data Repository [see footnote 1]). It should be noted that much of this material (notably the hyoliths) is still in need of systematic revision, so the generic assignments used here should only be regarded as tentative. The mineralogy of each higher group was assessed by reviewing the relevant literature (e.g., Bengtson and Conway Morris, 1992; Porter, 2010).

As described in Appendix section A6, chronometric dates were assigned to each carbon isotopic measurement, allowing a date to be placed on each fossil occurrence. Fossil occurrences for each genus were then placed in 2 m.y. time bins, and these were used to construct Figures 5 and 6. In Figures A2–A4, all Chinese sections were lumped together, as were all Mongolian sections, and all sections in the Lena-Aldan region (Dvortsy, Ulakhan Sulugur, Zhurinsky Mys, and Isit'). For Figure 6, the number of genera that first appear within each time bin was determined. To test the effects of individual sections on the pattern of first occurrences, the data for a particular section were omitted and the number of first occurrences recalculated. Similarly, to determine the contribution from each region (Siberia, Mongolia, or China), the data for the other two regions were omitted and the number of first occurrences recalculated.

A8. Paleogeography Methods

Traditionally, plate reconstructions are made by rotating paleomagnetic poles of similar age from different continents into collinearity. Then, one continent is moved around the mutual pole (i.e., across lines of paleolongitude) until an acceptable paleogeographic fit is achieved. Figure 3 is an example of such a plate reconstruction for ca. 525 Ma using the paleomagnetic poles collected in Table A1 and the rotations in Table A2. However, this paleogeography is poorly constrained and almost certainly inaccurate in detail.

First, no two poles from different continents are of the same quality or age (Table A1). Two Lower Cambrian poles exist for Laurentia. The Wichita Mountains granite (Oklahoma) is precisely dated with a U/Pb zircon age of 533 ± 3 Ma (Wright et al., 1996). Although there is some suggestion of a positive baked contact test with the discordantly underlying Glen Mountains Anorthosite (Roggenthen et al., 1981), the Wichita granite paleomagnetic pole has no rigorous positive field test and is substantially differ-

ent from the only other Lower Cambrian pole from Laurentia. The Mont Rigaud and Chatham-Grenville pole comes from two shallowly emplaced syenite intrusions along the failed rift arm of the Iapetus ocean (western Quebec) (Kumarapeli and Saull, 1966). The intrusions are dated using $^{40}\text{Ar}/^{39}\text{Ar}$ on hornblende and potassium feldspar, but neither passes a conclusive field test (McCausland et al., 2007). Paleomagnetic poles from Baltica (Torneråsk Formation; Torsvik and Rehnström, 2001) and Siberia (Kessyusa Formation and overlying Erket Formation, Khorbusuonka; Pisarevsky et al., 1997) come from sedimentary units with no radiometric ages, yet they are well-constrained in age in the context of the new U/Pb- $\delta^{13}\text{C}_{\text{CaCO}_3}$ age model presented in this paper. Unfortunately, none of these poles from Baltica or Siberia has undergone a rigorous field test. The $^{40}\text{Ar}/^{39}\text{Ar}$ age of 525 ± 5 Ma and the positive baked contact test make the Itabaiana mafic dikes (northeast Brazil, Amazonia) a particularly relevant paleomagnetic pole for Early Cambrian plate reconstructions (Trindade et al., 2006). The Ntonya igneous ring complex (Malawi-Congo craton) has an $^{40}\text{Ar}/^{39}\text{Ar}$ age of 522 ± 13 Ma, but no positive field test (Briden, 1968; Briden et al., 1993).

In the absence of paleomagnetic poles with positive field tests and statistically indistinguishable ages, an alternative way to create plate reconstructions is to fit small circle arcs representing the apparent polar wander (APW) path of paleomagnetic poles for each craton. Assuming constant long-term plate motion, specific ages can be interpolated along the APW paths and used as reconstruction points. Additionally, if each craton has two or more paleomagnetic poles that fall on a small circle, then the APW path for each craton should overlap, and the need for individual poles of identical age diminishes. Unfortunately, few cratons moved together during the continued continental dispersal of the Early Cambrian (e.g., Hoffman, 1991), and even western Gondwana (shown nearly joined in Fig. 3) may not have been sutured yet (Tohver et al., 2006). In the absence of combined individual pole and APW path constraints, relative paleolongitudes, and thus parameters such as the width of the Iapetus Ocean, remain unknown.

Not only are APW paths of marginal utility for the 525 Ma reconstruction, but even the high-quality Itabaiana dykes pole for Amazonia may not strictly constrain the latitude of West Africa if the continents had yet to be sutured. This point is particularly important because the fairly traditional (e.g., Hoffman, 1991; Cawood and Pisarevsky, 2006; McCausland et al., 2007) reconstruction in Figure 3 shows the 2-km-thick stromatolite/thrombolite/microbialite- and later archaeocyath-dominated carbonate platform of Morocco poleward of the Antarctic Circle. There are three possible solutions to this problem. (1) Tommotian–Atdabanian climate was similar to that of the middle Cretaceous (e.g., Huber et al., 1995; Herman and Spicer, 1996; Jenkyns et al., 2004) or early Eocene (e.g., Shackleton and Boersma, 1981; Greenwood and Wing, 1995; Sloan et al., 1995; Huber and Sloan, 2001), with generally warm temperatures and a very small equator- to-pole temperature gradient (e.g., Sloan and Pollard, 1998). However, this solution may be inconsistent with the observation that first and last appearances of archaeocyath reefs seem to be latitude-dependent, since they appear and disappear as continents such as Laurentia move through the carbonate belt (e.g., Debrenne and Courjault-Radé, 1994). Also, even during the equable climates of the mid-Cretaceous and Eocene, framework carbonate reefs did not develop poleward of 45°

latitude. (2) The Anti-Atlas margin may be allochthonous to West Africa prior to the Early Ordovician (Mitchell et al., 2010). However, the basement to the Anti-Atlas mountains consists of 2070 Ma metasediments (Walsh et al., 2002) intruded by 2050–2032 Ma granitoids (Walsh et al., 2002; Thomas et al., 2002; Roger et al., 2001; Hassenforder et al., 2001; Mortaj et al., 2000; Ait Malek et al., 1998), similar in age to the Birimian crust that makes up most of the West African craton (Boher et al., 1992). The Anti-Atlas Mountains would have to represent a ribbon continent rifted from West Africa during the Paleoproterozoic, and amalgamated with a Neoproterozoic arc complex prior to Late Cambrian or Early Ordovician collision with West Africa along a hidden suture beneath the Tindouf basin. Not only is this hypothesis ad hoc, but in the paleogeographic framework of Figure 3, it is not clear where the Anti-Atlas ribbon continent could have resided such that it enjoyed low latitudes during the Early Cambrian (i.e., far from northwestern Gondwana) but joined West Africa by Early Ordovician time. (3) The paleomagnetic data from Amazonia is younger than the $^{40}\text{Ar}/^{39}\text{Ar}$ age implies, or Gondwana was moving very rapidly during the Early Cambrian (see following).

Even during the preceding Ediacaran Period, the APW-based approach to plate reconstructions has been unsuccessful. While it is possible to choose or to reject subsets of any continent's paleomagnetic database in order to create a time-progressive APW path that does not require unrealistic rates of plate motion, it is impossible to do so entirely within the bounds of any objective quality filter (e.g., Kirschvink et al., 1997; Torsvik et al., 1998; Evans et al., 1998; Pisarevsky et al., 2000; Meert et al., 2001). This problem has led a number of authors to propose that the Early Cambrian was characterized by anomalously high plate motions or true polar wander (TPW—the wholesale rotation of the mantle and crust relative to the fluid outer core) (Kirschvink et al., 1997; Evans, 1998; Mitchell et al., 2010). True polar wander causes paleomagnetic poles to carve out great circle arcs perpendicular to the paleo-nonhydrostatic minimum moment of inertia, rather than the small circle arcs about Euler poles predicted for plate tectonic-driven motion. Additionally, if rapid TPW is oscillatory and fast (beyond the time resolution of the paleomagnetic database), the great circle distribution of poles may look like a zigzagging smear, rather than an age-progressive path. In a world where continental motion is dominated by rapid (e.g., <10 m.y.) oscillatory TPW events, poles from different cratons of sufficiently similar age (e.g., ± 1 m.y.) to warrant linear reconstruction may not exist at all, rendering traditional plate reconstruction methods impossible. However, a paleogeography can be reconstructed by rotating the great circle fits to paleomagnetic poles from individual cratons into coplanarity, thus bypassing the relative age of individual poles and capturing the effect of TPW on plate motions (Maloof, 2004; Raub et al., 2007). Maloof (2004) and Raub et al. (2007) performed this exercise using paleomagnetic poles spanning the 600–500 Ma time window and found that a plate reconstruction remarkably similar to that shown in Figure 3 could be generated, with Gondwana together and geologically consistent positions for Laurentia, Baltica, Siberia, and South China.

Unfortunately, even the TPW great circle technique does not bring us closer to defining the latitudinal distribution of the continents between 542 and 517 Ma. Whether we constrain the plate reconstruction using geology, individual paleomagnetic poles, APW paths, or TPW great circles, we typically arrive at a geography similar to that shown in Figure 3.

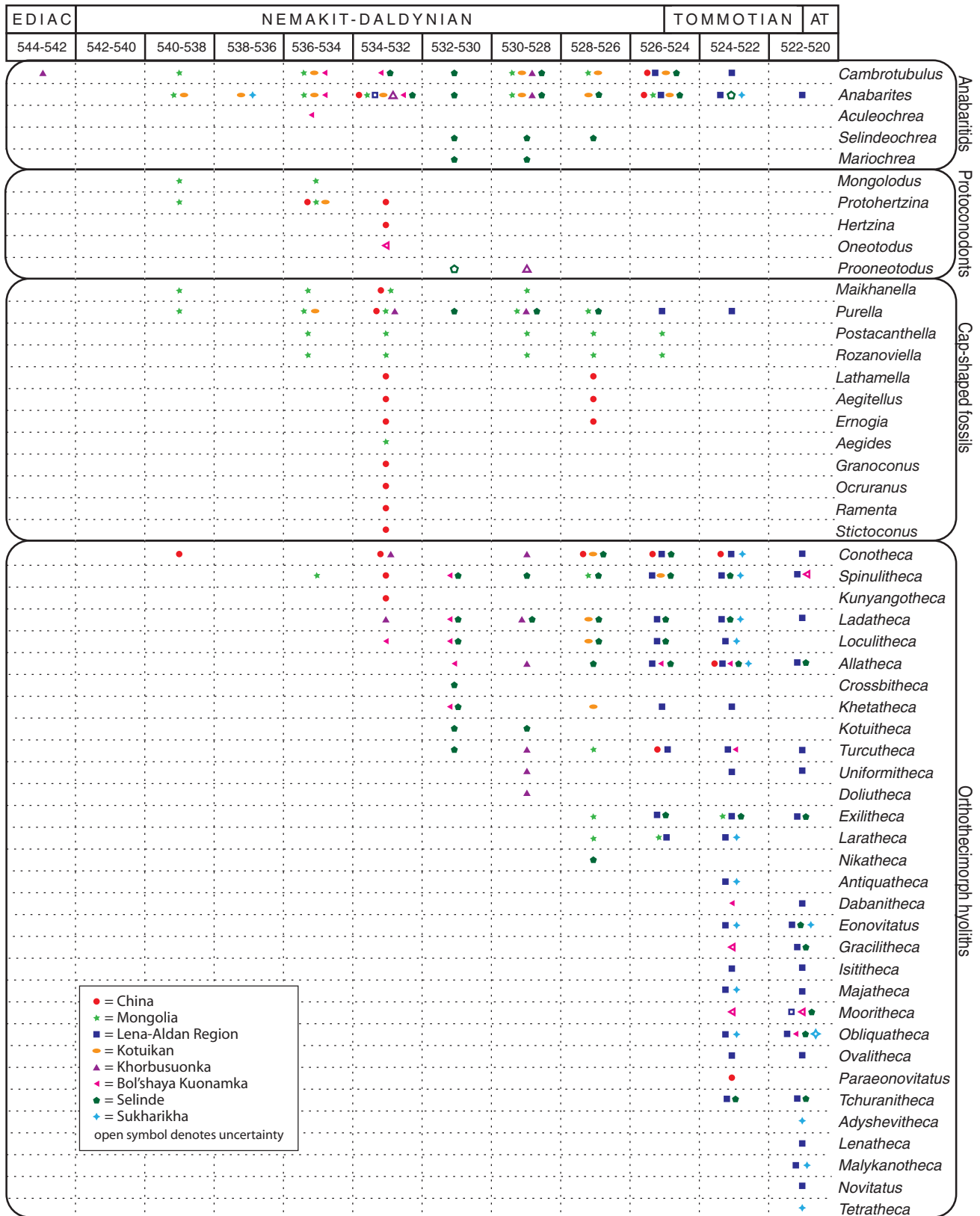


Figure A2. Occurrence data for 150 skeletal metazoan genera that are present in the earliest Cambrian (page 1 of 3). Genera are grouped according to higher taxa; orthothecimorph and hyolithomorph hyoliths are shown separately. Age boxes are defined by the U/Pb-calibrated $\delta^{13}C_{CaCO_3}$ age model, independent of the fossil first appearances themselves. See Appendix section A7 for detailed information regarding the construction of this figure.

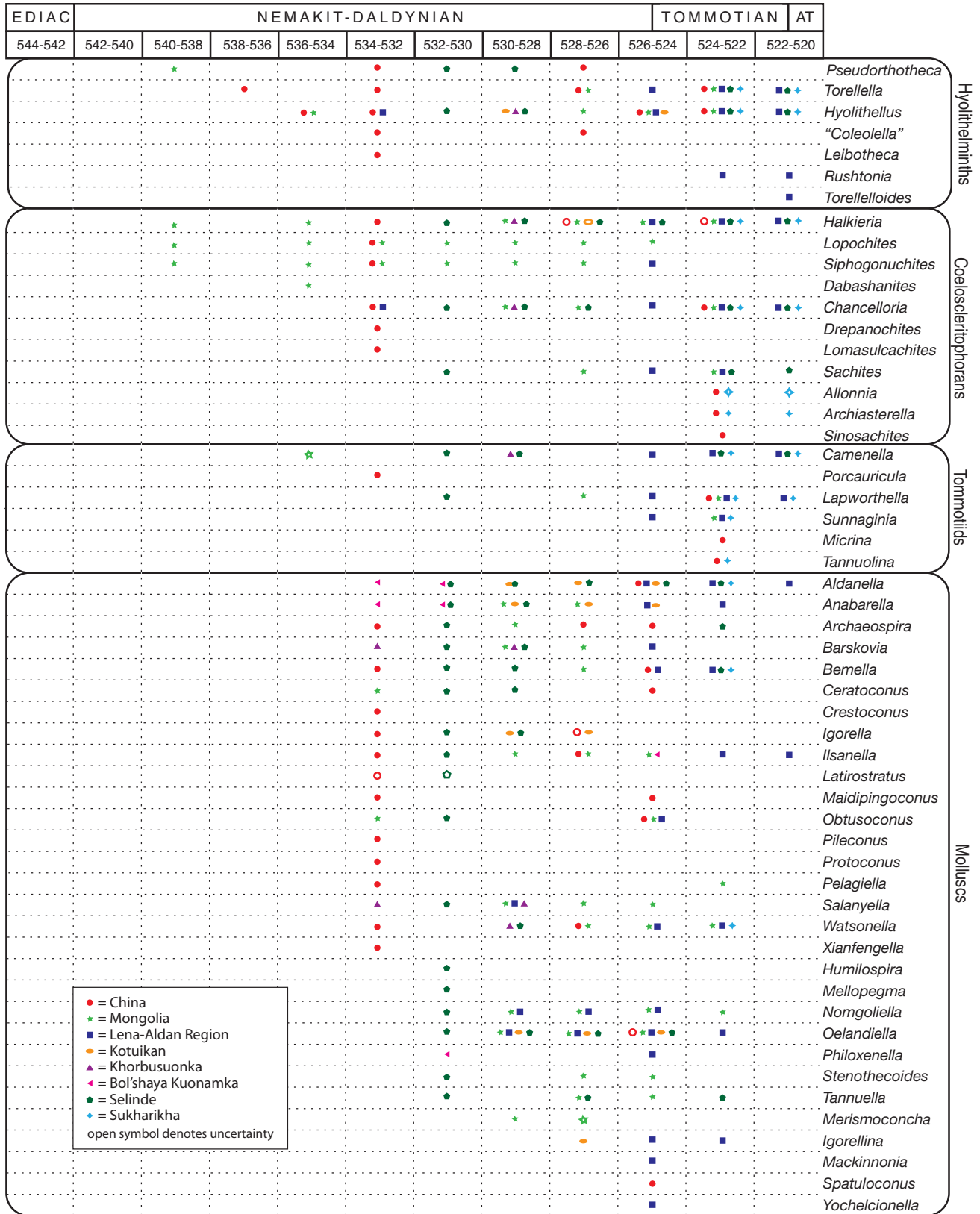


Figure A3. Occurrence data for 150 skeletal metazoan genera that are present in the earliest Cambrian (page 2 of 3). Genera are grouped according to higher taxa; orthothecimorph and hyolithomorph hyoliths are shown separately. Age boxes are defined by the U/Pb-calibrated $\delta^{13}\text{C}_{\text{CaCO}_3}$ age model, independent of the fossil first appearances themselves. See Appendix section A7 for detailed information regarding the construction of this figure.

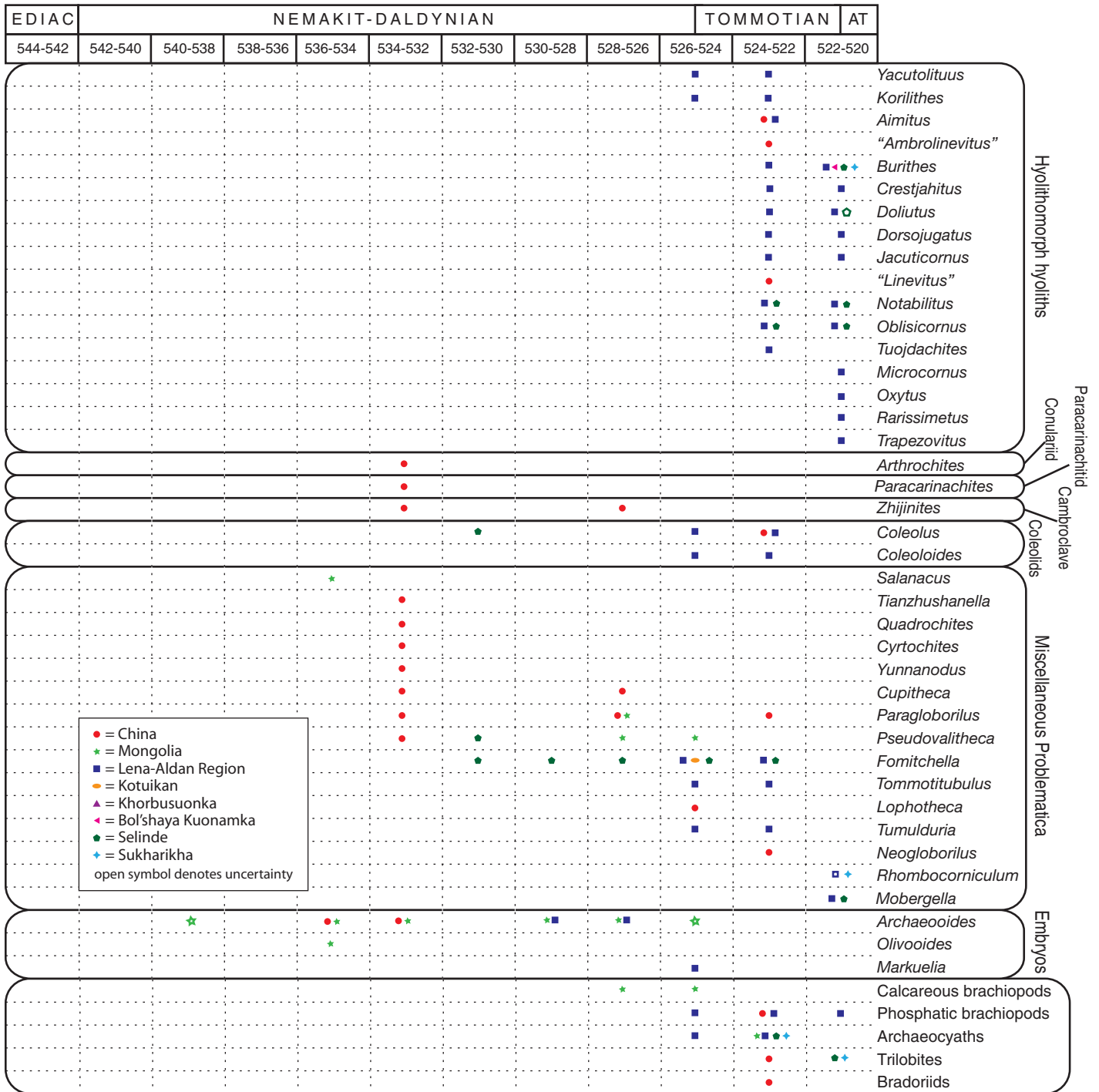


Figure A4. Occurrence data for 150 skeletal metazoan genera that are present in the earliest Cambrian (page 3 of 3). Genera are grouped according to higher taxa; orthothecimorph and hyolithomorph hyoliths are shown separately. Age boxes are defined by the U/Pb-calibrated $\delta^{13}\text{C}_{\text{CaCO}_3}$ age model, independent of the fossil first appearances themselves. See Appendix section A7 for detailed information regarding the construction of this figure.

TABLE A1. PALEOMAGNETIC POLES USED TO GENERATE THE PALEOGEOGRAPHY IN FIGURE 3

Craton	Unit	Code	PLAT	PLON	A ₉₅	Q	Unit age (Ma)	Age method
Laurentia	Wichita Granite (1)	WG	-2.0	327.0	8.5	4	533 ± 3 (2)	²⁰⁶ Pb/ ²³⁸ U
Laurentia	Mt. Rigaud and Chatham-Grenville (3)	MR	11.9	4.6	4.8	5	532 ± 2 (3)	⁴⁰ Ar/ ³⁹ Ar
Baltica	Tornetråsk Formation (4)	TT	56.0	116.0	12.0	4	533 ± 9	stratigraphic
Siberia	Kessyusa Formation (5)	KE	-37.6	165.0	9.3	4	533 ± 8	stratigraphic
Siberia	Erkeket Formation (5)	EK	-44.8	158.7	5.7	4	522 ± 3	stratigraphic
Amazonia	Itabaiana dikes (6)	IB	31.4	331.0	10.0	6	525 ± 5 (6)	⁴⁰ Ar/ ³⁹ Ar
Congo	Ntonya Ring (7)	NT	27.7	344.9	1.8	4	522 ± 13 (8)	⁴⁰ Ar/ ³⁹ Ar

Note: South China and Mongolia have no Lower Cambrian paleomagnetic constraints. PLAT, PLON, A₉₅, and Q refer to the latitude, longitude, 95% confidence circle, and quality factor (van der Voo, 1990) for each paleomagnetic pole. (1) Spall (1968) and Vincenz et al. (1975); (2) Wright et al. (1996); (3) McCausland et al. (2007); (4) Torsvik and Rehnström (2001); (5) Pisarevsky et al. (1997); (6) Trindade et al. (2006); (7) Briden (1968); (8) Briden et al. (1993).

The reconstructions still lack rigorous constraints on parameters such as the width of the Iapetus Ocean and the absolute rates of plate motion and true polar wander, and the reconstruction places Morocco at a latitude that appears too high for such thick shallow-water microbial carbonate accumulation. Better-resolved paleogeographic solutions may lie in paleomagnetic studies of the same sediments that contain the stratigraphic records of $\delta^{13}\text{C}_{\text{CaCO}_3}$, $^{87}\text{Sr}/^{86}\text{Sr}$, and fossils (e.g., Pisarevsky et al., 1997; Maloof et al., 2006; Mitchell et al., 2010).

A9. Are $\delta^{13}\text{C}_{\text{CaCO}_3}$ Data Records of the Global Ocean?

We hypothesize that the $\delta^{13}\text{C}_{\text{CaCO}_3}$ data from peritidal Lower Cambrian carbonates record a global signal linked to the open ocean. However, new $\delta^{13}\text{C}_{\text{CaCO}_3}$ data from upper Cenozoic carbonate platforms (Swart and Eberli, 2005; Swart, 2008) have called into question the assumption that ancient shelfal carbonates necessarily record the $\delta^{13}\text{C}$ of open-ocean dissolved inorganic carbon. Furthermore, two recent papers (Knauth and Kennedy, 2009; Derry, 2010) suggest that negative $\delta^{13}\text{C}_{\text{CaCO}_3}$ with covarying $\delta^{13}\text{C}_{\text{CaCO}_3}$ and $\delta^{18}\text{O}_{\text{CaCO}_3}$ are necessarily diagenetic in origin.

Ocean Drilling Project Leg 166 retrieved five cores from 362–658 m water depth on the leeward (western) slope of the Great Bahama Bank (Ginsburg, 2001). These aragonitic sediment cores depict a consistent Pliocene–Pleistocene rise in $\delta^{13}\text{C}_{\text{CaCO}_3}$ from ambient Miocene and Pliocene values of 1.5‰ to 2.5‰ to Pleistocene values of 3.0‰–4.5‰ (Swart and Eberli, 2005). In contrast, open-ocean planktonic foraminifera (low-Mg calcite) during the same interval record mean $\delta^{13}\text{C}$ values of 1‰ to 2‰ during the late Miocene (7–8 Ma) (Billups et al., 2008), followed by fluctuating mean values of -0.5‰ to 1.0‰ during the Pliocene (Billups et al., 2008), Pleistocene (Shackleton et al., 1983; Curry and Crowley, 1987), and Holocene (Wefer and Berger, 1991), with an ~1‰ gradient between ocean basins. Therefore, the leeward slope of the Great Bahama Bank appears to be anticorrelated with planktonic foraminifera of the open ocean during the Pliocene–Pleistocene (Swart and Eberli, 2005; Swart, 2008).

Swart and Eberli (2005) showed that the Bahamas cores each recorded a positive correlation between aragonite:calcite ratio and $\delta^{13}\text{C}_{\text{CaCO}_3}$. They speculated that the source of the ^{13}C -enriched aragonite found in the slope cores is mud precipitated by the calcifying green algae (e.g., *Halimeda*, *Penicillius*, and *Udotea*) inhabiting the shallows (1–10 m water depth) of the Great Bahama Bank (Swart and Eberli, 2005). Preferential uptake of ^{12}C by highly productive benthic sea grasses, algae, and microbial mats coupled to relatively sluggish mixing of shallow Great Bahama Bank waters with the open ocean (i.e., semi-closed-system

TABLE A2. TOTAL ROTATION FOR EACH CRATON USED TO CONSTRUCT FIGURE 3

Craton	Code	RLAT	RLON	Counterclockwise rotation
Laurentia	LAUR	37	208	-151
Baltica	BALT	24	210	-148
Siberia	SIB	17	220	-139
Amazonia	AM	9	216	-141
West Africa	WA	-4	244	-136
South China	SC	-62	140	107

Note: RLAT and RLON refer to the latitude and longitude, respectively, of the Euler pole for rotating the continent. The Mongolia ribbon continent is drawn without quantitative rotation.

behavior) tend to elevate $\delta^{13}\text{C}$ in any carbonate precipitated on the Great Bahama Bank (Lowenstam and Epstein, 1957; Andres et al., 2006). Additionally, at low to moderate water temperatures, aragonite is naturally enriched in ^{13}C by 1‰–2‰ compared to low-Mg calcite precipitated from the same waters (Rubinson and Clayton, 1969; Emrich et al., 1970; Romanek et al., 1992), further increasing $\delta^{13}\text{C}$ in Great Bahama Bank aragonite. Thus, Swart and Eberli (2005) proposed that $\delta^{13}\text{C}_{\text{CaCO}_3}$ preserved in Great Bahama Bank slope sediments does not record changes in the global carbon cycle, but instead reflects the relative efficiency of mud export from platform to slope. This aragonite mud transport efficiency, in turn, depends on relative sea level and the geometry of the carbonate bank (e.g., open ramp or flat-topped platform). Although the positive Pliocene–Pleistocene $\delta^{13}\text{C}_{\text{CaCO}_3}$ trend is damped, Swart (2008) demonstrated a similar anticorrelation between $\delta^{13}\text{C}_{\text{CaCO}_3}$ from open-ocean planktonic foraminifera and the slopes adjacent to platform carbonates in the Maldives and around Australia. Ironically, periplatform carbonates do not seem to be simple recorders of changes in open-ocean $\delta^{13}\text{C}_{\text{CaCO}_3}$, and yet they record a synchronous Pliocene–Pleistocene rise in $\delta^{13}\text{C}_{\text{CaCO}_3}$ and suggest that a global forcing, such as sea-level change, is controlling the efficiency of aragonite export from platforms (Swart, 2008).

In contrast to the western slope of the Great Bahama Bank, some carbonates on the bank itself do not record the Pliocene–Pleistocene positive $\delta^{13}\text{C}_{\text{CaCO}_3}$ shift. For example, Holocene aragonite muds from inner regions of the Great Bahama Bank (northwest Andros Island; Maloof, 2008, personal obs.) and Florida Bay (Patterson and Walter, 1994) have low $\delta^{13}\text{C}$ ranging from 1‰ to 2‰, consistent with similarly depleted ΣCO_2 in adjacent water. This signal is thought to be caused by progressive enrichment of ^{12}C from respired organic matter in aging water masses. Patterson and Walter (1994) likened this mechanism of ^{12}C enrichment to the vertical evolution of open-ocean water under the influence of the biological pump, with increasing ΣCO_2 and oxygen utilization with age and depth of the water mass (Kroopnick, 1985).

Even cores from the outer edge of the Great Bahama Bank itself (Clino and Unda; Ginsburg, 2001)

do not record the Pliocene–Pleistocene positive $\delta^{13}\text{C}$ swing that is documented on the slope. Swart and Eberli (2005) interpreted the Pleistocene $\delta^{13}\text{C}$ shift in Great Bahama Bank carbonates to values between -0.3‰ and -3.0‰ as a record of meteoric diagenesis during subaerial exposure caused by repeated glacial-interglacial sea-level changes of ~100 m.

Fluids responsible for meteoric diagenesis of carbonate rocks are rich in oxygen and poor in carbon. Therefore, altered specimens that show severe oxygen-isotope depletion still may faithfully record the $\delta^{13}\text{C}$ of oceanic DIC (Banner and Hanson, 1990; Jacobsen and Kaufman, 1999). However, work on the upper Cenozoic carbonates from the Great Bahama Bank (Swart and Eberli, 2005; Swart, 2008) suggests that even $\delta^{13}\text{C}_{\text{CaCO}_3}$ can be shifted a few per mil toward more negative values through diagenetic interactions with coastal pore fluids charged in isotopically depleted organic carbon. Covariant $\delta^{13}\text{C}_{\text{CaCO}_3}$ and $\delta^{18}\text{O}_{\text{CaCO}_3}$ values have been proposed as an index for differentiating between pristine and adulterated $\delta^{13}\text{C}$ values in diagenetically altered carbonates (Irwin et al., 1977; Kaufman et al., 1991). Knauth and Kennedy (2009) even suggested that highly depleted $\delta^{13}\text{C}_{\text{CaCO}_3}$ and covariation in $\delta^{13}\text{C}_{\text{CaCO}_3}$ and $\delta^{18}\text{O}_{\text{CaCO}_3}$ during the middle Ediacaran “Shuram” anomaly (Burns and Matter, 1993; Fike et al., 2006; McFadden et al., 2008) are diagenetic in origin and indicative of terrestrial “greening.” However, in another attempt to explain the very deep Shuram $\delta^{13}\text{C}_{\text{CaCO}_3}$ anomaly, Derry (2010) found that covarying $\delta^{13}\text{C}_{\text{CaCO}_3}$ - $\delta^{18}\text{O}_{\text{CaCO}_3}$ only resulted when two fluids (a CO_2 -charged water depleted in ^{13}C from interactions with organic matter and an ^{18}O -enriched brine) were allowed to alter the sediments at ~100°C during burial diagenesis.

Despite the apparent decoupling of Pliocene–Pleistocene carbonate shelf and open-marine $\delta^{13}\text{C}_{\text{CaCO}_3}$ records and the new ideas for meteoric or basinal brine diagenesis, there are several reasons to think that the carbon isotope data in the Lower Cambrian record a global DIC signal, and not just internal processes related to (1) meteoric diagenesis, (2) basin restriction, (3) riverine input, and (4) changes in aragonite mud transport efficiency:

Meteorite Diagenesis

In Lower Cambrian limestones and dolostones, lower $\delta^{13}\text{C}_{\text{CaCO}_3}$ values are not necessarily associated with lower $\delta^{18}\text{O}_{\text{CaCO}_3}$. In fact, there is no statistically significant covariation between $\delta^{13}\text{C}_{\text{CaCO}_3}$ and $\delta^{18}\text{O}_{\text{CaCO}_3}$, whether carbon and oxygen are compared between continents (Fig. A5) or by mineralogy and lithofacies (and thus initial porosity and permeability) in Morocco (Fig. A6F). For example, the ND-T transition is characterized by a 9‰ drop in $\delta^{13}\text{C}_{\text{CaCO}_3}$ over 50–200 m (Fig. 5). No sympathetic negative $\delta^{18}\text{O}_{\text{CaCO}_3}$ shift is observed across the ND-T boundary. Instead, $\delta^{18}\text{O}_{\text{CaCO}_3}$ varies chaotically between -5‰ and -8‰ throughout the entire interval, with no significant correlation to $\delta^{13}\text{C}_{\text{CaCO}_3}$ or lithofacies (Maloof et al., 2005).

Subaerial exposure surfaces are abundant in Morocco, and yet brecciated and recrystallized dolostones immediately below exposure surfaces rarely show ^{13}C depletion of more than 1‰. It is impossible to assess accurately the duration of subaerial exposure on these surfaces. However, we can infer a maximum average duration of 10–30 k.y. based on the ~26 exposure surfaces recorded during the ND-T transition at Zawyat n' Bougzoul and Sidi M'Sal. We also suggest that base-level drops were minimal because, with very few exceptions, karstic relief never exceeds 10 cm. Perhaps large base-level drops (50–120 m) of long duration (30–90 k.y.) typical of the Pleistocene (Siddall et al., 2003; Bintanja et al., 2005) and a substantial terrestrial biomass are required to impart a diagenetic $\delta^{13}\text{C}_{\text{CaCO}_3}$ signal to subaerial exposure surfaces.

Basin Restriction

In Morocco, wavy laminated carbonate muds and silts from interior lagoonal environments (Fig. 4A, 11—Zawyat n' Bougzoul and 16—Sidi M'Sal) are offset -1‰ to -3‰ from outer-shelf stromatolites and microbialites of the central Tiout-Aguerd trough (Fig. 4A, 7—Oued Sdas) (Maloof et al., 2010a). This isotopic offset is similar to that observed today in Florida Bay (Patterson and Walter, 1994) and may represent progressive depletion in ^{13}C as aging water masses on the poorly mixed interior of the shelf accumulated ^{13}C from respired marine organic matter. We also think that geometry, restriction, and water depth associated with coalescence and isolation of shelf areas, or changing sea level through time could lead to vertical $\delta^{13}\text{C}_{\text{CaCO}_3}$ variability not associated with changes in global ocean DIC. For example, Immenhauser et al. (2003) explained a 1‰ – 2‰ positive shift in $\delta^{13}\text{C}_{\text{CaCO}_3}$ that is progressively damped landward across the late Carboniferous platform of northern Spain as the transition from shallow, old, ^{13}C -depleted water and frequent meteorite diagenesis to deeper water better connected to the open ocean. Holmden et al. (1998) made a similar argument for a 0‰ – 3‰ positive $\delta^{13}\text{C}_{\text{CaCO}_3}$ excursion damped across the Mohawkian (Ordovician) epicontinental seaway of North America, and demonstrated that different $\delta^{13}\text{C}_{\text{CaCO}_3}$ values are associated with unique conodont ϵ_{Nd} compositions, indicating that shelfal waters were mixing slower than the ~300 yr residence time of Nd in the ocean. Although epeiric seas are bound to develop geochemically distinct and time-varying water, we have not found related mechanisms that could be responsible for the large-amplitude 4‰ – 9‰ variability observed in at least approximately contemporaneous Lower Cambrian $\delta^{13}\text{C}_{\text{CaCO}_3}$ records in Morocco, Siberia, Mongolia, and China (Fig. 5).

Riverine Input

Although the Cambrian shelf in Morocco is similar in size to the Great Bahama Bank, the Anti-Atlas margin fringed the large emergent continent of West

Africa and was not permanently isolated from riverine input the way the Great Bahama Bank is today. The Lie de Vin Formation heralds a westward (modern day coordinates) progradation of fluvial sands from the continent, which would have increased freshwater discharge into the basin. However, 75% of the ND-T $\delta^{13}\text{C}_{\text{CaCO}_3}$ negative shift was accomplished within the Adoudonian Formation, prior to any indication of increased siliciclastic input to the system.

Aragonite vs. Calcite

A transition from aragonite seas to calcite seas did occur sometime during the Nemakit-Daldynian Stage, perhaps near the ND-T boundary (Fig. 6; Porter, 2007), which could be linked to a 1‰ – 2‰ negative shift in $\delta^{13}\text{C}_{\text{CaCO}_3}$ (4–8× smaller than the observed ND-T boundary negative $\delta^{13}\text{C}_{\text{CaCO}_3}$ shift; Maloof et al., 2010a). However, the idea that stratigraphic $\delta^{13}\text{C}_{\text{CaCO}_3}$ variability is due to changes in the export efficiency of carbon-isotopically distinct platform material to the slope is not tenable for at least two reasons. First, calcareous plankton had not yet evolved in the Early Cambrian (Lipps, 1993; Hou et al., 1996; Katz et al., 2007), so platformal benthic skeletal debris and muds were likely the dominant source of carbonate both on the platform and on the slope. Second, in Morocco, virtually the entire 2.5 km stack of sediment preserved in the Anti-Atlas Mountains was deposited above storm wave base, and most of the material was deposited in the photic zone on the continental shelf, where slope processes are irrelevant. In fact, narrow periplatform slope environments tend to get severely deformed during orogenesis and rarely are preserved in large, structurally simple mappable units. Therefore, most Cambrian stratigraphic successions (including the Siberian, Mongolian, and Chinese sections in Fig. 5) record almost exclusively platformal signals.

One of the most striking arguments against an internal-process origin for anything but small-amplitude $\delta^{13}\text{C}_{\text{CaCO}_3}$ variability in Morocco is that Lower Cambrian $\delta^{13}\text{C}_{\text{CaCO}_3}$ from Siberia and Mo-

rocco can be matched peak for peak without violating biostratigraphic or geochronological constraints (Maloof et al., 2005). Such consistent correlation between geographically distant sedimentary basins characterized by very different lithologies and sedimentation rates suggests that global forcing played a dominant role. We conclude that high-amplitude $\delta^{13}\text{C}_{\text{CaCO}_3}$ variability in Lower Cambrian shelfal carbonates records an open-ocean signature of a changing global carbon cycle.

A10. Diagenesis and $^{87}\text{Sr}/^{86}\text{Sr}$, Uranium, and Vanadium

While the isotopic composition of major constituents like carbon may remain intact during neomorphism and recrystallization, trace elements such as strontium may be ejected from the carbonate lattice and replaced with better-fitting magnesium, calcium, or manganese. Dolomite ($\text{CaMg}[\text{CO}_3]_2$) is a major constituent of Lower Cambrian carbonate rocks, but it is rare in Holocene sediments (Given and Wilkinson, 1987; Sun, 1994). The origin of ancient dolostones (Zenger et al., 1980; Purser et al., 1994) has been interpreted as replacement of CaCO_3 at elevated burial temperatures (e.g., Mountjoy and Amthor, 1994), replacement of CaCO_3 below the sediment-water interface in suboxic environments where sulfate (a possible kinetic inhibitor to dolomite formation) is removed and alkalinity is added by bacterial sulfate reduction (e.g., Baker and Burns, 1985; Vasconcelos and McKenzie, 1997; Warthmann et al., 2000), or as primary dolomite precipitated under changing global ocean conditions (e.g., Arvidson and Mackenzie, 1999; Burns et al., 2000). Limestones likely began as aragonite or high-Mg calcite that later neomorphosed to more stable calcite spar.

It is common to exclude altered samples based on cutoff values of isotopic and elemental characteristics identified in general studies of Neoproterozoic carbonates (Derry et al., 1989; Kaufman et al., 1993;

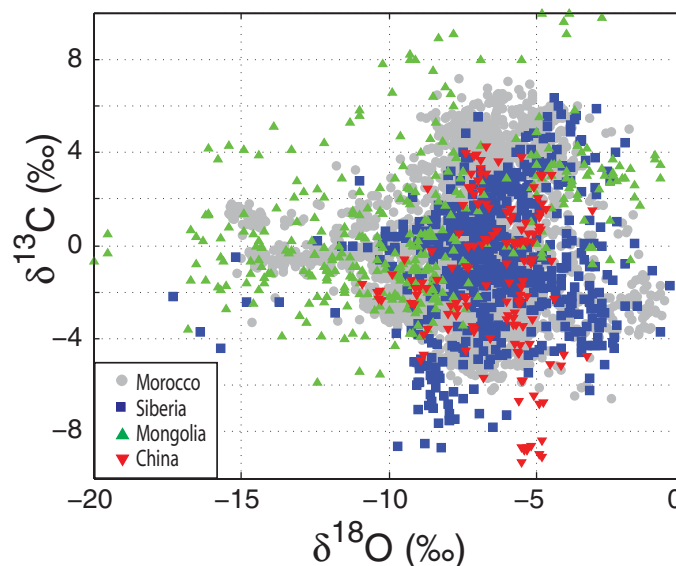


Figure A5. $\delta^{18}\text{O}_{\text{CaCO}_3}$ vs. $\delta^{13}\text{C}_{\text{CaCO}_3}$ cross plot. Data from Morocco (including all measured sections from Maloof et al., 2005), Siberia, Mongolia, and China all depict a similar population with no $\delta^{18}\text{O}$ - $\delta^{13}\text{C}$ covariance.

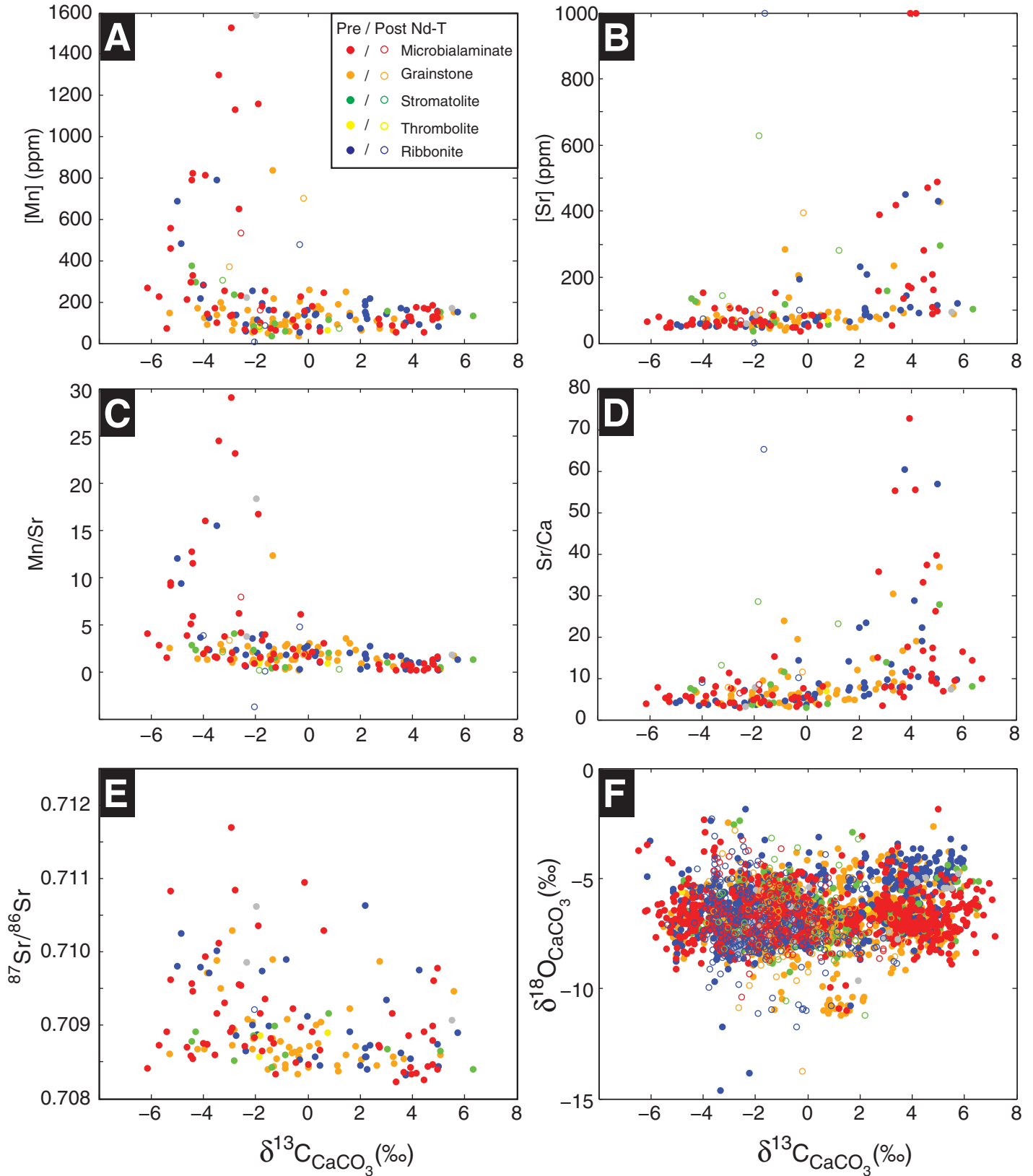


Figure A6. Cross plots depicting (A) [Mn], (B) [Sr], (C) Mn/Sr, (D) Sr/Ca, (E) $^{87}\text{Sr}/^{86}\text{Sr}$, and (F) $\delta^{18}\text{O}_{\text{CaCO}_3}$ versus $\delta^{13}\text{C}_{\text{CaCO}_3}$ show no statistically significant covariation. Furthermore, no lithofacies-dependent trends emerge, such as would be expected if diagenetic alteration were controlled by primary porosity and permeability.

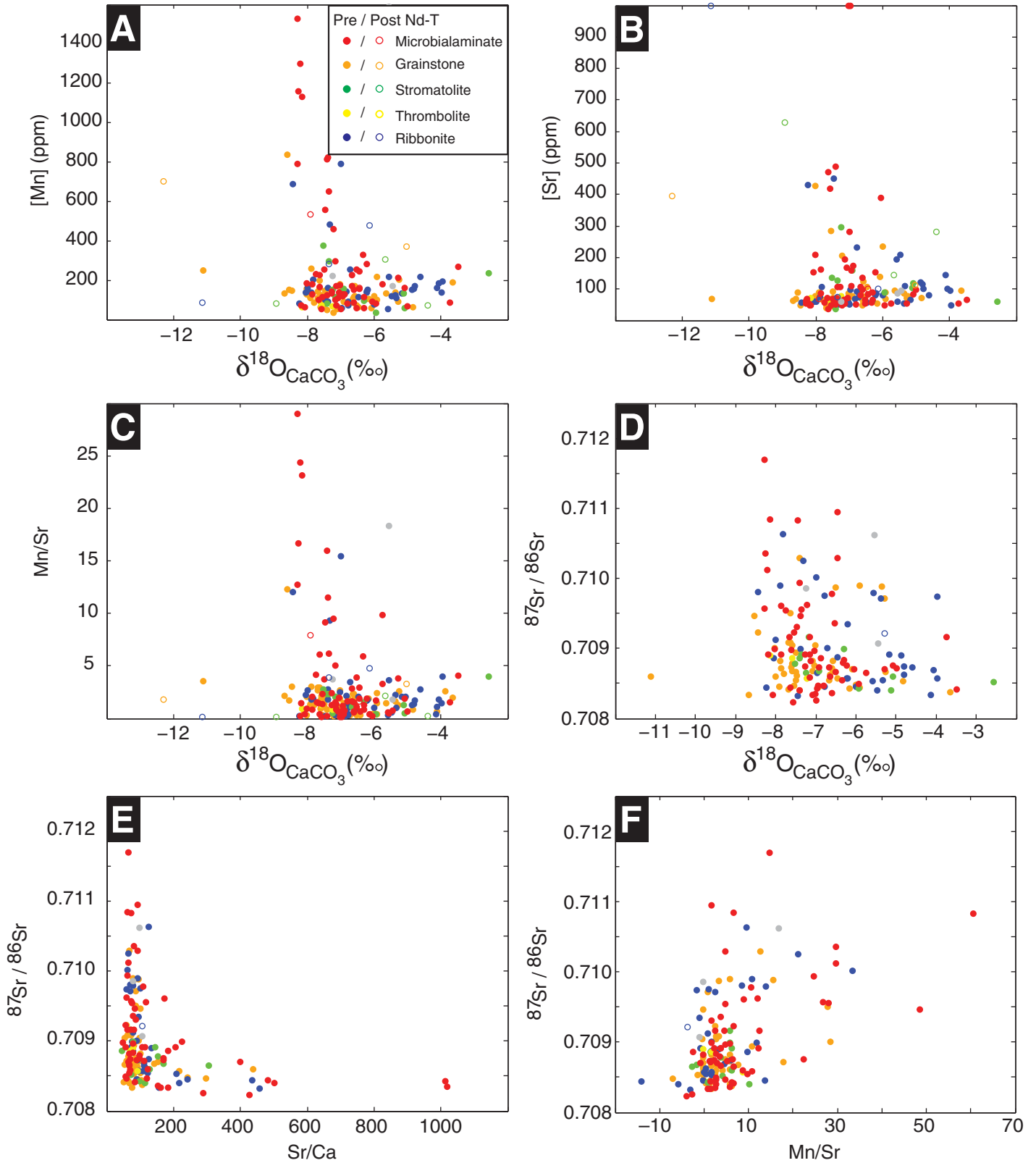


Figure A7. Cross plots depicting (A) [Mn], (B) [Sr], (C) Mn/Sr, and (D) $^{87}\text{Sr}/^{86}\text{Sr}$ versus $\delta^{18}\text{O}_{\text{CaCO}_3}$; (E) $^{87}\text{Sr}/^{86}\text{Sr}$ versus Sr/Ca; and (F) $^{87}\text{Sr}/^{86}\text{Sr}$ versus Mn/Sr. No lithofacies-dependent trends emerge, such as would be expected if diagenetic alteration were controlled by primary porosity and permeability.

Fölling and Frimmel, 2002). We prefer to establish the geochemical criteria for excluding altered samples on a case-by-case basis because there is no reason to assume that rocks with different geological histories should have experienced the same alteration pathways (Bartley et al., 2001; Halverson et al., 2007). We find that Sr concentration (Figs. A7 and A8) is the most useful single parameter for assessing the potential preservation of primary seawater $^{87}\text{Sr}/^{86}\text{Sr}$ (Halverson et al., 2007). Mn/Sr (Fig. A7F) also is a sensitive indicator of meteoric diagenesis (Brand and Veizer, 1980; Banner and Hanson, 1990; Jacobsen and Kaufman, 1999), although high [Mn] may indicate primary carbonate precipitation from dysoxic waters. Another potential metric for diagenetic alteration is $\delta^{18}\text{O}_{\text{CaCO}_3}$. However, in Morocco, Siberia, Mongolia, and China, there is no consistent covariation between $\delta^{18}\text{O}_{\text{CaCO}_3}$ and $^{87}\text{Sr}/^{86}\text{Sr}$ (Fig. A7D).

We are justified in basing our selection criterion on [Sr] since most alteration pathways decrease [Sr] (but see Derry, 2010), thus increasing the susceptibility of a given $^{87}\text{Sr}/^{86}\text{Sr}$ signature to overprinting (Brand and Veizer, 1980; Veizer, 1989; Banner and

Hanson, 1990). The result of diagenetic overprinting is a sharp increase in $^{87}\text{Sr}/^{86}\text{Sr}$ below a threshold [Sr] (Fig. A8), as predicted by water-rock geochemical models (e.g., Banner and Hanson, 1990; Jacobsen and Kaufman, 1999). Because the initial [Sr] of carbonates differs significantly as a function of original mineralogy (calcite vs. aragonite) and varying seawater [Sr] (e.g., Stoll et al., 1999), and due to variable [Sr] concentrations in diagenetic fluids, this [Sr] threshold is different for every rock. We establish the cutoff [Sr] based on a cross plot of $^{87}\text{Sr}/^{86}\text{Sr}$ versus [Sr] for each Lower Cambrian section (i.e., Morocco, Siberia, Mongolia, and China; Fig. A8). A similar Mn/Sr versus $^{87}\text{Sr}/^{86}\text{Sr}$ cross plot (Fig. A7F) results in a nearly identical filter.

Redox-sensitive trace elements such as uranium and vanadium are sensitive to the same diagenetic processes that reduce [Sr] and increase Mn/Sr in carbonates, and we may apply the same filter that we derived for $^{87}\text{Sr}/^{86}\text{Sr}$ to exclude altered U and V data. However, the ammonium acetate leaching method (see Appendix section A3), which effectively removes radiogenically ingrown (non-carbonate-

lattice-bound) ^{87}Sr from the decay of rubidium-rich clays, was not applied to solutions used for U and V analyses. Therefore, there is the potential that some of the U and V measured in carbonate powders is detrital in origin, preserved in clays mixed into the rocks rather than U and V complexes in the carbonate lattice itself. To correct for terrestrial contamination, we use Th, which is virtually absent in normal seawater, as a proxy for terrestrial contamination, and subtract U and V using the U/Th and V/Th ratios of post-Archean average shale (PAAS) compositions (Taylor and McLennan, 1985). The data set was normalized to aid in visualization.

A11. Numerical Model of Mg, Ca, and Sr in Seawater

The geochemical cycles of magnesium, calcium, and strontium in seawater reflect the balance between sources and sinks:

$$\frac{d\text{Mg}}{dt} = W_{\text{Mg-carb}} + W_{\text{Mg-sil}} - H_{\text{Mg-clays}} - P_{\text{Mg-carb}} \quad (\text{A1})$$

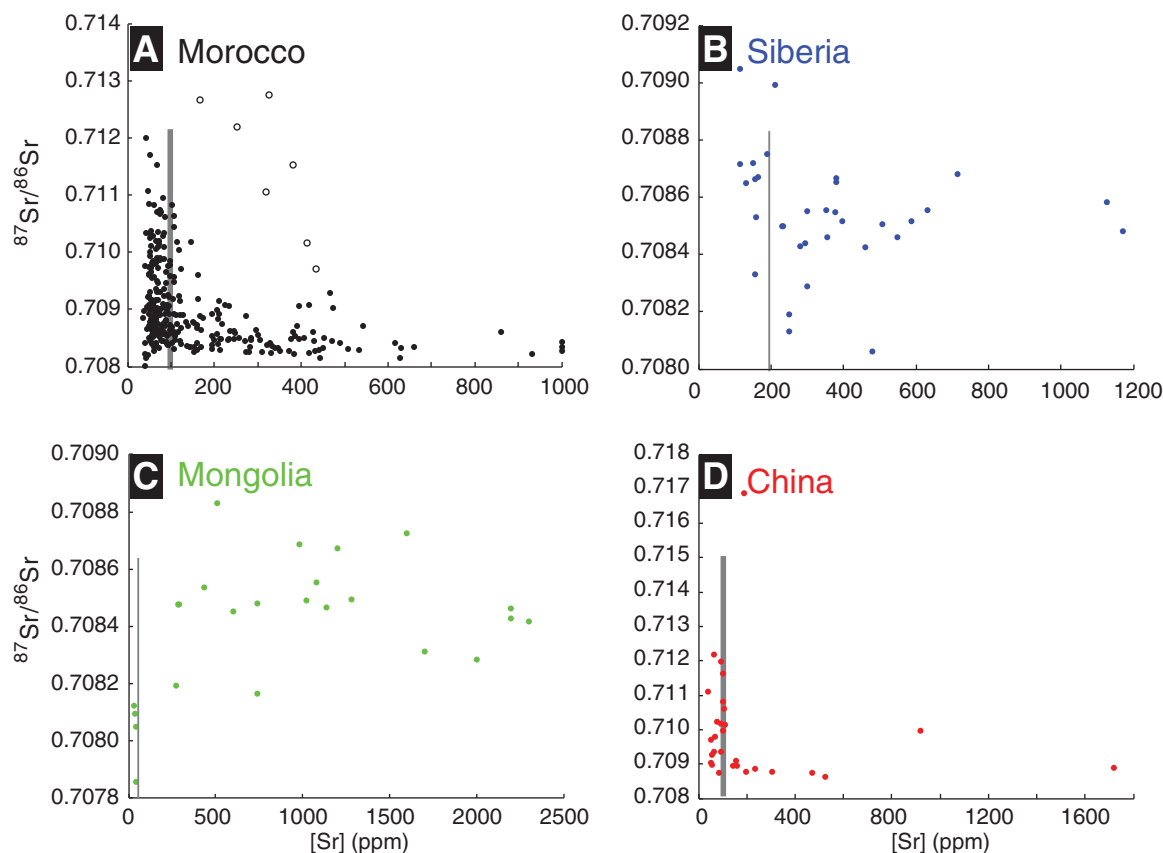


Figure A8. Low concentrations of Sr suggest diagenetic removal of Sr from the carbonate lattice, and make bulk carbonate $^{87}\text{Sr}/^{86}\text{Sr}$ more susceptible to contamination by rubidium decay in clays and the ingrowth of non-lattice-bound ^{87}Sr . For Morocco (A) and China (D), the [Sr] cutoff is obvious and marked with a thick gray vertical line, while for Siberia (B) and Mongolia (C), the relationship between [Sr] and $^{87}\text{Sr}/^{86}\text{Sr}$ is less clear, and the filter is less reliable. For Morocco, a Mn/Sr-based filter is slightly less stringent but yields a similar result. The open symbols in A are from strongly recrystallized archaeocyath reefs at Talat n' Yissi and Sidi M'Sal (Fig. 4A), and it is not known why that unit has uniquely high $^{87}\text{Sr}/^{86}\text{Sr}$ and [Sr]. The effect of filtering the Morocco data is depicted in stratigraphic context in Figure A9. Filtered $^{87}\text{Sr}/^{86}\text{Sr}$ data for Morocco, Siberia, Mongolia, and China are plotted together in the $\delta^{13}\text{C}_{\text{CaCO}_3}$ age model in Figure 9.

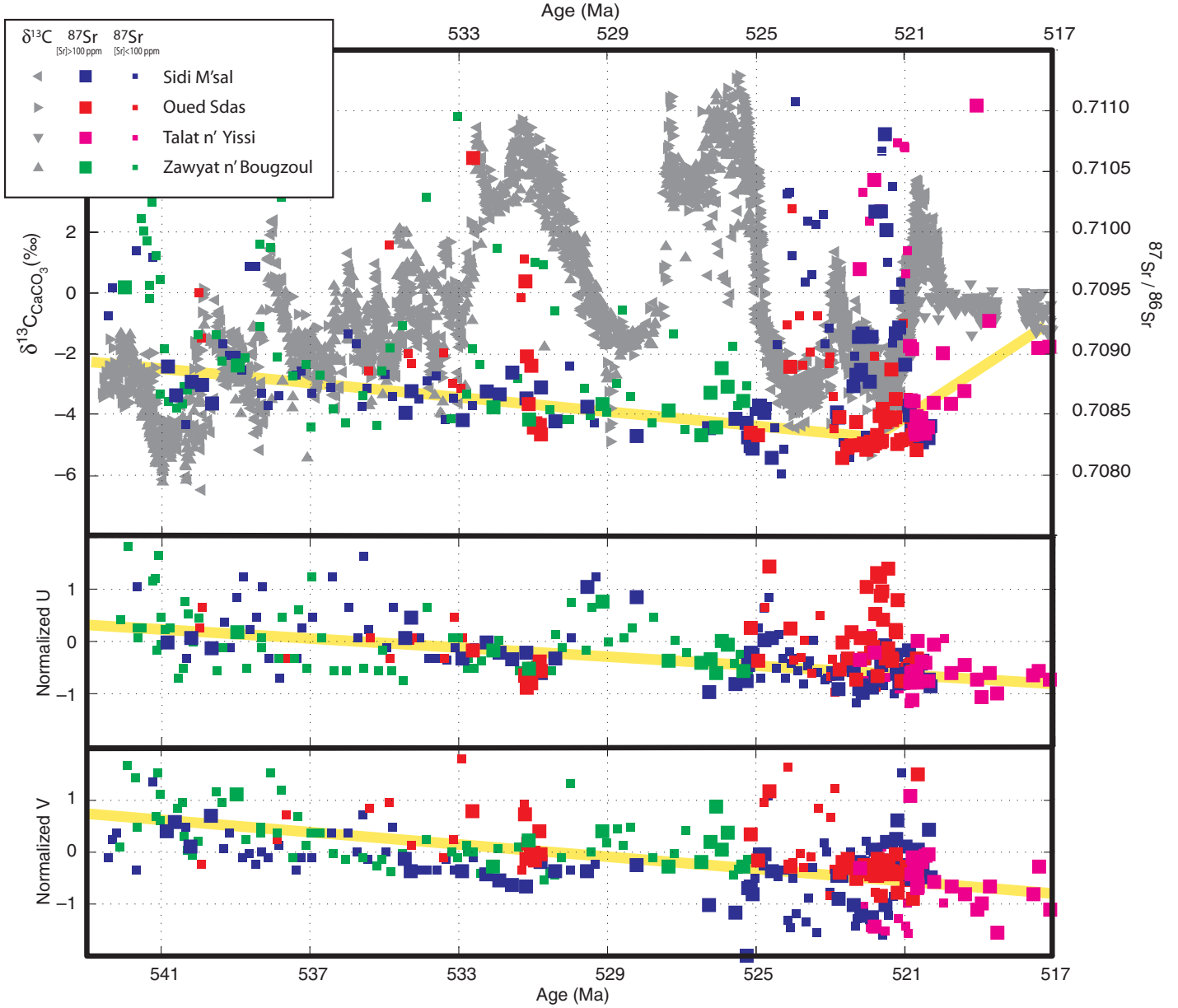


Figure A9. Time evolution of $\delta^{13}\text{C}_{\text{CaCO}_3}$, $^{87}\text{Sr}/^{86}\text{Sr}$, uranium, and vanadium for Morocco. Colors depict different stratigraphic sections, and symbol size indicates whether a sample passes (large) or fails (small) the [Sr] and Mn/Sr tests for diagenetic alteration (see Fig. A8). The very high $^{87}\text{Sr}/^{86}\text{Sr}$ values that pass the [Sr] filter between 522 and 519 Ma are from recrystallized archaeocyath reefs at Sidi M'Sal and Talat n' Yissi.

$$\frac{dCa}{dt} = W_{\text{Ca-carb}} + W_{\text{Ca-sil}} + H_{\text{Ca-basalt}} - P_{\text{Ca-carb}} \quad (\text{A2})$$

$$\frac{d^{n}\text{Sr}}{dt} = W_{n\text{Sr-carb}} + W_{n\text{Sr-sil}} + H_{n\text{Sr-basalt}} - P_{n\text{Sr-carb}} \quad (\text{A3})$$

where $W_{\text{Ca-carb}}$ and $W_{\text{Ca-sil}}$ are the fluxes of magnesium, calcium, and strontium due to subaerial weathering of carbonate and silicate rocks (Meybeck, 2003), $H_{\text{Mg-clays}}$ is the loss of magnesium in seawater due to the precipitation of clay minerals, and $H_{\text{Ca-basalt}}$ and $H_{\text{Sr-basalt}}$ are the sources of calcium and strontium associated with the weathering of ocean crust during hydrothermal circulation on mid-ocean-ridge crests and flanks (Edmond et al., 1979; Mottl and Wheat, 1994).

$P_{\text{X-carb}}$ is the magnesium, calcium, or strontium sink associated with the formation of carbonate minerals (aragonite, calcite, dolomite), and n refers to each isotope of Sr: ^{86}Sr , ^{87}Sr , and ^{88}Sr . The $^{87}\text{Sr}/^{86}\text{Sr}$ ratio of seawater is calculated by dividing the two appropriate equations. Equations A1–A3 are solved numerically in Matlab given estimates of global magnesium/calcium/strontium fluxes and the strontium isotopic composition of the various sources (silicates, carbonates, hydrothermal). Initial conditions for these fluxes and other model variables are given in Tables 1 and A3. The model is initially run to a steady state over ~100 m.y., which presumably reflects seawater composition in the Ediacaran. Following spin-up, fluxes or isotopic composition of the fluxes are varied over

the 22 m.y. window (543–521 Ma) to fit the observed Mg/Ca and Sr isotope data. The quality of the fit is established by visual inspection.

A12. Final Table

Please see the spreadsheet entitled “2010293.xls” in the GSA Data Repository materials (see footnote 1). The spreadsheet presents all of the data on fossil occurrences, $\delta^{13}\text{C}_{\text{CaCO}_3}$, $\delta^{18}\text{O}_{\text{CaCO}_3}$, $\delta^{13}\text{C}_{\text{org}}$, $^{87}\text{Sr}/^{86}\text{Sr}$, uranium, and vanadium for each of the sections used in this paper. It also includes composite $\delta^{13}\text{C}_{\text{CaCO}_3}$ (and $\delta^{18}\text{O}_{\text{org}}$ and $^{87}\text{Sr}/^{86}\text{Sr}$ where available), $\delta^{18}\text{O}_{\text{CaCO}_3}$, and biostratigraphic data, as well as a table of current generic assignments for all of the small shelly fossil taxa found in our literature sources.

TABLE A3. VARIABLES USED IN THE NUMERICAL MODEL OF Mg, Ca, AND Sr

Weathering		Hydrothermal	
$W_{Mg-carb}$	1.7×10^{12} mol/yr (1)	k	3.75×10^{13} kg H ₂ O/yr (3)
$W_{Ca-carb}$	12.0×10^{12} mol/yr (1)	$H_{Mg-clays}$	$k \cdot [Mg]$
$W_{Sr-carb}$	1.1×10^{10} mol/yr (2)	$H_{Sr-basalt}$	$\alpha_{Sr/Ca} \cdot H_{Ca-basalt}$
W_{Mg-sil}	3.1×10^{12} mol/yr (1)	$\alpha_{Mg/Ca}$	1 (4)
W_{Ca-sil}	4.0×10^{12} mol/yr (1)	$\alpha_{Sr/Ca}$	0.0013 (5)
W_{Sr-sil}	0.8×10^{10} mol/yr (2)		
⁸⁷ Sr/ ⁸⁶ Sr		Precipitation	
$W_{87/86Sr-sil}$	0.7150 (2)	$P_{Ca-carb}$	18.75×10^{12} mol/yr (6)
$W_{87/86Sr-carb}$	0.7070 (2)	$P_{Mg-carb}$	1.8×10^{12} mol/yr (7)
$H_{87/86Sr-basalt}$	0.7030 (2)	$P_{Sr-carb}$	$(Sr/Ca)_{seawater} \cdot K_{Sr} \cdot P_{Ca-carb}$
		K_{Sr}	0.2 (8)

Note: (1) adapted from Meybeck (2003); (2) adapted from Allègre et al. (2010); (3) flux of H₂O in hydrothermal systems assuming 100% of the heat flux at 350 °C (Elderfield and Schultz, 1996); (4) assumes 1:1 stoichiometry between Mg uptake and Ca release during basalt alteration; (5) calculated assuming 200 ppm Sr and 10 wt% CaO; (6) calculated assuming carbonate minerals are the only alkalinity sink; (7) estimated from the long-term rate of dolomitization (Wilkinson and Algeo, 1989); (8) homogeneous distribution coefficient for Sr in calcite (Mucci and Morse, 1983).

ACKNOWLEDGMENTS

Malooof and Bowring were supported by National Science Foundation (NSF) Sedimentary Geology & Paleobiology grants EAR-0638660 and EAR-0638634, respectively, and Higgins was supported by a Hess Postdoctoral Fellowship. Michael Bender, David Evans, John Grotzinger, Paul Hoffman, Matt Hurtgen, Jon Husson, Jamie Kellogg, Andy Knoll, Francis Macdonald, Jon Payne, Denis Poussart, Pascale Poussart, Sara Pruss, Jahandar Ramezani, Catherine Rose, Dan Rothman, Blair Schoene, Frederik Simons, Dan Schrag, and Danny Sigman challenged us with stimulating discussions. Claire Calmet, Jessica Creveling, Doug Erwin, Galen Haver-son, Gawen Jenkin, Sören Jensen, David Jones, Artem Kouchinsky, Michael Melchin, Jon Payne, and Nick Swanson-Hysell provided detailed reviews of the manuscript. Brendan Murphy supported the project and edited the paper. Lahssen Baidder and Université Hassan II, Said Mazouad, Mhamed Mouaacha, and Driss Najid provided generous logistical support. Mohamed Mazouad, Ryan Ewing, Jay Ewing, Lida Teneva, and Guoxiang Li assisted us in the field. Claire Calmet, Christine Chen, Will Jacobsen, Becca Levin, Julie Michelman, Jacqui Nesbit, Catherine Rose, Justin Strauss, Lija Treijbergs, and Nora Xu helped with sample preparation. Roger Summons made his MIT laboratory available for sample preparation and analysis. Jenn Kasbohm and Benita Sonntag helped with Figure 4. Maoyan Zhu graciously allowed us to use the δ¹³C data from Jijiapo (South China). Chris Emerling, Artem Kouchinsky, Michael Steiner, Michael Vendrasco, and Marites Villarosa Garcia provided fossil images for Figure 2.

REFERENCES CITED

Agatova, A.I., Sapozhnikov, V.V., and Torgunova, N.I., 1989, Noveye dannye po biogidrokhimii organicheskogo veshchestva v Chernom more: Doklady Akademii Nauk SSSR, v. 309, p. 706–710.
 Agatova, A.I., Lapina, N.M., Torgunova, N.I., and Kirpichev, K.B., 2001, Biogeochemical study of brackish-water marine ecosystems: Water Resources, v. 28, p. 428–437, doi: 10.1023/A:1010401907179.
 Ait Malek, H., Gasquet, D., Bertrand, J.-M., and Leterrier, J., 1998, Géochronologie U-Pb sur zircon de granitoïdes éburnéens et panafricanains dans les boutonnières protérozoïques d'Igherm, du Kerdous et du Bas Drâa (Anti-Atlas occidental, Maroc): Comptes Rendus de l'Académie des Sciences, sér. 2, Sciences de la Terre et des Planètes, v. 327, p. 819–826.
 Allègre, C.J., Louvat, P., Gaillardet, J., Meynadier, L., Rad, S., and Capmas, F., 2010, The fundamental role of is-

land arc weathering in the oceanic Sr isotope budget: Earth and Planetary Science Letters, v. 292, p. 51–56, doi: 10.1016/j.epsl.2010.01.019.
 Aller, R.C., Blair, N.E., Xia, Q., and Rude, P.D., 1996, Remineralization rates, recycling, and storage of carbon in Amazon shelf sediments: Continental Shelf Research, v. 16, p. 753–786, doi: 10.1016/0278-4343(95)00046-1.
 Amthor, J.E., Grotzinger, J.P., Schröder, S., Bowring, S.A., Ramezani, J., Martin, M.W., and Matter, A., 2003, Extinction of *Cloudina* and *Namacalathus* at the Precambrian-Cambrian boundary in Oman: Geology, v. 31, p. 431–434, doi: 10.1130/0091-7613(2003)031<0431:EOCANA>2.0.CO;2.
 Andres, M.S., Sumner, D.Y., Reid, R.P., and Swart, P.K., 2006, Isotopic fingerprints of microbial respiration in aragonite from Bahamian stromatolites: Geology, v. 34, p. 973–976, doi: 10.1130/G22859A.1.
 Aris-Brosou, S., and Yang, Z., 2003, Bayesian models of episodic evolution support a late Precambrian explosive diversification of the Metazoa: Molecular Biology and Evolution, v. 20, p. 1947–1954, doi: 10.1093/molbev/msg226.
 Arvidson, R.S., and Mackenzie, F.T., 1999, The dolomite problem: Control of precipitation kinetics by temperature and saturation state: American Journal of Science, v. 299, p. 275–288, doi: 10.2475/ajs.299.4.257.
 Asmerom, Y., Jacobsen, S.B., Knoll, A.H., Butterfield, N.J., and Swett, K., 1991, Strontium isotopic variations of Neoproterozoic seawater: Implications for crustal evolution: Geochimica et Cosmochimica Acta, v. 55, p. 2883–2894, doi: 10.1016/0016-7037(91)90453-C.
 Badarch, G., Cunningham, W.D., and Windley, B.F., 2002, A new terrane subdivision for Mongolia: Implications for the Phanerozoic crustal growth of Central Asia: Journal of Asian Earth Sciences, v. 21, p. 87–110, doi: 10.1016/S1367-9120(02)00017-2.
 Bahcall, J.N., Pinsonneault, M.H., and Basu, S., 2001, Solar models: Current epoch and time dependences, neutrinos, and helioseismological properties: The Astrophysical Journal, v. 555, p. 990–1012, doi: 10.1086/321493.
 Bailey, T.R., McArthur, J.M., Prince, H., and Thirlwall, M.F., 2000, Dissolution methods for strontium isotope stratigraphy: Whole rock analysis: Chemical Geology, v. 167, p. 313–319, doi: 10.1016/S0009-2541(99)00235-1.
 Baker, P.A., and Burns, S.J., 1985, Occurrence and formation of dolomite in organic-rich continental margin sediments: The American Association of Petroleum Geologists Bulletin, v. 69, p. 1917–1930.
 Balthasar, U., Skovsted, C.B., Holmer, L.E., and Brock, G.A., 2009, Homologous skeletal secretion in tomotoids and brachiopods: Geology, v. 37, p. 1143–1146, doi: 10.1130/G30323A.1.
 Banner, J.L., and Hanson, G.N., 1990, Calculation of simultaneous isotopic and trace element variations during water-rock interaction with applications to carbonate diagenesis: Geochimica et Cosmochimica Acta, v. 54, p. 3123–3137, doi: 10.1016/0016-7037(90)90128-8.

Barghoorn, E.S., and Tyler, S.A., 1965, Microorganisms from the Gunflint Chert: Science, v. 147, p. 563–575, doi: 10.1126/science.147.3658.563.
 Bartley, J.K., and Kah, L.C., 2004, Marine carbon reservoir, C_{org}-C_{carb} coupling, and the evolution of the Proterozoic carbon cycle: Geology, v. 32, p. 129–132, doi: 10.1130/G19939.1.
 Bartley, J.K., Semikhatov, M.A., Kaufman, A.J., Knoll, A.H., Pope, M.C., and Jacobsen, S.B., 2001, Global events across the Mesoproterozoic-Neoproterozoic boundary: C and Sr isotopic evidence from Siberia: Precambrian Research, v. 111, p. 165–202, doi: 10.1016/S0301-9268(01)00160-7.
 Bengtson, S., 1968, The problematic genus *Mobergella* from the Lower Cambrian of the Baltic area: Lethaia, v. 1, p. 325–351, doi: 10.1111/j.1502-3931.1968.tb01625.x.
 Bengtson, S., 1983, The early history of the Conodonta: Fossils and Strata, v. 15, p. 5–19.
 Bengtson, S., 1992a, Neoproterozoic and earliest Cambrian skeletal metazoans, in Schopf, J.W., and Klein, C., eds., The Proterozoic Biosphere: A Multidisciplinary Study: Cambridge, UK, Cambridge University Press, p. 1017–1033.
 Bengtson, S., 1992b, The cap-shaped Cambrian fossil *Maikhanella* and the relationship between coelocleritophorans and molluscs: Lethaia, v. 25, p. 401–420, doi: 10.1111/j.1502-3931.1992.tb01644.x.
 Bengtson, S., 2005, Mineralized skeletons and early animal evolution, in Briggs, D.E.G., ed., Evolving Form and Function: Fossils and development: Proceedings of a symposium honoring Adolf Seilacher for his contributions to paleontology, in celebration of his 80th birthday: New Haven, Connecticut, Peabody Museum of Natural History, p. 101–124.
 Bengtson, S., and Conway Morris, S., 1992, Early radiation of biomineralizing phyla, in Lipps, J.H., and Signor, P.W., eds., Origin and Early Evolution of the Metazoa: New York, Plenum Press, p. 447–481.
 Bengtson, S., and Hou Xianguang, 2001, The integument of Cambrian chancellorids: Acta Palaeontologica Polonica, v. 46, p. 1–22.
 Bengtson, S., and Missarzhevsky, V.V., 1981, Coelocleritophora—A major group of enigmatic Cambrian metazoans: U.S. Geological Survey Open-File Report 81–743, p. 19–21.
 Bengtson, S., Fedorov, A.B., Missarzhevsky, V.V., Rozanov, A.Yu., Zhegallo, E.A., and Zhuravlev, A.Yu., 1987, *Tumulduria incompta* and the case for Tommotian trilobites: Lethaia, v. 20, p. 361–370, doi: 10.1111/j.1502-3931.1987.tb00797.x.
 Bengtson, S., Conway Morris, S., Cooper, B.J., Jell, P.A., and Runnegar, B.N., 1990, Early Cambrian Fossils from South Australia: Association of Australasian Palaeontologists Memoir 9, 364 p.
 Berner, R.A., Lasaga, A.C., and Garrels, R.M., 1983, The carbonate-silicate geochemical cycle and its effects on atmospheric carbon dioxide over the past 100 million years: American Journal of Science, v. 283, p. 641–683.
 Billups, K., Kelly, C., and Pierce, E., 2008, The late Miocene to early Pliocene climate transition in the Southern Ocean: Palaeogeography, Palaeoclimatology, Palaeoecology, v. 267, p. 31–40, doi: 10.1016/j.palaeo.2008.05.013.
 Bintanja, R., van de Wal, R.S.W., and Oerlemans, J., 2005, Modelled atmospheric temperatures and global sea levels over the past million years: Nature, v. 437, p. 125–128, doi: 10.1038/nature03975.
 Blair, N.E., Leithold, E.L., Ford, S.T., Peeler, K.A., Holmes, J.C., and Perkey, D.W., 2003, The persistence of memory: The fate of ancient sedimentary organic carbon in a modern sedimentary system: Geochimica et Cosmochimica Acta, v. 67, p. 63–73, doi: 10.1016/S0016-7037(02)01043-8.
 Bockelie, T.G., and Yochelson, E.L., 1979, Variation in a species of “worm” from the Ordovician of Spitsbergen: Norsk Polarinstittut: Skrifter, v. 167, p. 225–237.
 Boher, M., Aouchami, W., Michard, A., Albarède, F., and Arndt, N.T., 1992, Crustal growth in West Africa at 2.1 Ga: Journal of Geophysical Research, v. 97, p. 345–369, doi: 10.1029/91JB01640.
 Bond, G.C., and Kominz, M.A., 1984, Construction of tectonic subsidence curves for the early Paleozoic mio-

- geocline, southern Canadian Rocky Mountains: Implications for subsidence mechanisms, age of breakup, and crustal thinning: *Geological Society of America Bulletin*, v. 95, p. 155–173, doi: 10.1130/0016-7606(1984)95<155:COTSCF>2.0.CO;2.
- Bond, G.C., Nickeson, P.A., and Kominz, M.A., 1984, Breakup of a supercontinent between 625 and 555 Ma: New evidence and implications for continental histories: *Earth and Planetary Science Letters*, v. 70, p. 325–345, doi: 10.1016/0012-821X(84)90017-7.
- Bond, G.C., Kominz, M.A., and Grotzinger, J.P., 1988, Cambro-Ordovician eustasy: Evidence from geophysical modeling of Cordilleran and Appalachian miogeoclines, in Kleinspehn, K., and Paola, C., eds., *New Perspectives in Basin Analysis*: Berlin, Springer-Verlag, p. 129–160.
- Bottjer, D.J., Hagadorn, J.W., and Dornbos, S.Q., 2000, The Cambrian substrate revolution: *GSA Today*, v. 10, no. 9, p. 1–7.
- Bowring, S.A., Grotzinger, J.P., Isachsen, C.E., Knoll, A.H., Pelechaty, S.M., and Kolosov, P., 1993, Calibrating rates of Early Cambrian evolution: *Science*, v. 261, p. 1293–1298, doi: 10.1126/science.11539488.
- Bowring, S.A., Grotzinger, J.P., Condon, D.J., Ramezani, J., Newall, M.J., and Allen, P.A., 2007, Geochronologic constraints on the chronostratigraphic framework of the Neoproterozoic Huqf Supergroup, Sultanate of Oman: *American Journal of Science*, v. 307, p. 1097–1145, doi: 10.2475/10.2007.01.
- Boyce, C.K., 2005, Patterns of segregation and convergence in the evolution of fern and seed plant leaf morphologies: *Paleobiology*, v. 31, p. 117–140, doi: 10.1666/0094-8373(2005)031<0117:POSACL>2.0.CO;2.
- Brand, U., and Veizer, J., 1980, Chemical diagenesis of a multicomponent carbonate system: 2. Stable isotopes: *Journal of Sedimentary Petrology*, v. 51, p. 987–997.
- Brasier, M.D., 1984, Microfossils and small shelly fossils from the Lower Cambrian *Hyolithes* Limestone at Nuneaton, English Midlands: *Geological Magazine*, v. 121, p. 229–253, doi: 10.1017/S0016756800028296.
- Brasier, M.D., 1996, The basal Cambrian transition and Cambrian bio-events, in Walliser, O.H., ed., *Global Events and Event Stratigraphy in the Phanerozoic*: Berlin, Springer-Verlag, p. 113–138.
- Brasier, M.D., and Sukhov, S.S., 1998, The falling amplitude of carbon isotopic oscillations through the Lower to Middle Cambrian: Northern Siberia data: *Canadian Journal of Earth Sciences*, v. 35, p. 353–373, doi: 10.1139/cjes-35-4-353.
- Brasier, M.D., Magaritz, M., Corfield, R., Luo Huilin, Wu Xiche, Ouyang Lin, Jiang Zhiwen, Hamdi, B., He Tinggui, and Fraser, A.G., 1990, The carbon- and oxygen-isotope record of the Precambrian-Cambrian boundary interval in China and Iran and their correlation: *Geological Magazine*, v. 127, p. 319–332.
- Brasier, M.D., Khomentovsky, V.V., and Corfield, R.M., 1993, Stable isotopic calibration of the earliest skeletal fossil assemblages in eastern Siberia (Precambrian-Cambrian boundary): *Terra Nova*, v. 5, p. 225–232, doi: 10.1111/j.1365-3121.1993.tb00253.x.
- Brasier, M., Cowie, J., and Taylor, M., 1994a, Decision on the Precambrian-Cambrian boundary stratotype: Episodes, v. 17, p. 3–8.
- Brasier, M.D., Rozanov, A.Yu., Zhuravlev, A.Yu., Corfield, R.M., and Derry, L.A., 1994b, A carbon isotope reference scale for the Lower Cambrian succession in Siberia: Report of IGCP Project 303: *Geological Magazine*, v. 131, p. 767–783, doi: 10.1017/S0016756800012851.
- Brasier, M.D., Corfield, R.M., Derry, L.A., Rozanov, A.Yu., and Zhuravlev, A.Yu., 1994c, Multiple $\delta^{13}\text{C}$ excursions spanning the Cambrian explosion to the Botomian crisis in Siberia: *Geology*, v. 22, p. 455–458, doi: 10.1130/0091-7613(1994)022<0455:MCESTC>2.3.CO;2.
- Brasier, M.D., Shields, G., Kuleshov, V.N., and Zhegallo, E.A., 1996, Integrated chemo- and biostratigraphic calibration of early animal evolution: Neoproterozoic–Early Cambrian of southwest Mongolia: *Geological Magazine*, v. 133, p. 445–485, doi: 10.1017/S0016756800007603.
- Brasier, M., Green, O., and Shields, G., 1997, Ediacarian sponge spicule clusters from southwestern Mongolia and the origins of the Cambrian fauna: *Geology*, v. 25, p. 303–306, doi: 10.1130/0091-7613(1997)025<0303:ESSCFS>2.3.CO;2.
- Braun, A., Chen, J., Waloszek, D., and Maas, A., 2007, First Early Cambrian Radiolaria, in Vickers-Rich, P., and Komarow, P., eds., *The Rise and Fall of the Ediacaran Biota*: Geological Society of London Special Publication 286, p. 143–149.
- Briden, J.C., 1968, Paleomagnetism of the Ntonya ring structure, Malawi: *Journal of Geophysical Research*, v. 73, p. 725–733, doi: 10.1029/JB073i002p00725.
- Briden, J.C., McClelland, E., and Rex, D.C., 1993, Proving the age of a paleomagnetic pole: The case of the Ntonya ring structure, Malawi: *Journal of Geophysical Research*, v. 98, p. 1743–1749, doi: 10.1029/92JB01254.
- Briggs, D.E.G., Erwin, D.H., and Collier, F.J., 1994, *The Fossils of the Burgess Shale*: Washington, D.C., Smithsonian Institution Press, 238 p.
- Bristow, T.F., and Kennedy, M.J., 2008, Carbon isotope excursions and the oxidant budget of the Ediacaran atmosphere and ocean: *Geology*, v. 36, p. 863–866, doi: 10.1130/G24968A.1.
- Broecker, W.S., and Peng, T.-H., 1982, *Tracers in the Sea*: Palisades, New York, Lamont-Doherty Geological Observatory, 690 p.
- Bromham, L., Rambaut, A., Fortey, R., Cooper, A., and Penny, D., 1998, Testing the Cambrian explosion hypothesis by using a molecular dating technique: Proceedings of the National Academy of Sciences of the United States of America, v. 95, p. 12,386–12,389, doi: 10.1073/pnas.95.21.12386.
- Brooks, B.-G.J., Crowley, J.L., Bowring, S.A., Cervato, C., and Jin Yugan, 2006, A new U/Pb date for the basal Meishucun section and implications for the timing of the Cambrian explosion: University of Sheffield, The Palaeontological Association, 50th Annual Meeting Abstracts, p. 18.
- Budd, G.E., 2002, A palaeontological solution to the arthropod head problem: *Nature*, v. 417, p. 271–275, doi: 10.1038/417271a.
- Budd, G.E., 2008, The earliest fossil record of the animals and its significance: *Philosophical Transactions of the Royal Society, ser. B*, v. 363, p. 1425–1434, doi: 10.1098/rstb.2007.2232.
- Budd, G.E., and Jensen, S., 2000, A critical reappraisal of the fossil record of the bilaterian phyla: *Biological Reviews of the Cambridge Philosophical Society*, v. 75, p. 253–295, doi: 10.1017/S000632310000548X.
- Burns, S.J., and Matter, A., 1993, Carbon isotopic record of the latest Proterozoic from Oman: *Eclogae Geologicae Helvetiae*, v. 86, p. 595–607.
- Burns, S.J., McKenzie, J.A., and Vasconcelos, C., 2000, Dolomite formation and biogeochemical cycles in the Phanerozoic: *Sedimentology*, v. 47, suppl. 1, p. 49–61, doi: 10.1046/j.1365-3091.2000.00004.x.
- Butterfield, N.J., 1997, Plankton ecology and the Proterozoic–Phanerozoic transition: *Paleobiology*, v. 23, p. 247–262.
- Calver, C.R., 2000, Isotope stratigraphy of the Ediacarian (Neoproterozoic III) of the Adelaide Rift complex, Australia, and the overprint of water column stratification: *Precambrian Research*, v. 100, p. 121–150, doi: 10.1016/S0301-9268(99)00072-8.
- Campbell, I.H., and Squire, R.J., 2010, The mountains that triggered the Late Neoproterozoic increase in oxygen: The second great oxidation event: *Geochimica et Cosmochimica Acta*, v. 74, p. 4187–4206, doi: 10.1016/j.gca.2010.04.064.
- Caron, J.-B., Scheltema, A., Schander, C., and Rudkin, D., 2006, A soft-bodied mollusc with radula from the Middle Cambrian Burgess Shale: *Nature*, v. 442, p. 159–163, doi: 10.1038/nature04894.
- Cauwet, G., Déliat, G., Krastev, A., Shtereva, G., Becquevort, S., Lancelot, C., Momzikoff, A., Saliot, A., Cociasu, A., and Popa, L., 2002, Seasonal DOC accumulation in the Black Sea: A regional explanation for a general mechanism: *Marine Chemistry*, v. 79, p. 193–205, doi: 10.1016/S0304-4203(02)00064-6.
- Cawood, P.A., and Pisarevsky, S.A., 2006, Was Baltica right-way-up or upside-down in the Neoproterozoic?: *Journal of the Geological Society of London*, v. 163, p. 753–759, doi: 10.1144/0016-76492005-126.
- Chen Ping, 1984, [Discovery of Lower Cambrian small shelly fossils from Jijiapo, Yichang, west Hubei and its significance]: *Professional Papers of Stratigraphy and Palaeontology*, v. 13, p. 49–66, 2 pl. (in Chinese with English summary).
- Chen Zhe, Bengtson, S., Zhou Chuanming, and Yue Zhao, 2008, Tube structure and original composition of *Sinotubulites*: Shelly fossils from the late Neoproterozoic in southern Shaanxi, China: *Lethaia*, v. 41, p. 37–45.
- Cloud, P.E., Jr., 1948, Some problems and patterns of evolution exemplified by fossil invertebrates: *Evolution*: International Journal of Organic Evolution, v. 2, p. 322–350.
- Cloud, P.E., Jr., 1965, Significance of the Gunflint (Precambrian) microfiora: *Science*, v. 148, p. 27–35, doi: 10.1126/science.148.3666.27.
- Cohen, P.A., Bradley, A., Knoll, A.H., Grotzinger, J.P., Jensen, S., Abelson, J., Hand, K., Love, G., Metz, J., McLoughlin, N., Meister, P., Shepard, R., Tice, M., and Wilson, J.P., 2009, Tubular compression fossils from the Ediacaran Nama Group, Namibia: *Journal of Paleontology*, v. 83, p. 110–122, doi: 10.1666/09-040R.1.
- Compston, W., Williams, I.S., Kirschvink, J.L., Zhang Zichao, and Ma Guogan, 1992, Zircon U-Pb ages from the Early Cambrian time-scale: *Journal of the Geological Society of London*, v. 149, p. 171–184, doi: 10.1144/gsjgs.149.2.0171.
- Compston, W., Zhang Zichao, Cooper, J.A., Ma Guogan, and Jenkins, R.J.F., 2008, Further SHRIMP geochronology on the Early Cambrian of South China: *American Journal of Science*, v. 308, p. 399–420, doi: 10.2475/04.2008.01.
- Condon, D., Zhu Maoyan, Bowring, S., Wang Wei, Yang Aihua, and Jin Yugan, 2005, U-Pb ages from the Neoproterozoic Doushantuo Formation, China: *Science*, v. 308, p. 95–98.
- Conrad, C.P., and Husson, L., 2009, Influence of dynamic topography on sea level and its rate of change: *Lithosphere*, v. 1, p. 110–120, doi: 10.1130/L32.1.
- Conrad, C.P., and Lithgow-Bertelloni, C., 2007, Faster sea-floor spreading and lithosphere production during the mid-Cenozoic: *Geology*, v. 35, p. 29–32, doi: 10.1130/G22759A.1.
- Conway Morris, S., and Chapman, A.J., 1996, Lower Cambrian coelocleritophorans (*Ninella*, *Siphonuchites*) from Xinjiang and Shaanxi, China: *Geological Magazine*, v. 133, p. 33–51, doi: 10.1017/S0016756800007238.
- Conway Morris, S., and Chapman, A.J., 1997, Mobergelans from the Lower Cambrian of Mongolia, Sweden, and the United States: Molluscs or opercula of incertae sedis?: *Journal of Paleontology*, v. 71, p. 968–985.
- Conway Morris, S., and Chen Meng'e, 1991, Cambroclaves and paracarinarachitids, early skeletal problematica from the Lower Cambrian of South China: *Palaeontology*, v. 34, p. 357–397.
- Conway Morris, S., and Chen Meng'e, 1992, Carinachitids, hexagonulaconulariids, and *Punctatus*: Problematic metazoans from the Early Cambrian of South China: *Journal of Paleontology*, v. 66, p. 384–406.
- Conway Morris, S., and Peel, J.S., 1995, Articulated halkieriids from the Lower Cambrian of North Greenland and their role in the early protostome evolution: *Philosophical Transactions of the Royal Society of London, ser. B*, *Biological Sciences*, v. 347, p. 305–358, doi: 10.1098/rstb.1995.0029.
- Conway Morris, S., Crampton, J.S., Xiao Bing, and Chapman, A.J., 1997, Lower Cambrian cambroclaves (*incertae sedis*) from Xinjiang, China, with comments on the morphological variability of sclerites: *Palaeontology*, v. 40, p. 167–189.
- Cook, P.J., and Shergold, J.H., 1984, Phosphorus, phosphorites and skeletal evolution at the Precambrian-Cambrian boundary: *Nature*, v. 308, p. 231–236, doi: 10.1038/308231a0.
- Corsetti, F.A., and Hagadorn, J.W., 2000, Precambrian-Cambrian transition: Death Valley, United States: *Geology*, v. 28, p. 299–302, doi: 10.1130/0091-7613(2000)28<299:PTDVUS>2.0.CO;2.
- Crimes, T.P., 1987, Trace fossils and correlation of late Precambrian and Early Cambrian strata: *Geological Magazine*, v. 124, p. 97–119, doi: 10.1017/S0016756800015922.
- Curry, W.B., and Crowley, T.J., 1987, The $\delta^{13}\text{C}$ of equatorial Atlantic surface waters: Implications for ice-age

- $p\text{CO}_2$ levels: *Paleoceanography*, v. 2, p. 489–517, doi: 10.1029/PA002i005p00489.
- Darwin, C., 1859, *On the Origin of Species by Means of Natural Selection, or the Preservation of Favoured Races in the Struggle for Life*: London, John Murray, 479 p.
- Debrenne, F., and Courjault-Radé, P., 1994, Répartition paléogéographique des archéocyathes et délimitation des zones intertropicales au Cambrien inférieur: *Bulletin de la Société Géologique de France*, v. 165, p. 459–467.
- Debrenne, F., Lafuste, J., and Zhuravlev, A., 1990, Corallo-morphes et spongiomorphes à l'aube du Cambrien: *Bulletin du Muséum d'Histoire Naturelle, Paris, section C, sér. 4*, v. 12, p. 17–39.
- Derry, L.A., 2010, A burial diagenesis origin for the Ediacaran Shuram-Wonoka carbon isotope anomaly: *Earth and Planetary Science Letters*, v. 294, p. 152–162, doi: 10.1016/j.epsl.2010.03.022.
- Derry, L.A., and France-Lanord, C., 1996, Neogene Himalayan weathering history and river $^{87}\text{Sr}/^{86}\text{Sr}$: Impact on the marine Sr record: *Earth and Planetary Science Letters*, v. 142, p. 59–74, doi: 10.1016/0012-821X(96)00091-X.
- Derry, L.A., Keto, L.S., Jacobsen, S.B., Knoll, A.H., and Swett, K., 1989, Sr isotopic variations in Upper Proterozoic carbonates from Svalbard and East Greenland: *Geochimica et Cosmochimica Acta*, v. 53, p. 2331–2339, doi: 10.1016/0016-7037(89)90355-4.
- Derry, L.A., Brasier, M.D., Corfield, R.M., Rozanov, A.Yu., and Zhuravlev, A.Yu., 1994, Sr and C isotopes in Lower Cambrian carbonates from the Siberian craton: A paleoenvironmental record during the 'Cambrian explosion': *Earth and Planetary Science Letters*, v. 128, p. 671–681, doi: 10.1016/0012-821X(94)90178-3.
- Des Marais, D.J., Strauss, H., Summons, R.E., and Hayes, J.M., 1992, Carbon isotope evidence for the stepwise oxidation of the Proterozoic environment: *Nature*, v. 359, p. 605–609, doi: 10.1038/359605a0.
- Dong, L., Xiao, S., Shen, B., Zhou Chuanming, Li Guoxiang, and Yao Jinxian, 2009, Basal Cambrian microfossils from the Yangtze Gorges area (South China) and the Aksu area (Tarim block, northwestern China): *Journal of Paleontology*, v. 83, p. 30–44, doi: 10.1666/07-147R.1.
- Donnadieu, Y., Goddés, Y., Ramstein, G., Nédélec, A., and Meert, J., 2004, A 'snowball Earth' climate triggered by continental break-up through changes in runoff: *Nature*, v. 428, p. 303–306, doi: 10.1038/nature02408.
- Donoghue, P.C.J., Kouchinsky, A., Waloszek, D., Bengtson, S., Dong Xiping, Val'kov, A.K., Cunningham, J.A., and Repetski, J.E., 2006a, Fossilized embryos are widespread but the record is temporally and taxonomically biased: *Evolution & Development*, v. 8, p. 232–238, doi: 10.1111/j.1525-142X.2006.00093.x.
- Donoghue, P.C.J., Bengtson, S., Dong Xiping, Gostling, N.J., Huldgren, T., Cunningham, J.A., Yin Chongyu, Yue Zhao, Peng Fan, and Stampanoni, M., 2006b, Synchrotron X-ray tomographic microscopy of fossil embryos: *Nature*, v. 442, p. 680–683.
- Dornbos, S.Q., Bottjer, D.J., and Chen Junyuan, 2004, Evidence for seafloor microbial mats and associated metazoan lifestyles in Lower Cambrian phosphorites of southwest China: *Lethaia*, v. 37, p. 127–137, doi: 10.1080/00241160410004764.
- Drenzek, N.J., Huguen, K.A., Montluçon, D.B., Southon, J.R., dos Santos, G.M., Druffel, E.R.M., Giosan, L., and Eglinton, T.I., 2009, A new look at old carbon in active margin sediments: *Geology*, v. 37, p. 239–242, doi: 10.1130/G25351A.1.
- Droser, M.L., and Bottjer, D.J., 1988, Trends in depth and extent of bioturbation in Cambrian carbonate marine environments, western United States: *Geology*, v. 16, p. 233–236, doi: 10.1130/0091-7613(1988)016<0233:TIDAEO>2.3.CO;2.
- Droser, M.L., Jensen, S., and Gehling, J.G., 2002, Trace fossils and substrates of the terminal Proterozoic-Cambrian transition: Implications for the record of early bilaterians and sediment mixing: *Proceedings of the National Academy of Sciences of the United States of America*, v. 99, p. 12,572–12,576, doi: 10.1073/pnas.202322499.
- Droser, M.L., Gehling, J.G., and Jensen, S., 2005, Ediacaran trace fossils: True and false, in Briggs, D.E.G., ed., *Evolving Form and Function: Fossils and Development: Proceedings of a symposium honoring Adolf Seilacher for his contributions to paleontology, in celebration of his 80th birthday*: New Haven, Connecticut, Peabody Museum of Natural History, p. 125–138.
- Dzik, J., 1991, Is fossil evidence consistent with traditional views of the early metazoan phylogeny?, in Simonetta, A.M., and Conway Morris, S., eds., *The Early Evolution of Metazoa and the Significance of Problematic Taxa*: Cambridge, UK, Cambridge University Press, p. 47–56.
- Dzik, J., 1994, Evolution of 'small shelly fossils' assemblages of the early Paleozoic: *Acta Paleontologica Polonica*, v. 39, p. 247–313.
- Dzik, J., 2005, Behavioral and anatomical unity of the earliest burrowing animals and the cause of the 'Cambrian explosion': *Paleobiology*, v. 31, p. 503–521, doi: 10.1666/0094-8373(2005)031[0503:BAAUOT]2.0.CO;2.
- Edmond, J.M., 1992, Himalayan tectonics, weathering processes, and strontium isotope record in marine limestones: *Science*, v. 258, p. 1594–1597, doi: 10.1126/science.258.5088.1594.
- Edmond, J.M., Measures, C., McDuff, R.E., Chan, L.H., Collier, R., Grant, B., Gordon, L.I., and Corliss, J.B., 1979, Ridge crest hydrothermal activity and the balances of the major and minor elements in the ocean: The Galapagos data: *Earth and Planetary Science Letters*, v. 46, p. 1–18, doi: 10.1016/0012-821X(79)90061-X.
- Elderfield, H., and Schultz, A., 1996, Mid-ocean ridge hydrothermal fluxes and the chemical composition of the ocean: *Annual Review of Earth and Planetary Sciences*, v. 24, p. 191–224, doi: 10.1146/annurev.earth.24.1.191.
- Emrich, K., Ehhalt, D.H., and Vogel, J.C., 1970, Carbon isotope fractionation during the precipitation of calcium carbonate: *Earth and Planetary Science Letters*, v. 8, p. 363–371, doi: 10.1016/0012-821X(70)90109-3.
- Endonzhams, Zh., and Lkhasuren, B., 1988, Stratigrafiya pograničnykh tolsch dokembriya i kembriya Dzhankhanskoj zony, in *Khomentovskij, V.V., and Shenfil', V.Yu., eds., Pozdnyj dokembriy i rannij paleozoy Sibiri, Rifej i vend: Novosibirsk, Institut Geologii i Geofiziki, Sibirskoe Otdelenie, Akademiya Nauk SSSR*, p. 150–162.
- Engelbreton, D.C., Kelley, K.P., Cashman, H.J., and Richards, M.A., 1992, 180 million years of subduction: *GSA Today*, v. 2, p. 93–95, 100.
- Esakova, N.V., and Zhegallo, E.A., 1996, Biotstratigrafiya i fauna nizhnego kembriya Mongolii: *Sovmestnaya Rossijsko-Mongol'skaya Paleontologičeskaya Ekspeditsiya*, *Trudy*, v. 46, 216 p., 24 pl.
- Evans, D.A., 1998, True polar wander, a supercontinental legacy: *Earth and Planetary Science Letters*, v. 157, p. 1–8, doi: 10.1016/S0012-821X(98)00031-4.
- Evans, D.A., Ripperdan, R.L., and Kirschvink, J.L., 1998, Polar wander and the Cambrian (response): *Science*, v. 279, p. 9 (correction p. 307).
- Evans, M.J., Derry, L.A., and France-Lanord, C., 2008, Degassing of metamorphic carbon dioxide from the Nepal Himalaya: *Geochemistry, Geophysics, Geosystems*, v. 9, no. 4, art. 04021, 18 p.
- Fedonkin, M.A., 1985, Paleichnology of Vendian Metazoa, in Sokolov, B.S., and Iwanowski, A.B., eds., *The Vendian System, Volume 1*: Berlin, Springer-Verlag p. 132–137.
- Fedonkin, M.A., and Waggoner, B.M., 1997, The Late Precambrian fossil *Kimberella* is a mollusc-like bilaterian organism: *Nature*, v. 388, p. 868–871, doi: 10.1038/42242.
- Fike, D.A., 2007, Carbon and Sulfur Isotopic Constraints on Ediacaran Biogeochemical Processes, *Huqf Supergroup, Sultanate of Oman* [Ph.D. thesis]: Cambridge, Massachusetts, Massachusetts Institute of Technology, 231 p.
- Fike, D.A., Grotzinger, J.P., Pratt, L.M., and Summons, R.E., 2006, Oxidation of the Ediacaran ocean: *Nature*, v. 444, p. 744–747, doi: 10.1038/nature05345.
- Fölling, P.G., and Frimmel, H.E., 2002, Chemostratigraphic correlation of carbonate successions in the Gariep and Saldania belts, Namibia and South Africa: *Basin Research*, v. 14, p. 69–88, doi: 10.1046/j.1365-2117.2002.00167.x.
- Foote, M., 1997, The evolution of morphological diversity: *Annual Review of Ecology and Systematics*, v. 28, p. 129–152, doi: 10.1146/annurev.ecolsys.28.1.129.
- Ford, T.D., 1958, Pre-Cambrian fossils from Charnwood Forest: *Proceedings of the Yorkshire Geological Society*, v. 31, p. 211–217, doi: 10.1144/pygs.31.3.211.
- Galy, A., France-Lanord, C., and Derry, L.A., 1999, The strontium isotopic budget of Himalayan rivers in Nepal and Bangladesh: *Geochimica et Cosmochimica Acta*, v. 63, p. 1905–1925, doi: 10.1016/S0016-7037(99)00081-2.
- Gao, G., Dworkin, S.I., Land, L.S., and Elmore, R.D., 1996, Geochemistry of Late Ordovician Viola Limestone, Oklahoma: Implications for marine carbon mineralogy and isotopic compositions: *The Journal of Geology*, v. 104, p. 359–367, doi: 10.1086/629831.
- Gehling, J.G., and Rigby, J.K., 1996, Long expected sponges from the Neoproterozoic Ediacara fauna of South Australia: *Journal of Paleontology*, v. 70, p. 185–195.
- Gehling, J.G., Jensen, S., Droser, M.L., Myrow, P.M., and Narbonne, G.M., 2001, Burrowing below the basal Cambrian GSSP, Fortune Head, Newfoundland: *Geological Magazine*, v. 138, p. 213–218, doi: 10.1017/S001675680100509X.
- Geyer, G., 1989, Late Precambrian to early Middle Cambrian lithostratigraphy of southern Morocco: *Beringeria*, v. 1, p. 115–143.
- Geyer, G., 1994, Middle Cambrian mollusks from Idaho and early conchiferan evolution: *New York State Museum Bulletin*, v. 481, p. 69–86.
- Geyer, G., and Landing, E., 1995, The Cambrian of the Moroccan Atlas regions, in Geyer, G., and Landing, E., eds., *Morocco '95: The Lower-Middle Cambrian Standard of Western Gondwana*: Würzburg, Beringeria Special Issue 2, p. 7–46.
- Ginsburg, R.N., 2001, The Bahamas drilling project: Background and acquisition of cores and logs, in Ginsburg, R.N., ed., *Subsurface Geology of a Prograding Carbonate Platform Margin, Great Bahama Bank: Results of the Bahamas Drilling Project: Society for Sedimentary Geology (SEPM) Special Publication 70*, p. 3–16.
- Giri, B.J., Bano, N., and Hollibaugh, J.T., 2004, Distribution of RuBisCO genotypes along a redox gradient in Mono Lake, California: *Applied and Environmental Microbiology*, v. 70, p. 3443–3448, doi: 10.1128/AEM.70.6.3443-3448.2004.
- Given, R.K., and Wilkinson, B.H., 1987, Dolomite abundance and stratigraphic age: Constraints on rates and mechanisms of Phanerozoic dolostone formation: *Journal of Sedimentary Petrology*, v. 57, p. 1068–1078.
- Glaessner, M.F., and Wade, M., 1966, The Late Precambrian fossils from Ediacara, South Australia: *Paleontology*, v. 9, p. 599–628, pl. 97–103.
- Gnilovskaya, M.B., 1985, Vendotaenids—Vendian metaphytes, in Sokolov, B.S., and Iwanowski, A.B., eds., *The Vendian System, Volume 1*: Berlin, Springer-Verlag, p. 138–147.
- Goldammer, T., Brüchert, V., Ferdelman, T.G., and Zabel, M., 2010, Microbial sequestration of phosphorus in anoxic upwelling sediments: *Nature Geoscience*, v. 3, p. 557–561, doi: 10.1038/ngeo913.
- Gould, S.J., 1989, *Wonderful Life: The Burgess Shale and the Nature of History*: New York, W.W. Norton, 347 p.
- Grant, S.W.F., 1990, Shell structure and distribution of *Cloudina*, a potential index fossil for the terminal Proterozoic: *American Journal of Science*, v. 290-A, p. 261–294.
- Greenwood, D.R., and Wing, S.L., 1995, Eocene continental climates and latitudinal temperature gradients: *Geology*, v. 23, p. 1044–1048, doi: 10.1130/0091-7613(1995)023<1044:ECCALT>2.3.CO;2.
- Grigor'eva, N.V., Mel'nikova, L.M., and Pel'man, Yu.L., 1983, Brachiopods, ostracodes (bradoriids) and problematical fossils from the stratotype region of the Lower Cambrian stages: *Paleontological Journal*, v. 17, no. 3, p. 51–56.
- Grotzinger, J.P., Bowring, S.A., Saylor, B.Z., and Kaufman, A.J., 1995, Biostratigraphic and geochronologic constraints on early animal evolution: *Science*, v. 270, p. 598–604, doi: 10.1126/science.270.5236.598.
- Grotzinger, J.P., Watters, W.A., and Knoll, A.H., 2000, Calcified metazoans in thrombolite-stromatolite reefs of

- the terminal Proterozoic Nama Group, Namibia: *Paleobiology*, v. 26, p. 334–359, doi: 10.1666/0094-8373(2000)026<0334:CMITSR>2.0.CO;2.
- Gubanov, A.P., and Peel, J.S., 2000, Cambrian monoplacophoran molluscs (class Helcionelloida): *American Malacological Bulletin*, v. 15, p. 139–145.
- Guo Junfeng, Li Yong, Han Jian, Zhang Xingliang, Zhang Zhifei, Ou Qiang, Liu Jianni, Shu Degan, Maruyama, S., and Komiya, T., 2008, Fossil association from the Lower Cambrian Yanjiahe Formation in the Yangtze Gorges area, Hubei, South China: *Acta Geologica Sinica (English edition)*, v. 82, p. 1124–1132.
- Gurnis, M., 1990, Ridge spreading, subduction, and sea level fluctuations: *Science*, v. 250, p. 970–972, doi: 10.1126/science.250.4983.970.
- Hallam, A., and Wignall, P.B., 1999, Mass extinctions and sea-level changes: *Earth-Science Reviews*, v. 48, p. 217–250, doi: 10.1016/S0012-8252(99)00055-0.
- Halverson, G.P., Hoffman, P.F., Schrag, D.P., Malooof, A.C., and Rice, A.H.N., 2005, Toward a Neoproterozoic composite carbon-isotope record: *Geological Society of America Bulletin*, v. 117, p. 1181–1207, doi: 10.1130/B25630.1.
- Halverson, G.P., Dudás, F.O., Malooof, A.C., and Bowring, S.A., 2007, Evolution of the $^{87}\text{Sr}/^{86}\text{Sr}$ composition of Neoproterozoic seawater: *Palaeogeography, Palaeoclimatology, Palaeoecology*, v. 256, p. 103–129, doi: 10.1016/j.palaeo.2007.02.028.
- Halverson, G.P., Wade, B.P., Hurtgen, M.T. and Barovich, K.M., 2010, Neoproterozoic chemostratigraphy: Precambrian Research (in press), doi:10.1016/j.precamres.2010.04.007.
- Hambrey, M.J., and Harland, W.B., eds., 1981, *Earth's Pre-Pleistocene Glacial Record*: Cambridge, UK, Cambridge University Press, 1004 p.
- Hansell, D.A., and Carlson, C.A., 2001, Marine dissolved organic matter and the carbon cycle: *Oceanography (Washington, D.C.)*, v. 14, no. 4, p. 41–49.
- Haq, B.U., and Schutter, S.R., 2008, A chronology of Paleozoic sea-level changes: *Science*, v. 322, p. 64–68, doi: 10.1126/science.1161648.
- Haq, B.U., Hardenbol, J., and Vail, P.R., 1987, Chronology of fluctuating sea levels since the Triassic: *Science*, v. 235, p. 1156–1167, doi: 10.1126/science.235.4793.1156.
- Hardie, L.A., 1996, Secular variation in seawater chemistry: An explanation for the coupled secular variation in the mineralogies of marine limestones and potash evaporites over the past 600 m.y.: *Geology*, v. 24, p. 279–283, doi: 10.1130/0091-7613(1996)024<0279:SVISCA>2.3.CO;2.
- Harland, W.B., Cox, A.V., Llewellyn, P.G., Pickton, C.A.G., Smith, A., and Walters, R., 1982, *A Geologic Time Scale*: Cambridge, UK, Cambridge University Press, 131 p.
- Harland, W.B., Armstrong, R.L., Cox, A.V., Craig, L.E., Smith, A.G., and Smith, D.G., 1990, *A Geologic Time Scale 1989*: Cambridge, UK, Cambridge University Press, 263 p.
- Hassenforder, B., Roger, J., Baudin, T., Chalot-Prat, F., Gasquet, D., Berrahma, A., Chèvremont, P., Marquer, D., Razin, P., and Benlakhdim, A., 2001, Feuille NHI-29-X-1c, Sidi Bou'Addi: Carte Géologique du Maroc à 1:50,000: Notes et Mémoires du Service Géologique du Maroc 414, 1 sheet, scale 1:50,000.
- Hayes, J.M., and Waldbauer, J.R., 2006, The carbon cycle and associated redox processes through time: *Philosophical Transactions of the Royal Society of London*, ser. B, *Biological Sciences*, v. 361, p. 931–950, doi: 10.1098/rstb.2006.1840.
- Hayes, J.M., Strauss, H., and Kaufman, A.J., 1999, The abundance of ^{13}C in marine organic matter and isotopic fractionation in the global biogeochemical cycle of carbon during the past 800 Ma: *Chemical Geology*, v. 161, p. 103–125, doi: 10.1016/S0009-2541(99)00083-2.
- Herman, A.B., and Spicer, R.A., 1996, Palaeobotanical evidence for a warm Cretaceous Arctic Ocean: *Nature*, v. 380, p. 330–333, doi: 10.1038/380330a0.
- Higgins, J.A., and Schrag, D.P., 2006, Beyond methane: Towards a theory for the Paleocene–Eocene thermal maximum: *Earth and Planetary Science Letters*, v. 245, p. 523–537, doi: 10.1016/j.epsl.2006.03.009.
- Higgins, J.A., Fischer, W.W., and Schrag, D.P., 2009, Oxygenation of the ocean and sediments: Consequences for the seafloor carbonate factory: *Earth and Planetary Science Letters*, v. 284, p. 25–33, doi: 10.1016/j.epsl.2009.03.039.
- Hoffman, P.F., 1991, Did the breakout of Laurentia turn Gondwanaland inside-out?: *Science*, v. 252, p. 1409–1412, doi: 10.1126/science.252.5011.1409.
- Hoffman, P.F., Kaufman, A.J., Halverson, G.P., and Schrag, D.P., 1998, A Neoproterozoic snowball Earth: *Science*, v. 281, p. 1342–1346, doi: 10.1126/science.281.5381.1342.
- Hoffmann, K.-H., Condon, D.J., Bowring, S.A., and Crowley, J.L., 2004, U-Pb zircon date from the Neoproterozoic Ghaub Formation, Namibia: Constraints on Marinoan glaciation: *Geology*, v. 32, p. 817–820, doi: 10.1130/G20519.1.
- Holland, H.D., and Zimmermann, H., 2000, The dolomite problem revisited: *International Geology Review*, v. 42, p. 481–490, doi: 10.1080/00206810009465093.
- Holmden, C., Creaser, R.A., Muehlenbachs, K., Leslie, S.A., and Bergström, S.M., 1998, Isotopic evidence for geochemical decoupling between ancient epicritic seas and bordering oceans: Implications for secular curves: *Geology*, v. 26, p. 567–570, doi: 10.1130/0091-7613(1998)026<0567:IEFGDB>2.3.CO;2.
- Holmer, L.E., Skovsted, C.B., Brock, G.A., Valentine, J.L., and Paterson, J.R., 2008, The Early Cambrian tomotiid *Micrina*, a sessile bivalved stem group brachiopod: *Biology Letters*, v. 4, p. 724–728, doi: 10.1098/rsbl.2008.0277.
- Holmes, A., 1960, A revised geological time-scale: *Transactions of the Edinburgh Geological Society*, v. 17, p. 183–216.
- Holser, W.T., Schidlowski, M., Mackenzie, F.T., and Maynard, J.B., 1988, Geochemical cycles of carbon and sulphur, in Gregory, C.B., Garrels, R.M., Mackenzie, F.T., and Maynard, J.B., eds., *Chemical Cycles in the Evolution of the Earth*: New York: John Wiley & Sons, p. 105–173.
- Hou Xianguang, Siveter, D.J., Williams, M., Walossek, D., and Bergström, J., 1996, Appendages of the arthropod *Kunmingella* from the Early Cambrian of China: Its bearing on the systematic position of the Bradoriida and the fossil record of the Ostracoda: *Philosophical Transactions of the Royal Society of London*, ser. B, v. 351, p. 1131–1145.
- Hou Xianguang, Aldridge, R.J., Bergström, J., Siveter, D.J., Siveter, D.J., and Feng Xianghong, 2004, *The Cambrian Fossils of Chengjiang, China: The Flowering of Early Animal Life*: Oxford, Blackwell Science, 233 p.
- Hua Hong, Chen Zhe, Yuan Xunlai, Zhang Luyi, and Xiao, S., 2005, Skeletogenesis and asexual reproduction in the earliest biomineralizing animal *Cloudina*: *Geology*, v. 33, p. 277–280, doi: 10.1130/G21198.1.
- Huber, B.T., Hodell, D.A., and Hamilton, C.P., 1995, Middle–Late Cretaceous climate of the southern high latitudes: Stable isotopic evidence for minimal equator-to-pole thermal gradients: *Geological Society of America Bulletin*, v. 107, p. 1164–1191, doi: 10.1130/0016-7606(1995)107<1164:MLCCOT>2.3.CO;2.
- Huber, M., and Sloan, L.C., 2001, Heat transport, deep waters, and thermal gradients: Coupled simulation of an Eocene greenhouse climate: *Geophysical Research Letters*, v. 28, p. 3481–3484, doi: 10.1029/2001GL012943.
- Huntley, J.W., Xiao, S., and Kowalewski, M., 2006, On the morphological history of Proterozoic and Cambrian acritarchs, in Xiao, S., and Kaufman, A.J., eds., *Neoproterozoic Geobiology and Paleobiology*: Dordrecht, Springer, p. 23–56.
- Husson, L., and Conrad, C.P., 2006, Tectonic velocities, dynamic topography, and relative sea level: *Geophysical Research Letters*, v. 33, art. L18303, 5 p.
- Immenhauser, A., Della Porta, G., Kenter, J.A.M., and Bahamonde, J.R., 2003, An alternative model for positive shifts in shallow-marine carbonate $\delta^{13}\text{C}$ and $\delta^{18}\text{O}$: *Sedimentology*, v. 50, p. 953–959, doi: 10.1046/j.1365-3091.2003.00590.x.
- Ingall, E., and Jahnke, R., 1997, Influence of water-column anoxia on the elemental fractionation of carbon and phosphorus during sediment diagenesis: *Marine Geology*, v. 139, p. 219–229, doi: 10.1016/S0025-3227(96)00112-0.
- Ingall, E.D., and Van Cappellen, P., 1990, Relation between sedimentation rate and burial of organic phosphorus and organic carbon in marine sediments: *Geochimica et Cosmochimica Acta*, v. 54, p. 373–386, doi: 10.1016/0016-7037(90)90326-G.
- Ingall, E.D., Bustin, R.M., and Van Cappellen, P., 1993, Influence of water column anoxia on the burial and preservation of carbon and phosphorus in marine shales: *Geochimica et Cosmochimica Acta*, v. 57, p. 303–316, doi: 10.1016/0016-7037(93)90433-W.
- Irwin, H., Curtis, C., and Coleman, M., 1977, Isotopic evidence for source of diagenetic carbonates formed during burial of organic-rich sediments: *Nature*, v. 269, p. 209–213, doi: 10.1038/269209a0.
- Ishikawa, T., Ueno, Y., Komiya, T., Sawaki, Y., Han Jian, Shu Degan, Li Yong, Maruyama, S., and Yoshida, N., 2008, Carbon isotope chemostratigraphy of a Precambrian/Cambrian boundary section in the Three Gorge area, South China: Prominent global-scale isotope excursions just before the Cambrian explosion: *Gondwana Research*, v. 14, p. 193–208.
- Ivantsov, A.Yu., 1990, New data on the ultrastructure of sabelliditids (Pogonophora?): *Paleontological Journal*, v. 24, no. 4, p. 125–128.
- Jacobsen, S.B., and Kaufman, A.J., 1999, The Sr, C and O isotopic evolution of Neoproterozoic seawater: *Chemical Geology*, v. 161, p. 37–57, doi: 10.1016/S0009-2541(99)00080-7.
- James, N.P., and Klappa, C.F., 1983, Petrogenesis of Early Cambrian reef limestones, Labrador, Canada: *Journal of Sedimentary Petrology*, v. 53, p. 1051–1096.
- James, N.P., Bone, Y., and Kyser, T.K., 2005, Where has all the aragonite gone? Mineralogy of Holocene neritic cool-water carbonates, southern Australia: *Journal of Sedimentary Research*, v. 75, p. 454–463, doi: 10.2110/jsr.2005.035.
- Janussen, D., Steiner, M., and Zhu Maoyan, 2002, New well-preserved scleritomes of Chancelloriidae from the Early Cambrian Yuanshan Formation (Chengjiang, China) and the Middle Cambrian Wheeler Shale (Utah, USA) and paleobiological implications: *Journal of Paleontology*, v. 76, p. 596–606, doi: 10.1666/0022-3360(2002)076<0596:NWPSOC>2.0.CO;2.
- Jenkins, R.J.F., Cooper, J.A., and Compston, W., 2002, Age and biostratigraphy of Early Cambrian tuffs from SE Australia and southern China: *Journal of the Geological Society of London*, v. 159, p. 645–658, doi: 10.1144/0016-764901-127.
- Jenkyns, H.C., Forster, A., Schouten, S., and Simminghe Damsté, J.S., 2004, High temperatures in the Late Cretaceous Arctic Ocean: *Nature*, v. 432, p. 888–892, doi: 10.1038/nature03143.
- Jensen, S., 1997, Trace Fossils from the Lower Cambrian Mickwitzia Sandstone, South-Central Sweden: *Fossils and Strata*: Oslo, Scandinavian University Press, no. 42, 111 p.
- Jensen, S., 2003, The Proterozoic and earliest Cambrian trace fossil record; patterns, problems and perspectives: *Integrative and Comparative Biology*, v. 43, p. 219–228, doi: 10.1093/icb/43.1.219.
- Jensen, S., Gehling, J.G., and Droser, M.L., 1998, Ediacaratype fossils in Cambrian sediments: *Nature*, v. 393, p. 567–569, doi: 10.1038/31215.
- Jensen, S., Saylor, B.Z., Gehling, J.G., and Germs, G.J.B., 2000, Complex trace fossils from the terminal Proterozoic of Namibia: *Geology*, v. 28, p. 143–146, doi: 10.1130/0091-7613(2000)28<143:CTFFTT>2.0.CO;2.
- Jensen, S., Droser, M.L., and Gehling, J.G., 2006, A critical look at the Ediacaran trace fossil record, in Xiao, S., and Kaufman, A.J., eds., *Neoproterozoic Geobiology and Paleobiology*: Dordrecht, Springer, p. 115–157.
- Jernvall, J., Hunter, J.P., and Fortelius, M., 1996, Molar tooth diversity, disparity, and ecology in Cenozoic ungulate radiations: *Science*, v. 274, p. 1489–1492, doi: 10.1126/science.274.5292.1489.
- Jones, B., and Manning, D.A.C., 1994, Comparison of geochemical indices used for the interpretation of palaeoredox conditions in ancient mudstones: *Chemical Geology*, v. 111, p. 111–129, doi: 10.1016/0009-2541(94)90085-X.
- Junge, C.E., Schidlowski, M., Eichmann, R., and Pietrek, H., 1975, Model calculations for the terrestrial

- carbon cycle: Carbon isotope geochemistry and evolution of photosynthetic oxygen: *Journal of Geophysical Research*, v. 80, p. 4542–4552, doi: 10.1029/JC080i033p04542.
- Karlova, G.A., 1987, Pervye nakhodki skelnetoy fauny v turkustskoy svite Olenekskogo podnyatiya: *Doklady Akademii Nauk SSSR*, v. 292, p. 204–205, 1 pl.
- Karlova, G.A., and Vodanyuk, S.A., 1985, Novye dannye o perekhodnykh k kembriyu otlozheniyakh basseyna r. Khorbusuonki (Olenekskoe podnyatie), in *Khomentovskiy, V.V., ed., Stratigrafiya pozdnego dokembriya i rannego paleozoya Sibiri, Vend i rifej: Novosibirsk, Institut Geologii i Geofiziki, Sibirskoe Otdelenie, Akademiya Nauk SSSR*, p. 3–13.
- Katz, M.E., Fennel, K., and Falkowski, P.G., 2007, Geochemical and biological consequences of phytoplankton evolution, in *Falkowski, P.G., and Knoll, A.H., eds., Evolution of Primary Producers in the Sea: Amsterdam, Elsevier*, p. 405–430.
- Kaufman, A.J., Hayes, J.M., Knoll, A.H., and Germs, G.J.B., 1991, Isotopic compositions of carbonates and organic carbon from Upper Proterozoic successions in Namibia: Stratigraphic variation and the effects of diagenesis and metamorphism: *Precambrian Research*, v. 49, p. 301–327, doi: 10.1016/0301-9268(91)90039-D.
- Kaufman, A.J., Jacobsen, S.B., and Knoll, A.H., 1993, The Vendian record of Sr and C isotopic variations in seawater: Implications for tectonics and paleoclimate: *Earth and Planetary Science Letters*, v. 120, p. 409–430, doi: 10.1016/0012-821X(93)90254-7.
- Kaufman, A.J., Knoll, A.H., Semikhatov, M.A., Grotzinger, J.P., Jacobsen, S.B., and Adams, W., 1996, Integrated chronostratigraphy of Proterozoic–Cambrian boundary beds in the western Anabar region, northern Siberia: *Geological Magazine*, v. 133, p. 509–533, doi: 10.1017/S0016756800007810.
- Khain, E.V., Bibikova, E.V., Salnikova, E.B., Kröner, A., Gibsher, A.S., Didenko, A.N., Degtyarev, K.E., and Fedotova, A.A., 2003, The palaeo-Asian ocean in the Neoproterozoic and early Palaeozoic: New geochronological data and palaeotectonic reconstructions: *Precambrian Research*, v. 122, p. 329–358, doi: 10.1016/S0301-9268(02)00218-8.
- Khomentovskiy, V.V., 1997, Sizing up the sub-Tommotian unconformity in Siberia: Comment: *Geology*, v. 25, p. 286, doi: 10.1130/0091-7613(1997)025<0286:SUTSTU>2.3.CO;2.
- Khomentovskiy, V.V., 2008, The Yudomian of Siberia, Vendian and Ediacaran systems of the international stratigraphic scale: *Stratigraphy and Geological Correlation*, v. 16, p. 581–598, doi: 10.1134/S0869593808060014.
- Khomentovskiy, V.V., and Gibsher, A.S., 1996, The Neoproterozoic–Lower Cambrian in northern Govi-Altay, western Mongolia: Regional setting, lithostratigraphy and biostratigraphy: *Geological Magazine*, v. 133, p. 371–390, doi: 10.1017/S001675680000755X.
- Khomentovskiy, V.V., and Karlova, G.A., 1986, O nizhney granitse pestrotsvetnoy svity v bassejne r. Aldan, in *Khomentovskiy, V.V., ed., Pozdnyy dokembriy i ranniy paleozoy Sibiri, Sibirskaya platforma i vneshchaya zona Altae-Sayanskoy skladchtoy oblasti: Novosibirsk, Institut Geologii i Geofiziki, Sibirskoe Otdelenie, Akademiya Nauk SSSR*, p. 3–22.
- Khomentovskiy, V.V., and Karlova, G.A., 1992, The Precambrian–Cambrian boundary and principles of its justification in Siberia: *Russian Geology and Geophysics*, v. 33, no. 11, p. 1–18.
- Khomentovskiy, V.V., and Karlova, G.A., 1993, Biostratigraphy of the Vendian–Cambrian beds and the Lower Cambrian boundary in Siberia: *Geological Magazine*, v. 130, p. 29–45, doi: 10.1017/S0016756800023700.
- Khomentovskiy, V.V., and Karlova, G.A., 2002, The boundary between Nemakit–Daldynian and Tommotian Stages (Vendian–Cambrian systems) of Siberia: *Stratigraphy and Geological Correlation*, v. 10, p. 217–238.
- Khomentovskiy, V.V., and Karlova, G.A., 2005, The Tommotian Stage base as the Cambrian lower boundary in Siberia: *Stratigraphy and Geological Correlation*, v. 13, p. 21–34.
- Kimura, H., and Watanabe, Y., 2001, Oceanic anoxia at the Precambrian–Cambrian boundary: *Geology*, v. 29, p. 995–998, doi: 10.1130/0091-7613(2001)029<0995:OAAATPC>2.0.CO;2.
- Kirschvink, J.L., Magaritz, M., Ripperdan, R.L., Zhuravlev, A.Yu., and Rozanov, A.Yu., 1991, The Precambrian/Cambrian boundary: Magnetostratigraphy and carbon isotopes resolve correlation problems between Siberia, Morocco, and South China: *GSA Today*, v. 1, p. 69–71, 87, 91.
- Kirschvink, J.L., Ripperdan, R.L., and Evans, D.A., 1997, Evidence for a large-scale reorganization of Early Cambrian continental masses by inertial interchange true polar wander: *Science*, v. 277, p. 541–545, doi: 10.1126/science.277.5325.541.
- Knauth, L.P., and Kennedy, M.J., 2009, The late Precambrian greening of the Earth: *Nature*, v. 460, p. 728–732.
- Knoll, A.H., 1994, Proterozoic and Early Cambrian protists: Evidence for accelerating evolutionary tempo: *Proceedings of the National Academy of Sciences of the United States of America*, v. 91, p. 6743–6750, doi: 10.1073/pnas.91.15.6743.
- Knoll, A.H., Hayes, J.M., Kaufman, A.J., Swett, K., and Lambert, I.B., 1986, Secular variation in carbon isotope ratios from Upper Proterozoic successions of Svalbard and East Greenland: *Nature*, v. 321, p. 832–838, doi: 10.1038/321832a0.
- Knoll, A.H., Grotzinger, J.P., Kaufman, A.J., and Kolosov, P., 1995a, Integrated approaches to terminal Proterozoic stratigraphy: An example from the Olenek Uplift, northeastern Siberia: *Precambrian Research*, v. 73, p. 251–270, doi: 10.1016/0301-9268(94)00081-2.
- Knoll, A.H., Kaufman, A.J., Semikhatov, M.A., Grotzinger, J.P., and Adams, W., 1995b, Sizing up the sub-Tommotian unconformity in Siberia: *Geology*, v. 23, p. 1139–1143, doi: 10.1130/0091-7613(1995)023<1139:SUTSTU>2.3.CO;2.
- Kominz, M.A., 1984, Oceanic ridge volumes and sea-level change—An error analysis, in *Schlee, J.S., ed., Interregional Unconformities and Hydrocarbon Accumulation: American Association of Petroleum Geologists Memoir 36*, p. 109–127.
- Korobov, M.N., and Missarzhevskiy, V.V., 1977, O pogranichnykh sloyakh kembriya i dokembriya Zapadnoy Mongolii (khrebet Khasadg-Khairkhan), in *Tatarinov, L.P., ed., Bespozvonochnye paleozoya Mongolii: Sovmestnaya Sovetskogo-Mongol'skaya Paleontologicheskaya Ekspeditsiya, Trudy*, v. 5, p. 7–9.
- Korshunov, V.I., Repina, L.N., and Sysoev, V.A., 1969, K stroeniyu pestrotsvetnoy svity vostoka Aldanskoy anteklizy: *Geologiya i Geofizika*, v. 1969, no. 10, p. 18–21.
- Kouchinsky, A.V., 2000, Skeletal microstructures of hyoliths from the Early Cambrian of Siberia: *Alcheringa*, v. 24, p. 65–81, doi: 10.1080/03115510008619525.
- Kouchinsky, A.V., 2001, Mollusks, hyoliths, stenotheoids, and coeloscleritophorans, in *Zhuravlev, A.Yu., and Riding, R., eds., The Ecology of the Cambrian Radiation: New York, Columbia University Press*, p. 326–349.
- Kouchinsky, A., Bengtson, S., Missarzhevskiy, V.V., Pelechaty, S., Torssander, P., and Val'kov, A.K., 2001, Carbon isotope stratigraphy and the problem of a pre-Tommotian Stage in Siberia: *Geological Magazine*, v. 138, p. 387–396, doi: 10.1017/S0016756801005684.
- Kouchinsky, A., Bengtson, S., Pavlov, V., Rungner, B., Val'kov, A., and Young, E., 2005, Pre-Tommotian age of the lower Pestrotsvet Formation in the Selinde section on the Siberian platform: Carbon isotopic evidence: *Geological Magazine*, v. 142, p. 319–325, doi: 10.1017/S0016756805000865.
- Kouchinsky, A., Bengtson, S., Pavlov, V., Rungner, B., Torssander, P., Young, E., and Ziegler, K., 2007, Carbon isotope stratigraphy of the Precambrian–Cambrian Sukharikha River section, northwestern Siberian platform: *Geological Magazine*, v. 144, p. 609–618, doi: 10.1017/S0016756807003354.
- Kouchinsky, A., Bengtson, S., Feng Weimin, Kutygin, R., and Val'kov, A., 2009, The Lower Cambrian fossil anabaritids: Affinities, occurrences and systematics: *Journal of Systematic Palaeontology*, v. 7, p. 241–298, doi: 10.1017/S1477201909002715.
- Kouchinsky, A., Bengtson, S., and Murdock, D.J.E., 2010, A new annuolinid problematic from the Lower Cambrian of the Sukharikha River in northern Siberia: *Acta Palaeontologica Polonica*, v. 55, p. 321–331, doi: 10.4202/app.2009.1102.
- Kroopnick, P.M., 1985, The distribution of ^{13}C of SCO_2 in the world oceans: *Deep-Sea Research*, v. 32, p. 57–84, doi: 10.1016/0198-0149(85)90017-2.
- Kruse, P.D., Zhuravlev, A.Yu., and James, N.P., 1995, Primmordial metazoan–calcmicrobial reefs: Tommotian (Early Cambrian) of the Siberian Platform: *Palaios*, v. 10, p. 291–321, doi: 10.2307/3515157.
- Kruse, P.D., Gandin, A., Debrenne, F., and Wood, R., 1996, Early Cambrian bioconstructions in the Zavkhan Basin of western Mongolia: *Geological Magazine*, v. 133, p. 429–444, doi: 10.1017/S0016756800007597.
- Kumarapeli, P.S., and Saull, V.A., 1966, The St. Lawrence valley system: A North American equivalent to the East African rift valley system: *Canadian Journal of Earth Sciences*, v. 3, p. 639–658.
- Kump, L.R., 1988, Terrestrial feedback in atmospheric oxygen regulation by fire and phosphorus: *Nature*, v. 335, p. 152–154, doi: 10.1038/335152a0.
- Kump, L.R., 1991, Interpreting carbon-isotopic excursions: Strangelove oceans: *Geology*, v. 19, p. 299–302, doi: 10.1130/0091-7613(1991)019<0299:ICIESO>2.3.CO;2.
- Kump, L.R., and Arthur, M.A., 1999, Interpreting carbon-isotope excursions: Carbonates and organic matter: *Chemical Geology*, v. 161, p. 181–198.
- Kuzmichev, A.B., Bibikova, E.V., and Zhuravlev, D.Z., 2001, Neoproterozoic (~800 Ma) orogeny in the Tuva-Mongolia Massif (Siberia): Island arc–continent collision at the northeast Rodinia margin: *Precambrian Research*, v. 110, p. 109–126, doi: 10.1016/S0301-9268(01)00183-8.
- Lahajnar, N., Rixen, T., Gaye-Haake, B., Schäfer, P., and Ittekkot, V., 2005, Dissolved organic carbon (DOC) fluxes of deep-sea sediments from the Arabian Sea and NE Atlantic: *Deep-Sea Research, Part II. Topical Studies in Oceanography*, v. 52, p. 1947–1964, doi: 10.1016/j.dsr2.2005.05.006.
- Landing, E., 1988, Lower Cambrian of eastern Massachusetts: Stratigraphy and small shelly fossils: *Journal of Paleontology*, v. 62, p. 661–695.
- Landing, E., 1991, Upper Precambrian through Lower Cambrian of Cape Breton Island: Faunas, paleoenvironments, and stratigraphic revision: *Journal of Paleontology*, v. 65, p. 570–595.
- Landing, E., 1993, In situ earliest Cambrian tube worms and the oldest metazoan-constructed biostrome (Placentian Series, southeastern Newfoundland): *Journal of Paleontology*, v. 67, p. 333–342.
- Landing, E., 1994, Precambrian–Cambrian boundary global stratotype ratified and a new perspective of Cambrian time: *Geology*, v. 22, p. 179–182, doi: 10.1130/0091-7613(1994)022<0179:PCBGRS>2.3.CO;2.
- Landing, E., and MacGabhann, B.A., 2010, First evidence for Cambrian glaciation provided by sections in Avalonian New Brunswick and Ireland: Additional data for Avalon–Gondwana separation by the earliest Palaeozoic: *Palaeogeography, Palaeoclimatology, Palaeoecology*, v. 285, p. 174–185, doi: 10.1016/j.palaeo.2009.11.009.
- Landing, E., Myrow, P., Benus, A.P., and Narbonne, G.M., 1989, The Placentian Series: Appearance of the oldest skeletalized faunas in southeastern Newfoundland: *Journal of Paleontology*, v. 63, p. 739–769.
- Landing, E., Bowring, S.A., Davidek, K.L., Westrop, S.R., Geyer, G., and Heldmaier, W., 1998, Duration of the Early Cambrian: U–Pb ages of volcanic ashes from Avalon and Gondwana: *Canadian Journal of Earth Sciences*, v. 35, p. 329–338, doi: 10.1139/cjes-35-4-329.
- Latham, A., and Riding, R., 1990, Fossil evidence for the location of the Precambrian/Cambrian boundary in Morocco: *Nature*, v. 344, p. 752–754, doi: 10.1038/344752a0.
- Laurie, J.R., 2000, Paterinata, in *Williams, A., Brunton, C.H.C., and Carlson, S.J., eds., Treatise on Invertebrate Paleontology, Part H, Brachiopoda (Revised), Volume 2: Boulder, Colorado, Geological Society of America*, p. 147–157.
- Lenton, T.M., and Watson, A.J., 2000, Redfield revisited: 1. Regulation of nitrate, phosphate, and oxygen in the ocean: *Global Biogeochemical Cycles*, v. 14, p. 225–248, doi: 10.1029/1999GB009005.
- Li Guoxiang, Zhang Junming, and Zhu Maoyan, 2001, Litho- and biostratigraphy of the Lower Cambrian

- Meishucunian Stage in the Xiaotan section, eastern Yunnan: *Acta Palaeontologica Sinica*, v. 40, supplement, p. 40–53.
- Li Guoxiang, Zhu Maoyan, and Steiner, M., 2003, Microstructure and functional morphology of the Early Cambrian problematical fossil *Rhombocorniculium*: *Progress in Natural Science*, v. 13, p. 831–835, doi: 10.1080/10020070312331344510.
- Li Guoxiang, Steiner, M., Zhu Xuejian, Yang Aihua, Wang Haifeng, and Erdtmann, B.-D., 2007, Early Cambrian metazoan fossil record of South China: Generic diversity and radiation patterns: *Palaeogeography, Palaeoclimatology, Palaeoecology*, v. 254, p. 229–249.
- Li, Z.X., 1998, Tectonic history of the major East Asian lithospheric blocks since the mid-Proterozoic—A synthesis, in Martin, F.J., Chung, S.-L., Lo, C.-H., and Lee, T.-Y., eds., *Mantle Dynamics and Plate Interactions in East Asia*: American Geophysical Union (AGU) Geodynamics Series 27, p. 221–243.
- Li, Z.X., Li, X.H., Kinny, P.D., Wang, J., Zhang, S., and Zhou, H., 2003, Geochronology of Neoproterozoic syn-rift magmatism in the Yangtze craton, South China, and correlations with other continents: Evidence for a mantle superplume that broke up Rodinia: *Precambrian Research*, v. 122, p. 85–109, doi: 10.1016/S0301-9268(02)00208-5.
- Lindsay, J.F., Brasier, M.D., Dorjnamjaa, D., Groling, R., Kruse, P.D., and Wood, R.A., 1996a, Facies and sequence controls on the appearance of the Cambrian biota in southwestern Mongolia: Implications for the Precambrian-Cambrian boundary: *Geological Magazine*, v. 133, p. 417–428, doi: 10.1017/S0016756800007585.
- Lindsay, J.F., Brasier, M.D., Shields, G., Khomentovsky, V.V., and Bat-Ireedui, Y.A., 1996b, Glacial facies associations in a Neoproterozoic back-arc setting, Zavkhan Basin, western Mongolia: *Geological Magazine*, v. 133, p. 391–402, doi: 10.1017/S0016756800007561.
- Lipps, J.H., ed., 1993, *Fossil prokaryotes and protists*: Boston, Blackwell Science, 342 p.
- Love, G.D., Grosjean, E., Stalvies, C., Fike, D.A., Grotzinger, J.P., Bradley, A.S., Kelly, A.E., Bhatia, M., Meredith, W., Snape, C.E., Bowring, S.A., Condon, D.J., and Summons, R.E., 2009, Fossil steroids record the appearance of Demospongiae during the Cryogenian period: *Nature*, v. 457, p. 718–721, doi: 10.1038/nature07673.
- Lowenstam, H.A., and Epstein, S., 1957, On the origin of sedimentary aragonite needles of the Great Bahama Bank: *The Journal of Geology*, v. 65, p. 364–375, doi: 10.1086/626439.
- Lowenstam, T.K., Timofeef, M.N., Brennan, S.T., Hardie, L.A., and Demicco, R.V., 2001, Oscillations in Phanerozoic seawater chemistry: Evidence from fluid inclusions: *Science*, v. 294, p. 1086–1088, doi: 10.1126/science.1064280.
- Luchinina, V.A., 1999, Reef frameworks on the Siberian Platform through the Vendian–Cambrian boundary: *Russian Geology and Geophysics*, v. 40, p. 1753–1762.
- Luchinina, V.A., Korovnikov, I.V., Sipin, D.P., and Fedoseev, A.V., 1997, Upper Vendian–Lower Cambrian biostratigraphy of the Sukharikha River section (Siberian Platform): *Russian Geology and Geophysics*, v. 38, p. 1385–1397.
- Luo Huilin, Wu Xiche, and Ouyang Lin, 1991, Facies and correlation of the Sinian–Cambrian boundary stratigraphy: *Sedimentary Facies and Palaeogeography*, v. 4, p. 27–35 (in Chinese with English abstract).
- Ma Lifong, chief compiler, 2004, *Geological Map of China*: Beijing, Geological Publishing House, scale 1:2,500,000, 1 sheet.
- Macdonald, F.A., Jones, D.S., and Schrag, D.P., 2009, Stratigraphic and tectonic implications of a newly discovered glacial diamictite–cap carbonate couplet in southwestern Mongolia: *Geology*, v. 37, p. 123–126, doi: 10.1130/G24797A.1.
- Magaritz, M., Holsler, W.T., and Kirschvink, J.L., 1986, Carbon isotope events across the Precambrian/Cambrian boundary on the Siberian Platform: *Nature*, v. 320, p. 258–259, doi: 10.1038/320258a0.
- Magaritz, M., Kirschvink, J.L., Latham, A.J., Zhuravlev, A.Yu., and Rozanov, A.Yu., 1991, Precambrian/Cambrian boundary problem: Carbon isotope correlations for Vendian and Tommotian time between Siberia and Morocco: *Geology*, v. 19, p. 847–850, doi: 10.1130/0091-7613(1991)019<0847:PCBPCL>2.3.CO;2.
- Malinky, J.M., 2009, First occurrence of *Orthotheca* Novák, 1886 (Hyalolitha, Early Devonian) in North America: *Journal of Paleontology*, v. 83, p. 588–596, doi: 10.1666/08-164R.1.
- Malinky, J.M., and Skovsted, C.B., 2004, Hyoliths and small shelly fossils from the Lower Cambrian of North-East Greenland: *Acta Palaeontologica Polonica*, v. 49, p. 551–578.
- Malinky, J.M., and Yochelson, E.L., 2007, On the systematic position of the Hyolitha (kingdom Animalia), in Laurie, J.R., and Paterson, J.R., eds., *Papers in Honour of John H. Shergold 1938–2006*: Association of Australasian Palaeontologists Memoir 34, p. 521–536.
- Maloof, A.C., 2004, Thermal Contraction Cracks, Polar Wandering, and Global Carbon Cycling: Non-Uniformitarian Changes that Shaped the Neoproterozoic and Early Cambrian Earth [Ph.D. thesis]: Cambridge, Massachusetts, Harvard University, 193 p.
- Maloof, A.C., Schrag, D.P., Crowley, J.L., and Bowring, S.A., 2005, An expanded record of Early Cambrian carbon cycling from the Anti-Atlas margin, Morocco: *Canadian Journal of Earth Sciences*, v. 42, p. 2195–2216, doi: 10.1139/e05-062.
- Maloof, A.C., Halverson, G.P., Kirschvink, J.L., Schrag, D.P., Weiss, B.P., and Hoffman, P.F., 2006, Combined paleomagnetic, isotopic, and stratigraphic evidence for true polar wander from the Neoproterozoic Akademikerbreen Group, Svalbard, Norway: *Geological Society of America Bulletin*, v. 118, p. 1099–1124, doi: 10.1130/B25892.1.
- Maloof, A.C., Ramezani, J., Bowring, S.A., Fike, D.A., Porter, S.M., and Mazouad, M., 2010a, Constraints on Early Cambrian carbon cycling from the duration of the Nemakit-Daldynian–Tommotian boundary $\delta^{13}\text{C}$ shift, Morocco: *Geology*, v. 38, p. 623–626, doi: 10.1130/G30726.1.
- Maloof, A.C., Rose, C.V., Beach, R., Samuels, B.M., Calmet, C.C., Erwin, D.H., Poirier, G.R., Yao, N. and Simons, F.J., 2010b, Possible animal-body fossils in pre-Marinoan limestones from South Australia: *Nature Geoscience*, v. 3, p. 653–659, doi: 10.1038/ngeo934.
- Marek, L., and Yochelson, E.L., 1976, Aspects of the biology of Hyolitha (Mollusca): *Lethaia*, v. 9, p. 65–82, doi: 10.1111/j.1502-3931.1976.tb00952.x.
- Marshall, C.R., 2006, Explaining the Cambrian “explosion” of animals: *Annual Review of Earth and Planetary Sciences*, v. 34, p. 355–384, doi: 10.1146/annurev.earth.33.031504.103001.
- Martí Mus, M., and Bergström, J., 2005, The morphology of hyolithids and its functional implications: *Palaeontology*, v. 48, p. 1139–1167, doi: 10.1111/j.1475-4983.2005.00511.x.
- Martí Mus, M., Palacios, T., and Jensen, S., 2008, Size of the earliest mollusks: Did small helcionellids grow to become large adults?: *Geology*, v. 36, p. 175–178, doi: 10.1130/G24218A.1.
- Martin, M.W., Grazhdankin, D.V., Bowring, S.A., Evans, D.A.D., Fedonkin, M.A., and Kirschvink, J.L., 2000, Age of Neoproterozoic bilaterian body and trace fossils, White Sea, Russia: Implications for metazoan evolution: *Science*, v. 288, p. 841–845, doi: 10.1126/science.288.5467.841.
- Matthews, S.C., and Cowie, J.W., 1979, Early Cambrian transgression: *Journal of the Geological Society of London*, v. 136, p. 133–135, doi: 10.1144/gsjgs.136.2.0133.
- Matthews, S.C., and Missarzhevsky, V.V., 1975, Small shelly fossils of late Precambrian and Early Cambrian age: A review of recent work: *Journal of the Geological Society of London*, v. 131, p. 289–304, 4 pl.
- Mattinson, J.M., 2000, Revisiting the “gold standard”—The uranium decay constants of Jaffey et al., 1971: *Eos (Transactions, American Geophysical Union)*, v. 81, Spring Meeting supplement, p. S444–S445.
- Mattinson, J.M., 2005, Zircon U-Pb chemical abrasion (“CA-TIMS”) method: Combined annealing and multi-step partial dissolution analysis for improved precision and accuracy of zircon ages: *Chemical Geology*, v. 220, p. 47–66, doi: 10.1016/j.chemgeo.2005.03.011.
- Mattinson, J.M., 2010, Analysis of the relative decay constants of ^{235}U and ^{238}U by multi-step CA-TIMS measurements of closed-system natural zircon samples: *Chemical Geology*, v. 275, p. 186–198, doi: 10.1016/j.chemgeo.2010.05.007.
- McCausland, P.J.A., Van der Voo, R., and Hall, C.M., 2007, Circum-Iapetus paleogeography of the Precambrian-Cambrian transition with a new paleomagnetic constraint from Laurentia: *Precambrian Research*, v. 156, p. 125–152, doi: 10.1016/j.precambres.2007.03.004.
- McFadden, K.A., Huang Jing, Chu Xuelei, Jiang Ganqing, Kaufman, A.J., Zhou Chuanming, Yuan Xunali, and Xiao, S., 2008, Pulsed oxidation and biological evolution in the Ediacaran Doushantuo Formation: *Proceedings of the National Academy of Sciences, U.S.A.*, v. 105, p. 3197–3202.
- McIlroy, D., Green, O.R., and Brasier, M.D., 2001, Palaeobiology and evolution of the earliest agglutinated Foraminifera: *Platysolenites*, *Spirosolenites* and related forms: *Lethaia*, v. 34, p. 13–29, doi: 10.1080/002411601300068170.
- McKie, T., 1993, Relative sea-level changes and the development of a Cambrian transgression: *Geological Magazine*, v. 130, p. 245–256, doi: 10.1017/S001675680009894.
- Meert, J.G., Van der Voo, R., Pisarevsky, S.A., Komissarova, R.A., and Khramov, A.N., 2001, New paleomagnetic result from Vendian red sediments in Cisbaikalia and the problem of the relationship of Siberia and Laurentia in the Vendian: Comment and reply: *Geophysical Journal International*, v. 146, p. 867–870, doi: 10.1046/j.0956-540x.2001.01474.x.
- Mehl, D., and Erdtmann, B.-D., 1994, *Sanshapentella dapingi* n. gen., n. sp.—A new hexactinellid sponge from the Early Cambrian (Tommotian) of China: *Berliner Geowissenschaftliche Abhandlungen E*, v. 13, p. 315–319.
- Meshkova, N.P., 1974, Kholiity nizhnego kembriya Sibirskoy platformy: *Akademiya Nauk SSSR, Sibirskoe Otdelenie, Trudy Instituta Geologii i Geofiziki*, v. 97, 111 p.
- Meybeck, M., 2003, Global analysis of river systems: From Earth system controls to Anthropocene syndromes: *Philosophical Transactions of the Royal Society of London, ser. B, Biological Sciences*, v. 358, p. 1935–1955, doi: 10.1098/rstb.2003.1379.
- Miller, K.G., Komzin, M.A., Browning, J.V., Wright, J.D., Mountain, G.S., Katz, M.E., Sugarman, P.J., Cramer, B.S., Christie-Blick, N., and Pekar, S.F., 2005, The Phanerozoic record of global sea-level change: *Science*, v. 310, p. 1293–1298, doi: 10.1126/science.1116412.
- Missarzhevsky, V.V., 1982, Subdivision and correlation of the Precambrian-Cambrian boundary sequences based on certain ancient groups of skeletal organisms: *International Geology Review*, v. 25, p. 745–759, doi: 10.1080/00206818309466763.
- Missarzhevsky, V.V., 1983, The stratigraphy of the oldest Phanerozoic sequences of the Anabar Massif: *International Geology Review*, v. 26, p. 394–406, doi: 10.1080/00206818409466566.
- Missarzhevsky, V.V., 1989, Drevneyshie skelentye okamenelosti i stratigrafiya pogranichnykh tolsch dokembriya i kembriya: *Akademiya Nauk SSSR, Ordena Trudovogo Krasnogo Znameni Geologicheskiiy Institut, Trudy*, v. 443, 238 p., 32 pl.
- Mitchell, R.N., Evans, D.A.D., and Kilian, T.M., 2010, Rapid Early Cambrian rotation of Gondwana: *Geology*, v. 38, p. 755–758, doi: 10.1130/G30910.1.
- Montañez, I.P., Banner, J.L., Osleger, D.A., Borg, L.E., and Bosserman, P.J., 1996, Integrated Sr isotope variations and sea-level history of Middle to Upper Cambrian platform carbonates: Implications for the evolution of Cambrian seawater $^{87}\text{Sr}/^{86}\text{Sr}$: *Geology*, v. 24, p. 917–920, doi: 10.1130/0091-7613(1996)024<0917:ISIVAS>2.3.CO;2.
- Mortaj, A., Ikenne, M., Gasquet, D., Barbey, P., and Stussi, J.M., 2000, Les graniitoïdes paléoproterozoïques des boutonnières du Bas Drâa et de la Tagragra d’Akka (Anti-Atlas occidental, Maroc): Un élément du puzzle

- géodynamique du craton ouest-africain: *Journal of African Earth Sciences*, v. 31, p. 523–538, doi: 10.1016/S0899-5362(00)80005-6.
- Mottl, M.J., and Wheat, C.G., 1994, Hydrothermal circulation through mid-ocean ridge flanks: Fluxes of heat and magnesium: *Geochimica et Cosmochimica Acta*, v. 58, p. 2225–2237, doi: 10.1016/0016-7037(94)90007-8.
- Moucha, R., Forte, A.M., Mitrovica, J.X., Rowley, D.B., Quéré, S., Simmons, N.A., and Grand, S.P., 2008, Dynamic topography and long-term sea-level variations: There is no such thing as a stable continental platform: *Earth and Planetary Science Letters*, v. 271, p. 101–108, doi: 10.1016/j.epsl.2008.03.056.
- Mountjoy, E.W., and Amthor, J.E., 1994, Has burial dolomitization come of age? Some answers from the Western Canada sedimentary basin, in Purser, B., Tucker, M., and Zenger, D., eds., *Dolomites: A Volume in Honour of Dolomieu*: Oxford, Blackwell Scientific, p. 203–229.
- Mucci, A., and Morse, J.W., 1983, The incorporation of Mg²⁺ and Sr²⁺ into calcite overgrowths: Influences of growth rate and solution composition: *Geochimica et Cosmochimica Acta*, v. 47, p. 217–233, doi: 10.1016/0016-7037(83)90135-7.
- Nalivkin, D.V., chief compiler, 1965, *Geologicheskaya Karta SSSR: Moscow, Ministerstvo Geologii*, scale 1:2,500,000, 17 sheets.
- Narbonne, G.M., Kaufman, A.J., and Knoll, A.H., 1994, Integrated chemostratigraphy and biostratigraphy of the Windermere Supergroup, northwestern Canada: Implications for Neoproterozoic correlations and the early evolution of animals: *Geological Society of America Bulletin*, v. 106, p. 1281–1292, doi: 10.1130/0016-7606(1994)106<1281:ICABOT>2.3.CO;2.
- Newell, N.D., 1952, Periodicity in invertebrate evolution: *Journal of Paleontology*, v. 26, p. 371–385.
- Newell, N.D., 1962, Paleontological gaps and geochronology: *Journal of Paleontology*, v. 36, p. 592–610.
- Nicholas, C.J., 1996, The Sr isotopic evolution of the oceans during the ‘Cambrian explosion’: *Journal of the Geological Society of London*, v. 153, p. 243–254, doi: 10.1144/gsjgs.153.2.0243.
- Norin, E., 1937, *Geology of western Qurug Tagh, eastern T’ien-Shan: Reports from the Scientific Expedition to the North-Western Provinces of China under the Leadership of Dr. Sven Hedin, III: Stockholm, Bokförlags Aktiebolaget Thule, Volume 1*, 194 p.
- O’Loughlin, E.J., and Chin, Y.-P., 2004, Quantification and characterization of dissolved organic carbon and iron in sedimentary porewater from Green Bay, WI, USA: *Biogeochemistry*, v. 71, p. 371–386, doi: 10.1007/s10533-004-0373-x.
- Orłowski, S., and Waksmundzki, B., 1986, The oldest Hyolitha in the Lower Cambrian of the Holy Cross Mountains: *Acta Geologica Polonica*, v. 36, p. 225–231, 2 pl.
- Parkhaev, P.Yu., 1998, Siphonocoelocera—A new class of Early Cambrian bivalved organisms: *Paleontological Journal*, v. 32, p. 1–15.
- Parkhaev, P.Yu., 2001, The functional morphology of the Cambrian univalved molluscs—Helcionellids: *Paleontological Journal*, v. 35, p. 470–475.
- Parkhaev, P.Yu., 2008, The Early Cambrian radiation of Mollusca, in Ponder, W.F., and Lindberg, D.R., eds., *Phylogeny and Evolution of the Mollusca*: Berkeley, University of California Press, p. 33–69.
- Parsons, B., 1982, Causes and consequences of the relation between area and age of the ocean floor: *Journal of Geophysical Research*, v. 87, p. 289–302, doi: 10.1029/JB087iB01p00289.
- Patterson, W.P., and Walter, L.M., 1994, Depletion of ¹³C in seawater E_{CO2} on modern carbonate platforms: Significance for the carbon isotopic record of carbonates: *Geology*, v. 22, p. 885–888, doi: 10.1130/0091-7613(1994)022<0885:DOCISC>2.3.CO;2.
- Peel, J.S., 1988, *Spirellus* and related helically coiled microfossils (Cyanobacteria) from the Lower Cambrian of North Greenland: *Grønlands Geologiske Undersøgelse Rapport*, v. 137, p. 5–32.
- Peel, J.S., 1991, Functional morphology of the class Helcionelloida nov., and the early evolution of the Mollusca, in Simonetta, A.M., and Conway Morris, S., eds., *The Early Evolution of Metazoa and the Significance of Problematic Taxa*: Cambridge, UK, Cambridge University Press, p. 157–177.
- Peel, J.S., and Skovsted, C.B., 2005, Problematic cap-shaped fossils from the Lower Cambrian of North-East Greenland: *Palaontologische Zeitschrift*, v. 79, p. 461–470.
- Pel'man, Yu.L., Ermak, V.V., Fedorov, A.B., Luchinina, V.A., Zhuravleva, I.T., Repina, L.N., Bondarev, V.I., and Borodaevskaya, Z.V., 1990, Novye dannye po stratigrafii i paleontologii verkhnego dokembriya i nizhnego kembriya r. Dzhandy (pravyy pritok r. Aldan), in Repina, L.N., ed., *Biostratigrafiya i paleontologiya kembriya Severnoy Azii: Akademiya Nauk SSSR, Sibirskoe Otdelenie, Trudy Instituta Geologii i Geofiziki*, v. 765, p. 3–32, 3 pl.
- Peters, S.E., 2005, Geologic constraints on the macroevolutionary history of marine animals: *Proceedings of the National Academy of Sciences of the United States of America*, v. 102, p. 12,326–12,331, doi: 10.1073/pnas.0502616102.
- Peterson, K.J., Lyons, J.B., Nowak, K.S., Takacs, C.M., Wargo, M.J., and McPeck, M.A., 2004, Estimating metazoan divergence times with a molecular clock: *Proceedings of the National Academy of Sciences of the United States of America*, v. 101, p. 6536–6541, doi: 10.1073/pnas.0401670101.
- Peterson, K.J., Cotton, J.A., Gehling, J.G., and Pisani, D., 2008, The Ediacaran emergence of bilaterians: Congruence between the genetic and the geological fossil records: *Philosophical Transactions of the Royal Society of London*, ser. B, *Biological Sciences*, v. 363, p. 1435–1443, doi: 10.1098/rstb.2007.2233.
- Piper, D.Z., 1994, Seawater as the source of minor elements in black shales, phosphorites and other sedimentary rocks: *Chemical Geology*, v. 114, p. 95–114, doi: 10.1016/0009-2541(94)90044-2.
- Piper, D.Z., and Isaacs, C.M., 1995, Minor elements in Quaternary sediment from the Sea of Japan: A record of surface-water productivity and intermediate-water redox conditions: *Geological Society of America Bulletin*, v. 107, p. 54–67, doi: 10.1130/0016-7606(1995)107<0054:MEIQSF>2.3.CO;2.
- Pisarevsky, S.A., Gurevich, E.L., and Khramov, A.N., 1997, Palaeomagnetism of Lower Cambrian sediments from the Olenek River section (northern Siberia): Palaeopoles and the problem of magnetic polarity in the Early Cambrian: *Geophysical Journal International*, v. 130, p. 746–756, doi: 10.1111/j.1365-246X.1997.tb01869.x.
- Pisarevsky, S.A., Komissarova, R.A., and Khramov, A.N., 2000, New palaeomagnetic results from Vendian red sediments in Cisbaikalia and the problem of the relationship of Siberia and Laurentia in the Vendian: *Geophysical Journal International*, v. 140, p. 598–610, doi: 10.1046/j.1365-246X.2000.101-1-00056.x.
- Pisarevsky, S.A., Wingate, M.T.D., Powell, C.M., Johnson, S., and Evans, D.A.D., 2003, Models of Rodinia assembly and fragmentation, in Yoshida, M., Windley, B.E., and Dasgupta, S., eds., *Proterozoic East Gondwana: Supercontinent Assembly and Breakup*: Geological Society of London Special Publication 206, p. 35–55.
- Pitman, W.C., III, 1978, Relationship between eustasy and stratigraphic sequences of passive margins: *Geological Society of America Bulletin*, v. 89, p. 1389–1403, doi: 10.1130/0016-7606(1978)89<1389:RBEASS>2.0.CO;2.
- Ponder, W.F., Parkhaev, P.Yu., and Beecher, D.L., 2007, A remarkable similarity in scaly shell structure in Early Cambrian univalved limpets (Monoplacophora; Maikhanellidae) and a Recent fissurellid limpet (Gastropoda: Vetigastropoda) with a review of Maikhanellidae: *Molluscan Research*, v. 27, p. 129–139.
- Popov, L.E., and Holmer, L.E., 2000, Obolletata, in Williams, A., Brunton, C.H.C., and Carlson, S.J., eds., *Treatise on Invertebrate Paleontology, Part H, Brachiopoda (Revised)*, Volume 2: Boulder, Colorado, Geological Society of America, p. 200–208.
- Popov, L.E., and Williams, A., 2000, Kutorginata, in Williams, A., Brunton, C.H.C., and Carlson, S.J., eds., *Treatise on Invertebrate Paleontology, Part H, Brachiopoda (Revised)*, Volume 2: Boulder, Colorado, Geological Society of America, p. 208–215.
- Porter, S.M., 2004a, Closing the phosphatization window: Testing for the influence of taphonomic megabias on the pattern of small shelly fossil decline: *Palaeos*, v. 19, p. 178–183, doi: 10.1669/0883-1351(2004)019<0178:CTPWTF>2.0.CO;2.
- Porter, S.M., 2004b, Halkierids in Middle Cambrian phosphatic limestones from Australia: *Journal of Paleontology*, v. 78, p. 574–590.
- Porter, S.M., 2007, Seawater chemistry and early carbonate biomineralization: *Science*, v. 316, p. 1302, doi: 10.1126/science.1137284.
- Porter, S.M., 2008, Skeletal microstructure indicates chancelloriids and halkierids are closely related: *Palaontology*, v. 51, p. 865–879, doi: 10.1111/j.1475-4983.2008.00792.x.
- Porter, S.M., 2010, Calcite and aragonite seas and the *de novo* acquisition of carbonate skeletons: *Geobiology*, v. 8, p. 256–277, doi: 10.1111/j.1472-4669.2010.00246.x.
- Purser, B., Tucker, M., and Zenger, D., eds., 1994, *Dolomites: A Volume in Honour of Dolomieu*: Oxford, Blackwell Scientific, 451 p.
- Qian Yi, 1977, [Hyolitha and some problematica from the Lower Cambrian Meishucun Stage in central and S.W. China]: *Acta Palaeontologica Sinica*, v. 16, p. 255–278, 3 pl. (in Chinese with English abstract).
- Qian Yi, 1989, Early Cambrian small shelly fossils of China with special reference to the Precambrian-Cambrian boundary: *Stratigraphy and palaeontology of systemic boundaries in China, Precambrian-Cambrian boundary, Volume 2*: Nanjing, Nanjing University Publishing House, 342 p., 99 pl.
- Qian Yi, ed., 1999, [Taxonomy and biostratigraphy of small shelly fossils in China]: Beijing, Science Press, 247 p. (in Chinese with English summary).
- Qian Yi, and Bengtson, S., 1989, Palaeontology and biostratigraphy of the Early Cambrian Meishucunian Stage in Yunnan Province, South China: *Fossils and Strata*, v. 24, 156 p.
- Qian Yi, Li Guoxiang, and Zhu Maoyan, 2001, The Meishucunian Stage and its small shelly fossil sequence in China: *Acta Palaeontologica Sinica*, v. 40, supplement, p. 54–62.
- Qian Yi, Li Guoxiang, Zhu Maoyan, Steiner, M., and Erdtmann, B.-D., 2004, Early Cambrian protoconodonts and conodont-like fossils from China: Taxonomic revisions and stratigraphic implications: *Progress in Natural Science*, v. 14, p. 173–180.
- Ragözina, A., Dorjnamjaa, D., Krayushkin, A., and Serezhnikova, E., 2008, *Treptichnus pedum* and the Vendian-Cambrian boundary, in 33rd International Geological Congress Abstracts: Oslo, abs. HPF-07.
- Randell, R.D., Lieberman, B.S., Hasiotis, S.T., and Pope, M.C., 2005, New chancelloriids from the Early Cambrian Sekwi Formation with a comment on chancelloriid affinities: *Journal of Paleontology*, v. 79, p. 987–996, doi: 10.1666/0022-3360(2005)079[0987:NCFTFC]2.0.CO;2.
- Raub, T.D., Kirschvink, J.L., and Evans, D.A.D., 2007, True polar wander: Linking deep and shallow geodynamics to hydro- and biospheric hypotheses, in Kono, M., ed., *Treatise on Geophysics: Volume 5. Geomagnetism*: Amsterdam, Elsevier, p. 565–589.
- Raymo, M.E., Ruddiman, W.F., and Froelich, P.N., 1988, Influence of late Cenozoic mountain building on ocean geochemical cycles: *Geology*, v. 16, p. 649–653, doi: 10.1130/0091-7613(1988)016<0649:IOLCMB>2.3.CO;2.
- Reitner, J., and Wörheide, G., 2002, Non-lithistid fossil Demospongiae—Origins of their palaeobiodiversity and highlights in history of preservation, in Hooper, J.N.A., and Van Soest, R., eds., *Systema Porifera*: New York, Kluwer/Plenum, p. 52–68.
- Repina, L.N., and Rozanov, A.Yu., eds., 1992, *Kembriy Sibiri: Rossiyskaya Akademiya Nauk, Sibirskoe Otdelenie, Trudy Instituta Geologii i Geofiziki*, v. 788, 135 p.
- Repina, L.N., Borodaevskaya, Z.V., and Ermak, V.V., 1988, Opornyy razrez po r. Selinde (yugo-vostochnaya okraina Aldanskogo shchita), in Zhuravleva, I.T., and Repina, L.N., eds., *Kembriy Sibiri i Sredney Azii: Akademiya Nauk SSSR, Sibirskoe Otdelenie, Trudy Instituta Geologii i Geofiziki*, v. 720, p. 3–31.
- Richter, F.M., Rowley, D.B., and DePaolo, D.J., 1992, Sr isotope evolution of seawater: The role of tectonics: *Earth and Planetary Science Letters*, v. 109, p. 11–23, doi: 10.1016/0012-821X(92)90070-C.

- Riding, R., 2001, Calcified algae and bacteria, in Zhuravlev, A. Yu., and Riding, R., eds., *The Ecology of the Cambrian Radiation*: New York, Columbia University Press, p. 445–473.
- Riding, R., and Zhuravlev, A. Yu., 1995, Structure and diversity of oldest sponge-microbe reefs: Lower Cambrian, Aldan River, Siberia: *Geology*, v. 23, p. 649–652, doi: 10.1130/0091-7613(1995)023<0649:SADOOS>2.3.CO;2.
- Roger, J., Gasquet, D., Baudin, T., Chalot-Prat, F., Hassenforder, B., Marquer, D., Chèvremont, P., Berrahma, A., Destombes, J., Razin, P., and Benlakhdim, A., 2001, Feuille NHI-29-X-1d, Tamazart: Carte Géologique du Maroc à 1:50,000: Notes et Mémoires du Service Géologique du Maroc 415, 1 sheet, scale 1:50,000.
- Roggenthen, W.M., Fischer, J.F., Napoleone, G., and Fischer, A.G., 1981, Paleomagnetism and age of mafic plutons, Wichita Mountains, Oklahoma: *Geophysical Research Letters*, v. 8, p. 133–136, doi: 10.1029/GL008i02p00133.
- Romanek, C.S., Grossman, E.L., and Morse, J.W., 1992, Carbon isotopic fractionation in synthetic aragonite and calcite: Effects of temperature and precipitation rate: *Geochimica et Cosmochimica Acta*, v. 56, p. 419–430, doi: 10.1016/0016-7037(92)90142-6.
- Rothman, D.H., Hayes, J.M., and Summons, R.E., 2003, Dynamics of the Neoproterozoic carbon cycle: Proceedings of the National Academy of Sciences of the United States of America, v. 100, p. 8124–8129, doi: 10.1073/pnas.0832439100.
- Rowland, S.M., 2001, Archaeocyaths—A history of phylogenetic interpretation: *Journal of Paleontology*, v. 75, p. 1065–1078, doi: 10.1666/0022-3360(2001)075<1065:AAHOP>2.0.CO;2.
- Rowland, S.M., Luchinina, V.A., Korovnikov, I.V., Sipin, D.P., Tarletskov, A.I., and Fedoseev, A.V., 1998, Biostratigraphy of the Vendian–Cambrian Sukharikha River section, northwestern Siberian Platform: *Canadian Journal of Earth Sciences*, v. 35, p. 339–352, doi: 10.1139/cjes-35-4-339.
- Rowley, D.B., 2002, Rate of plate creation and destruction: 180 Ma to present: *Geological Society of America Bulletin*, v. 114, p. 927–933, doi: 10.1130/0016-7606(2002)114<0927:ROPCAD>2.0.CO;2.
- Rozañov, A. Yu., 1984, The Precambrian–Cambrian boundary in Siberia: Episodes, v. 7, p. 20–24.
- Rozañov, A. Yu., and Missarzhevsky, V.V., 1966, Biostratigrafiya i fauna nizhnikh gorizontov kembriya: Akademiya Nauk SSSR, Geologicheskii Institut, Trudy, v. 148, 127 p., 13 pl.
- Rozañov, A. Yu., and Sokolov, B.S., eds., 1984, Yarusnoe raschlenenie nizhnego kembriya, Stratigrafiya: Moscow, Nauka, 184 p.
- Rozañov, A. Yu., and Zhuravlev, A. Yu., 1992, The Lower Cambrian fossil record of the Soviet Union, in Lipps, J.H., and Signor, P.W., eds., *Origin and Early Evolution of the Metazoa*: New York, Plenum Press, p. 205–282.
- Rozañov, A. Yu., Missarzhevsky, V.V., Volkova, N.A., Voronova, L.C., Krylov, I.N., Keller, B.M., Korolyuk, I.K., Lendzion, K., Michniak, R., Pykhova, N.G., and Sidorov, A.D., 1969, The Tommotian Stage and the Cambrian lower boundary problem: New Delhi, Amerind Publishing Co., 359 p., 55 pl.
- Rozañov, A. Yu., Khomentovsky, V.V., Shabanov, Yu. Ya., Karlova, G.A., Varlamov, A.I., Luchinina, V.A., Pegel', T.V., Demidenko, Yu.E., Parkhaev, P. Yu., Korovnikov, I.V., and Skortolova, N.A., 2008, To the problem of stage subdivision of the Lower Cambrian: *Stratigraphy and Geological Correlation*, v. 16, p. 1–19.
- Rubinson, M., and Clayton, R.N., 1969, Carbon-13 fractionation between aragonite and calcite: *Geochimica et Cosmochimica Acta*, v. 33, p. 997–1002, doi: 10.1016/0016-7037(69)90109-4.
- Runkel, A.C., Mackey, T.J., Cowan, C.A., and Fox, D.L., 2010, Tropical shoreline ice in the late Cambrian: Implications for Earth's climate between the Cambrian Explosion and the Great Ordovician Biodiversification Event: *GSA Today*, v. 20, no. 11, p. 4–10, doi: 10.1130/GSAT684A.1
- Runnegar, B., 1981, Muscle scars, shell form and torsion in Cambrian and Ordovician univalved molluscs: *Lethaia*, v. 14, p. 311–322, doi: 10.1111/j.1502-3931.1981.tb01104.x.
- Runnegar, B., and Pojeta, J., Jr., 1974, Molluscan phylogeny: The paleontological viewpoint: *Science*, v. 186, p. 311–317, doi: 10.1126/science.186.4161.311.
- Runnegar, B., Pojeta, J., Jr., Morris, N.J., Taylor, J.D., Taylor, M.E., and McClung, G., 1975, Biology of the Hyolitha: *Lethaia*, v. 8, p. 181–191, doi: 10.1111/j.1502-3931.1975.tb01311.x.
- Saadi, S., Hilali, E.K., Bensaid, M., Boudda, A., and Dahmani, M., 1985, Carte Géologique du Maroc: Rabat, Ministère de l'Énergie et des Mines, Service Géologique du Maroc, scale 1:1,000,000.
- Saltzman, M.R., 2005, Phosphorus, nitrogen, and the redox evolution of the Paleozoic oceans: *Geology*, v. 33, p. 573–576, doi: 10.1130/G21535.1.
- Saltzman, M.R., Ripperdan, R.L., Brasier, M.D., Lohmann, K.C., Robison, R.A., Chang, W.T., Peng Shanchi, Ergaliev, E.K., and Runnegar, B., 2000, A global carbon isotope excursion (SPICE) during the Late Cambrian: Relation to trilobite extinctions, organic-matter burial and sea level: *Palaeogeography, Palaeoclimatology, Palaeoecology*, v. 162, p. 211–223.
- Savitsky, V.E., Zhuravleva, I.T., Kir'yanov, V.V., Luchinina, V.A., Meshkova, N.P., and Shishkin, B.B., 1980, Nemakit-daldynskiy fatiostratotip granity dokembriya i kembriya Sibiri, in Sidorenko, A.V., ed., *Mezhdunarodnyy Geologicheskii Kongress, XXVI sessiya, Doklady sovetskikh geologov, Dokembriy: Moscow, Nauka*, p. 164–170.
- Sawaki, Y., Ohno, T., Fukushi, Y., Komiya, T., Ishikawa, T., Hirata, T., and Maruyama, S., 2008, Sr isotope excursion across the Precambrian–Cambrian boundary in the Three Gorges area, South China: *Gondwana Research*, v. 14, p. 134–147, doi: 10.1016/j.gr.2007.11.002.
- Schoene, B., Crowley, J.L., Condon, D.J., Schmitz, M.D., and Bowring, S.A., 2006, Reassessing the uranium decay constants for geochronology using ID-TIMS U-Pb data: *Geochimica et Cosmochimica Acta*, v. 70, p. 426–445, doi: 10.1016/j.gca.2005.09.007.
- Scholle, P.A., and Arthur, M.A., 1980, Carbon isotope fluctuations in Cretaceous pelagic limestones: Potential stratigraphic and petroleum exploration tool: *The American Association of Petroleum Geologists Bulletin*, v. 64, p. 67–87.
- Schopf, J.W., 2000, Solution to Darwin's dilemma: Discovery of the missing Precambrian record of life: Proceedings of the National Academy of Sciences of the United States of America, v. 97, p. 6947–6953, doi: 10.1073/pnas.97.13.6947.
- Schopf, T.J.M., 1974, Permo-Triassic extinctions: Relation to sea-floor spreading: *The Journal of Geology*, v. 82, p. 129–143, doi: 10.1086/627955.
- Schrag, D.P., Berner, R.A., Hoffman, P.F., and Halverson, G.P., 2002, On the initiation of a snowball Earth: *Geochimistry, Geophysics, Geosystems*, v. 3, no. 6, art. 1036, 21 p.
- Schröder, S., and Grotzinger, J.P., 2007, Evidence for anoxia at the Ediacaran–Cambrian boundary: The record of redox-sensitive trace elements and rare earth elements in Oman: *Journal of the Geological Society of London*, v. 164, p. 175–187, doi: 10.1144/0016-76492005-022.
- Seilacher, A., 1984, Late Precambrian and Early Cambrian Metazoa: Preservation or real extinctions?, in Holland, H.D., and Trendall, A.F., eds., *Patterns of Change in Earth Evolution*: Berlin, Springer-Verlag, p. 159–168.
- Sepkoski, J.J., Jr., 1992, Proterozoic–Early Cambrian diversification of metazoans and metaplates, in Schopf, J.W., and Klein, C., eds., *The Proterozoic Biosphere: A Multidisciplinary Study*: Cambridge, UK, Cambridge University Press, p. 553–561.
- Shackleton, N., and Boersma, A., 1981, The climate of the Eocene ocean: *Journal of the Geological Society of London*, v. 138, p. 153–157, doi: 10.1144/gsjgs.138.2.0153.
- Shackleton, N.J., Hall, M.A., Line, J., and Cang, S., 1983, Carbon isotope data in core V19–30 confirm reduced carbon dioxide concentrations in the ice age atmosphere: *Nature*, v. 306, p. 319–322, doi: 10.1038/306319a0.
- Shen, B., Dong, L., Xiao, S., and Kowalewski, M., 2008, The Avalon explosion: Evolution of Ediacara morphospace: *Science*, v. 319, p. 81–84, doi: 10.1126/science.1150279.
- Shen Yanan, and Schidlowski, M., 2000, New C isotope stratigraphy from southwest China: Implications for the placement of the Precambrian–Cambrian boundary on the Yangtze Platform and global correlations: *Geology*, v. 28, p. 623–626.
- Shu, D.-G., Conway Morris, S., Han, J., Chen, L., Zhang, X.-L., Zhang, Z.-F., Liu, H.-Q., Li, Y., and Liu, J.-N., 2001, Primitive deuterostomes from the Chengjiang Lagerstätte (Lower Cambrian, China): *Nature*, v. 414, p. 419–424, doi: 10.1038/35106514.
- Siddall, M., Rohling, E.J., Almqvist-Labin, A., Hemleben, C., Meischner, D., Schmelzer, I., and Smeed, D.A., 2003, Sea-level fluctuations during the last glacial cycle: *Nature*, v. 423, p. 853–858, doi: 10.1038/nature01690.
- Simberloff, D.S., 1974, Permo-Triassic extinctions: Effects of area on biotic equilibrium: *The Journal of Geology*, v. 82, p. 267–274, doi: 10.1086/627962.
- Skovsted, C.B., 2003, Mobergellans (Problematica) from the Cambrian of Greenland, Siberia and Kazakhstan: *Paläontologische Zeitschrift*, v. 77, p. 429–443.
- Skovsted, C.B., Brock, G.A., and Paterson, J.R., 2006, Bivalved arthropods from the Lower Cambrian Mernmerna Formation, Arrowie Basin, South Australia, and their implications for identification of Cambrian 'small shelly fossils', in Paterson, J.R., and Laurie, J.R., eds., *Cambro-Ordovician Studies II: Association of Australasian Palaeontologists Memoir 32*, p. 7–41.
- Skovsted, C.B., Brock, G.A., Paterson, J.R., Holmer, L.E., and Budd, G.E., 2008, The scleritome of *Eccentrotheca* from the Lower Cambrian of South Australia: Lophophorate affinities and implications for tomotiid phylogeny: *Geology*, v. 36, p. 171–174, doi: 10.1130/G24385A.1.
- Skovsted, C.B., Balthasar, U., Brock, G.A., and Paterson, J.R., 2009a, The tomotiid *Camenella reticulosa* from the Early Cambrian of South Australia: Morphology, scleritome reconstruction, and phylogeny: *Acta Palaeontologica Polonica*, v. 54, p. 525–540, doi: 10.4202/app.2008.0082.
- Skovsted, C.B., Holmer, L.E., Larsson, C.M., Högström, A.E.S., Brock, G.A., Topper, J.P., Balthasar, U., Paterson, J.R., and Paterson, J.R., 2009b, The scleritome of *Paterimitra*: An Early Cambrian stem group brachiopod from South Australia: Proceedings of the Royal Society B, *Biological Sciences*, v. 276, p. 1651–1656, doi: 10.1098/rspb.2008.1655.
- Sloan, L.C., and Pollard, D., 1998, Polar stratospheric clouds: A high latitude warming mechanism in an ancient greenhouse world: *Geophysical Research Letters*, v. 25, p. 3517–3520, doi: 10.1029/98GL02492.
- Sloan, L.C., Walker, J.C.G., and Moore, T.C., Jr., 1995, Possible role of oceanic heat transport in early Eocene climate: *Paleoceanography*, v. 10, p. 347–356, doi: 10.1029/94PA02928.
- Sloss, L.L., 1963, Sequences in the cratonic interior of North America: *Geological Society of America Bulletin*, v. 74, p. 93–114, doi: 10.1130/0016-7606(1963)74[93:SITCIO]2.0.CO;2.
- Smith, R.L., Miller, L.G., and Howes, B.L., 1993, The geochemistry of methane in Lake Fryxell, an amictic, permanently ice-covered, Antarctic lake: *Biogeochemistry*, v. 21, p. 95–115, doi: 10.1007/BF00000873.
- Smith, S.V., 1984, Phosphorus versus nitrogen limitation in the marine environment: *Limnology and Oceanography*, v. 29, p. 1149–1160, doi: 10.4319/lo.1984.29.6.1149.
- Sokolov, B.S., and Zhuravleva, I.T., 1983, Yarusnoe raschlenenie nizhnego kembriya Sibiri, Atlas okamenelostey: Akademiya Nauk SSSR, Sibirskoe Otdelenie, Trudy Instituta Geologii i Geofiziki, v. 558, 216 p., 72 pl.
- Spall, H., 1968, Paleomagnetism of basement granites of southern Oklahoma and its implications; progress report: *Oklahoma Geology Notes*, v. 28, p. 65–80.
- Sperling, E.A., Pisani, D., and Peterson, K.J., 2007, Poriferan paraphyly and its implications for Precambrian palaeobiology, in Vickers-Rich, P., and Komarower, P., eds., *The Rise and Fall of the Ediacaran Biota*: Geological Society of London Special Publication 286, p. 355–368.
- Sperling, E.A., Robinson, J.M., Pisani, D., and Peterson, K.J., 2010, Where's the glass? Biomarkers, molecu-

- lar clocks, and microRNAs suggest a 200-Myr missing Precambrian fossil record of siliceous sponge spicules: *Geobiology*, v. 8, p. 24–36, doi: 10.1111/j.1472-4669.2009.00225.x.
- Squire, R.J., Campbell, I.H., Allen, C.M., and Wilson, C.J.L., 2006, Did the Transgondwanan Supermountain trigger the explosive radiation of animals on Earth?: *Earth and Planetary Science Letters*, v. 250, p. 116–133, doi: 10.1016/j.epsl.2006.07.032.
- Stanley, S.M., 1973, An ecological theory for the sudden origin of multicellular life in the late Precambrian: *Proceedings of the National Academy of Sciences of the United States of America*, v. 70, p. 1486–1489, doi: 10.1073/pnas.70.5.1486.
- Stanley, S.M., and Hardie, L.A., 1998, Secular oscillations in the carbonate mineralogy of reef-building and sediment-producing organisms driven by tectonically forced shifts in seawater chemistry: *Palaeogeography, Palaeoclimatology, Palaeoecology*, v. 144, p. 3–19, doi: 10.1016/S0031-0182(98)00109-6.
- Steiner, M., Mehl, D., Reitner, J., and Erdtmann, B.-D., 1993, Oldest entirely preserved sponges and other fossils from the lowermost Cambrian and a new facies reconstruction of the Yangtze platform (China): *Berliner Geowissenschaftliche Abhandlungen E*, v. 9, p. 293–329.
- Steiner, M., Wallis, E., Erdtmann, B.-D., Zhao Yuanlong, and Yang Ruidong, 2001, Submarine hydrothermal exhalative ore layers in black shales from South China and associated fossils—Insights into a Lower Cambrian facies and bio-evolution: *Palaeogeography, Palaeoclimatology, Palaeoecology*, v. 169, p. 165–191.
- Steiner, M., Li Guoxiang, Qian Yi, and Zhu Maoyan, 2004a, Lower Cambrian small shelly fossils of northern Sichuan and southern Shaanxi (China), and their biostratigraphic importance: *Geobios*, v. 37, p. 259–273.
- Steiner, M., Zhu Maoyan, Li Guoxiang, Qian Yi, and Erdtmann, B.-D., 2004b, New Early Cambrian bilaterian embryos and larvae from China: *Geology*, v. 32, p. 833–836.
- Steiner, M., Li Guoxiang, Qian Yi, Zhu Maoyan, and Erdtmann, B.-D., 2007, Neoproterozoic to Early Cambrian small shelly fossil assemblages and a revised biostratigraphic correlation of the Yangtze Platform (China): *Palaeogeography, Palaeoclimatology, Palaeoecology*, v. 254, p. 67–99.
- Stoll, H.M., and Schrag, D.P., 1998, Effects of Quaternary sea level cycles on strontium in seawater: *Geochimica et Cosmochimica Acta*, v. 62, p. 1107–1118, doi: 10.1016/S0016-7037(98)00042-8.
- Stoll, H.M., Schrag, D.P., and Clemens, S.C., 1999, Are seawater Sr/Ca variations preserved in Quaternary foraminifera?: *Geochimica et Cosmochimica Acta*, v. 63, p. 3535–3547, doi: 10.1016/S0016-7037(99)00129-5.
- Sun, S.Q., 1994, A reappraisal of dolomite abundance and occurrence in the Phanerozoic: *Journal of Sedimentary Research*, v. A64, p. 396–404.
- Swanson-Hysell, N.L., Rose, C.V., Calmet, C.C., Halverson, G.P., Hurtgen, M.T., and Maloof, A.C., 2010, Cryogenian glaciation and the onset of carbon-isotope decoupling: *Science*, v. 328, p. 608–611, doi: 10.1126/science.1184508.
- Swart, P.K., 2008, Global synchronous changes in the carbon isotopic composition of carbonate sediments unrelated to changes in the global carbon cycle: *Proceedings of the National Academy of Sciences of the United States of America*, v. 105, p. 13,741–13,745, doi: 10.1073/pnas.0802841105.
- Swart, P.K., and Eberli, G., 2005, The nature of the $\delta^{13}\text{C}$ of periplatform sediments: Implications for stratigraphy and the global carbon cycle: *Sedimentary Geology*, v. 175, p. 115–129, doi: 10.1016/j.sedgeo.2004.12.029.
- Swart, P.K., Elderfield, H., and Ostlund, G., 2001, The geochemistry of pore fluids from bore holes in the Great Bahama Bank, in Ginsburg, R.N., ed., *Subsurface Geology of a Prograding Carbonate Platform Margin, Great Bahama Bank: Results of the Bahamas Drilling Project: Society for Sedimentary Geology (SEPM) Special Publication 70*, p. 163–174.
- Sysoev, V.A., 1972, *Biostratigrafiya i khliolity ortotetsimorfy nizhego kembriya Sibirskoy platformy*: Moscow, Nauka, 152 p.
- Szaniawski, H., 1982, Chaetognath grasping spines recognized among Cambrian protoconodonts: *Journal of Paleontology*, v. 56, p. 806–810.
- Szaniawski, H., 2002, New evidence for the protoconodont origin of chaetognaths: *Acta Palaeontologica Polonica*, v. 47, p. 405–419.
- Takacs, C.D., Priscu, J.C., and McKnight, D.M., 2001, Bacterial dissolved organic carbon demand in McMurdo Dry Valley lakes, Antarctica: *Limnology and Oceanography*, v. 46, p. 1189–1194, doi: 10.4319/lo.2001.46.5.1189.
- Taylor, S.R., and McLennan, S.M., 1985, *The Continental Crust: Its Composition and Evolution: An Examination of the Geochemical Record Preserved in Sedimentary Rocks*: Oxford, Blackwell Science, 312 p.
- Terman, M.J., chief compiler, 1973, *Tectonic Map of China and Mongolia*: Boulder, Colorado, Geological Society of America, scale 1:5,000,000, 1 sheet.
- Thomas, R.J., Chevallier, L.P., Gresse, P.G., Harmer, R.E., Eglington, B.M., Armstrong, R.A., de Beer, C.H., Martini, J.E.J., de Kock, G.S., Macey, P.H., and Ingram, B.A., 2002, Precambrian evolution of the Sirwa Window, Anti-Atlas orogen, Morocco: *Precambrian Research*, v. 118, p. 1–57, doi: 10.1016/S0301-9268(02)00075-X.
- Tohver, E., D'Agrella-Filho, M.S., and Trindade, R.I.F., 2006, Paleomagnetic record of Africa and South America for the 1200–500 Ma interval, and evaluation of Rodinia and Gondwana assemblies: *Precambrian Research*, v. 147, p. 193–222, doi: 10.1016/j.precamres.2006.01.015.
- Torgunova, N.I., 1994, New ideas on dissolved matter distribution in the Black Sea: *Oceanology (Moscow)*, v. 34, p. 50–54.
- Torsvik, T.H., and Rehnström, E.F., 2001, Cambrian palaeomagnetic data from Baltica: Implications for true polar wander and Cambrian palaeogeography: *Journal of the Geological Society of London*, v. 158, p. 321–329, doi: 10.1144/jgs.158.2.321.
- Torsvik, T.H., Meert, J.G., and Smethurst, M.A., 1998, Polar wander and the Cambrian: *Technical Comment: Science*, v. 279, p. 9.
- Towe, K.M., 1970, Oxygen-collagen priority and the early metazoan fossil record: *Proceedings of the National Academy of Sciences of the United States of America*, v. 65, p. 781–788, doi: 10.1073/pnas.65.4.781.
- Trindade, R.I.F., D'Agrella-Filho, M.S., Epof, I., and Brito Neves, B.J., 2006, Paleomagnetism of Early Cambrian Itabaiana mafic dikes (NE Brazil) and the final assembly of Gondwana: *Earth and Planetary Science Letters*, v. 244, p. 361–377, doi: 10.1016/j.epsl.2005.12.039.
- Tyler, S.A., and Barghoorn, E.S., 1954, Occurrence of structurally preserved plants in Pre-Cambrian rocks of the Canadian Shield: *Science*, v. 119, p. 606–608, doi: 10.1126/science.119.3096.606.
- Tyrell, T., 1999, The relative influences of nitrogen and phosphorous on oceanic primary production: *Nature*, v. 400, p. 525–531, doi: 10.1038/22941.
- Urbanek, A., and Mierzejewska, G., 1977, The fine structure of zooidal tubes in Sabelliditida and Pogonophora with reference to their affinity: *Acta Palaeontologica Polonica*, v. 22, p. 223–240, 18 pl.
- Ushatinskaya, G.T., 1987, Unusual inarticulate brachiopods from the Lower Cambrian sequence of Mongolia: *Paleontological Journal*, v. 21, no. 2, p. 59–66.
- Ushatinskaya, G.T., 2001, Brachiopods, in Zhuravlev, A.Yu., and Riding, R., eds., *The Ecology of the Cambrian Radiation*: New York, Columbia University Press, p. 350–369.
- Ushatinskaya, G.T., 2008, Origin and dispersal of the earliest brachiopods: *Paleontological Journal*, v. 42, p. 776–791, doi: 10.1134/S0031030108080029.
- Vail, P.R., Mitchum, R.M., Jr., Todd, R.G., Widmier, J.M., Thompson, S., III, Sangree, J.B., Bubb, J.N., and Hatlelid, W.G., 1977, Seismic stratigraphy and global changes of sea level, in C.E. Payton, ed., *Seismic stratigraphy—Applications to hydrocarbon exploration*: American Association of Petroleum Geologists Memoir 26, p. 49–212.
- Valentine, J.W., 1994, Late Precambrian bilaterians: Grades and clades: *Proceedings of the National Academy of Sciences of the United States of America*, v. 91, p. 6751–6757, doi: 10.1073/pnas.91.15.6751.
- Valentine, J.W., 2002, Prelude to the Cambrian explosion: *Annual Review of Earth and Planetary Sciences*, v. 30, p. 285–306, doi: 10.1146/annurev.earth.30.082901.092917.
- Valentine, J.W., 2004, *On the Origin of Phyla*: Chicago, University of Chicago Press, 614 p.
- Valentine, J.W., and Moores, E.M., 1970, Plate-tectonic regulation of faunal diversity and sea level: A model: *Nature*, v. 228, p. 657–659, doi: 10.1038/228657a0.
- Val'kov, A.K., 1975, *Biostratigrafiya i khliolity kembriya severo-vostoka Sibirskoy platformy*: Moscow, Nauka, 140 p.
- Val'kov, A.K., 1982, *Biostratigrafiya nizhego kembriya vostoka Sibirskoy platformy*: Moscow, Nauka, 92 p., 16 pl.
- Val'kov, A.K., 1983, Rasprostranenie drevneyshikh skeletnykh organizmov i korrelyatsiya nizhego granitsy kembriya v yugo-vostochnoy chasti Sibirskoy platformy, in Khomentovskiy, V.V., ed., *Pozdnyy dokembriy i ranniy paleozoy Sibiri, Vendskie otlozheniya*: Novosibirsk, Institut Geologii i Geofiziki, Sibirskoe Otdelenie, Akademiyi Nauk SSSR, p. 37–48.
- Val'kov, A.K., 1987, *Biostratigrafiya nizhego kembriya vostoka Sibirskoy platformy, Yudomo-Olenekskiy region*: Moscow, Nauka, 137 p., 16 pl.
- Van Cappellen, P., and Ingall, E.D., 1996, Redox stabilization of the atmosphere and oceans by phosphorous-limited marine productivity: *Science*, v. 271, p. 493–496, doi: 10.1126/science.271.5248.493.
- van der Voo, R., 1990, The reliability of paleomagnetic data: *Tectonophysics*, v. 184, p. 1–9, doi: 10.1016/0040-1951(90)90116-P.
- Van Iten, H., Zhu Maoyan, and Li Guoxiang, 2010, Redescription of *Hexaconularia* He and Yang, 1986 (Lower Cambrian, South China): Implications for the affinities of conulariid-like small shelly fossils: *Paleontology*, v. 53, p. 191–199.
- Vannier, J., Steiner, M., Renvoisé, E., Hu, S.-X., and Casanova, J.-P., 2007, Early Cambrian origin of modern food webs: Evidence from predator arrow worms: *Proceedings of the Royal Society B, Biological Sciences*, v. 274, p. 627–633, doi: 10.1098/rspb.2006.3761.
- Vannier, J., Calandra, I., Gaillard, C., and Żylińska, A., 2010, Priapulid worms: Pioneer horizontal burrowers at the Precambrian-Cambrian boundary: *Geology*, v. 38, p. 711–714, doi: 10.1130/G30829.1.
- Vasconcelos, C., and McKenzie, J.A., 1997, Microbial mediation of modern dolomite precipitation and diagenesis under anoxic conditions (Lagoa Vermelha, Rio de Janeiro, Brazil): *Journal of Sedimentary Research*, v. 67, p. 378–390.
- Vasil'eva, N.I., 1998, *Melkaya rakovinnaya fauna i biostratigrafiya nizhego kembriya Sibirskoy platformy: Saint Petersburg, Vserossiyskiy Neftyanoy Nauchno-Issledovatel'skiy Geologorazvedochnyy Institut*, 139 p., 50 pl.
- Veizer, J., 1989, Strontium isotopes in seawater through time: *Annual Review of Earth and Planetary Sciences*, v. 17, p. 141–167, doi: 10.1146/annurev.earth.17.050189.001041.
- Veizer, J., Ala, D., Azmy, K., Bruckschen, P., Buhl, D., Bruhn, F., Carden, G.A.F., Diener, A., Ebneth, S., Godderis, Y., Jasper, T., Korte, C., Pawellek, F., Podlaha, O.G., and Strauss, H., 1999, $^{87}\text{Sr}/^{86}\text{Sr}$, $\delta^{13}\text{C}$ and $\delta^{18}\text{O}$ evolution of Phanerozoic seawater: *Chemical Geology*, v. 161, p. 59–88, doi: 10.1016/S0009-2541(99)00081-9.
- Vendrasco, M.J., Li Guoxiang, Porter, S.M., and Fernandez, C.Z., 2009, New data on the enigmatic *Ocrurus-Eohalobia* group of Early Cambrian small skeletal fossils: *Paleontology*, v. 52, p. 1373–1396.
- Vendrasco, M.J., Porter, S.M., Kouchinsky, A., Li Guoxiang, and Fernandez, C.Z., 2010, New data on molluscs and their shell microstructures from the Middle Cambrian Gowers Formation, Australia: *Paleontology*, v. 53, p. 97–135.
- Vidal, G., and Moczydlowska-Vidal, M., 1997, Biodiversity, speciation, and extinction trends of Proterozoic and Cambrian phytoplankton: *Paleobiology*, v. 23, p. 230–246.
- Vincenz, S.A., Yaskawa, K., and Ade-Hall, J.M., 1975, Origin of the magnetization of the Wichita Mountains granites, Oklahoma: *Geophysical Journal of the Royal Astronomical Society*, v. 42, p. 21–48, doi: 10.1111/j.1365-246X.1975.tb05848.x.

- Vinn, O., 2006, Possible cnidarian affinities of *Torellella* (Hyolithelminthes, Upper Cambrian, Estonia): *Paläontologische Zeitschrift*, v. 80, p. 384–389.
- Vinther, J., and Nielsen, C., 2005, The Early Cambrian *Halkieria* is a mollusc: *Zoologica Scripta*, v. 34, p. 81–89, doi: 10.1111/j.1463-6409.2005.00177.x.
- Voronin, Yu.L., Voronova, L.G., Grigor'eva, N.V., Drozdova, N.A., Zhegallo, E.A., Zhuravlev, A.Yu., Ragozina, A.L., Rozanov, A.Yu., Sayutina, T.A., Sysoev, V.A., and Fomin, V.D., 1982, Granitsa dokembriya i kembriya v geosinklinal'nykh oblastiakh (opornyy razrez Salany-Gol, MNR): *Sovmestnaya Sovetskoye-Mongol'skaya Paleontologicheskaya Ekspeditsiya, Trudy*, v. 18, 150 p., 40 pl.
- Voronova, L.G., Grigor'eva, N.V., Zhegallo, E.A., Missar-zhevsky, V.V., and Sysoev, V.A., 1983, Vozrast sloev "Oelandiella" korobkovi-Anabarella plana na Sibirskoy platforme: *Izvestiya Akademii Nauk SSSR, Seriya Geologicheskaya*, v. 1983, no. 12, p. 80–84.
- Wagner, P.J., 1995, Diversity patterns among early gastropods: Contrasting taxonomic and phylogenetic descriptions: *Paleobiology*, v. 21, p. 410–439.
- Walsh, G.J., Aleinikoff, J.N., Benziane, F., Yazidi, A., and Armstrong, T.R., 2002, U-Pb zircon geochronology of the Paleoproterozoic Tagrara de Tata inlier and its Neoproterozoic cover, western Anti-Atlas, Morocco: *Precambrian Research*, v. 117, p. 1–20, doi: 10.1016/S0301-9268(02)00044-X.
- Walter, M.R., Veevers, J.J., Calver, C.R., Gorjan, P., and Hill, A.C., 2000, Dating the 840–544 Ma Neoproterozoic interval by isotopes of strontium, carbon, and sulfur in seawater, and some interpretive models: *Precambrian Research*, v. 100, p. 371–433, doi: 10.1016/S0301-9268(99)00082-0.
- Warthmann, R., van Lith, Y., Vasconcelos, C., McKenzie, J.A., and Karpoff, A.M., 2000, Bacterially induced dolomite precipitation in anoxic culture experiments: *Geology*, v. 28, p. 1091–1094, doi: 10.1130/0091-7613(2000)28<1091:BDPIA>2.0.CO;2.
- Weber, B., and Zhu Maoyan, 2003, Arthropod trace fossils from the Zhujiaqing Formation (Meishucunian, Yunnan) and their palaeobiological implications: *Progress in Natural Science*, v. 13, p. 795–800, doi: 10.1080/10020070312331344450.
- Weber, B., Steiner, M., and Zhu Maoyan, 2007, Precambrian-Cambrian trace fossils from the Yangtze Platform (South China) and the early evolution of bilaterian lifestyles: *Palaeogeography, Palaeoclimatology, Palaeoecology*, v. 254, p. 328–349, doi: 10.1016/j.palaeo.2007.03.021.
- Wefer, G., and Berger, W.H., 1991, Isotope paleontology: Growth and composition of extant calcareous species: *Marine Geology*, v. 100, p. 207–248, doi: 10.1016/0025-3227(91)90234-U.
- Wilkinson, B.H., and Algeo, T.J., 1989, Sedimentary carbonate record of calcium-magnesium cycling: *American Journal of Science*, v. 289, p. 1158–1194.
- Wille, M., Nägler, T., Lehmann, B., Schröder, S., and Kramers, J.D., 2008, Hydrogen sulphide release to surface waters at the Precambrian/Cambrian boundary: *Nature*, v. 453, p. 767–769, doi: 10.1038/nature07072.
- Wingate, M.T.D., Cambell, I.H., Compston, W., and Gibson, G.M., 1998, Ion microprobe U-Pb ages for Neoproterozoic basaltic magmatism in south-central Australia and implications for the breakup of Rodinia: *Precambrian Research*, v. 87, p. 135–159, doi: 10.1016/S0301-9268(97)00072-7.
- Wood, R.A., Grotzinger, J.P., and Dickson, J.A.D., 2002, Proterozoic modular biomineralized metazoan from the Nama Group, Namibia: *Science*, v. 296, p. 2383–2386, doi: 10.1126/science.1071599.
- Worsley, T.R., Nance, D., and Moody, J.B., 1984, Global tectonics and eustasy for the past 2 billion years: *Marine Geology*, v. 58, p. 373–400, doi: 10.1016/0025-3227(84)90209-3.
- Wray, G.A., Levinton, J.S., and Shapiro, L.H., 1996, Molecular evidence for deep Precambrian divergences among metazoan phyla: *Science*, v. 274, p. 568–573, doi: 10.1126/science.274.5287.568.
- Wright, J.E., Hogan, J.P., and Gilbert, M.C., 1996, The southern Oklahoma aulocogen: Not just another *B.L.L.P.*: *Eos (Transactions, American Geophysical Union)*, v. 77, Fall Meeting supplement, p. 845.
- Xiao, S., Zhang Yun, and Knoll, A.H., 1998, Three-dimensional preservation of algae and animal embryos in a Neoproterozoic phosphorite: *Nature*, v. 391, p. 553–558.
- Xiao, S., Yuan Xunlai, Steiner, M., and Knoll, A.H., 2002, Macroscopic carbonaceous compressions in a terminal Proterozoic shale: A systematic reassessment of the Miaohu biota, South China: *Journal of Paleontology*, v. 76, p. 347–376, doi: 10.1666/0022-3360(2002)076<0347:MCCIAT>2.0.CO;2.
- Xiao, S., Hu Jie, Yuan Xunlai, Parsley, R.L., and Cao Ruiji, 2005, Articulated sponges from the Lower Cambrian Hetang Formation in southern Anhui, South China: Their age and implications for the early evolution of sponges: *Palaeogeography, Palaeoclimatology, Palaeoecology*, v. 220, p. 89–117.
- Yao Jinxian, Xiao, S., Yin Leiming, Li Guoxiang, and Yuan Xunlai, 2005, Basal Cambrian microfossils from the Yurtus and Xishanblaq Formations (Tarim, north-west China): Systematic revision and biostratigraphic correlation of *Micrhystridium*-like acritarchs: *Palaeontology*, v. 48, p. 687–708.
- Yin Leiming, Zhu Maoyan, Knoll, A.H., Yuan Xunlai, Zhang Junming, and Hu Jie, 2007, Doushantuo embryos preserved inside diapause egg cysts: *Nature*, v. 446, p. 661–663.
- Yochelson, E.L., 1969, Stenothecoida, a proposed new class of Cambrian Mollusca: *Lethaia*, v. 2, p. 49–62, doi: 10.1111/j.1502-3931.1969.tb01250.x.
- Yochelson, E.L., 1978, An alternative approach to the interpretation of the phylogeny of ancient mollusks: *Malacologia*, v. 17, p. 165–191.
- Yue Zhao and Bengtson, S., 1999, Embryonic and post-embryonic development of the Early Cambrian cnidarian *Olivoides*: *Lethaia*, v. 32, p. 181–195.
- Zenger, D.H., Dunham, J.R., and Ethington, R.L., eds., 1980, Concepts and Models of Dolomitization: Society of Economic Paleontologists and Mineralogists Special Publication 28, 320 p.
- Zhang Junming, Li Guoxiang, Zhou Chuanming, Zhu Maoyan, and Yu Ziyi, 1997, Carbon isotope profiles and their correlation across the Neoproterozoic-Cambrian boundary interval on the Yangtze Platform, China: *Bulletin of the National Museum of Natural Science (Taiwan)*, v. 10, p. 107–116.
- Zhao Yuanlong, Steiner, M., Yang Ruidong, Erdtmann, B.-D., Guo Qingjun, Zhou Zhen, and Wallis, E., 1999, [Discovery and significance of the early metazoan biotas from the Lower Cambrian Niutitang Formation Zunyi, Guizhou, China]: *Acta Palaeontologica Sinica*, v. 38, supplement, p. 132–144, 2 pl. (in Chinese with English abstract).
- Zhou Chuanming, Zhang Junming, Li Guoxiang, and Yu Ziyi, 1997, Carbon and oxygen isotopic record of the Early Cambrian from the Xiaotan Section, Yunnan, South China: *Scientia Geologica Sinica*, v. 32, p. 201–211 (in Chinese with English abstract).
- Zhu Maoyan, Li Guoxiang, and Zhang Junming, 2001a, New C isotope stratigraphy from southwest China: Implications for the placement of the Precambrian-Cambrian boundary on the Yangtze Platform and global correlations: *Comment: Geology*, v. 29, p. 871–872, doi: 10.1130/0091-7613(2001)029<0871:NCISFS>2.0.CO;2.
- Zhu Maoyan, Li Guoxiang, Zhang Junming, Steiner, M., Qian Yi, and Jiang Zhiwen, 2001b, Early Cambrian stratigraphy of east Yunnan, southwestern China: A synthesis: *Acta Palaeontologica Sinica*, v. 40, supplement, p. 4–39.
- Zhuravlev, A.Yu., 1986a, Evolution of archaeocyaths and palaeobiogeography of the Early Cambrian: *Geological Magazine*, v. 123, p. 377–385, doi: 10.1017/S0016756800033471.
- Zhuravlev, A.Yu., 1986b, Radiocyathids, in Hoffman, A., and Nitecki, M.H., eds., *Problematic Fossil Taxa*: Oxford, Oxford University Press, p. 35–44.
- Zhuravlev, A.Yu., 2001, Biotic diversity and structure during the Neoproterozoic–Ordovician transition, in Zhuravlev, A.Yu., and Riding, R., eds., *The Ecology of the Cambrian Radiation*: New York, Columbia University Press, p. 173–199.
- Zhuravlev, A.Yu., and Wood, R.A., 2008, Eve of biomineralization: Controls on skeletal mineralogy: *Geology*, v. 36, p. 923–926, doi: 10.1130/G25094A.1.

MANUSCRIPT RECEIVED 4 JUNE 2010
 MANUSCRIPT ACCEPTED 3 AUGUST 2010

Printed in the USA